AD-A179 910 A STUDY OF PLASMA IRREGULARITIES IN THE HIGH-LATITUDE REGION(U) REGIS COLL RESEARCH CENTER WESTON MA D R WEIMER ET AL. 27 OCT 86 AFGL-TR-86-0233 1/2

UNCLASSIFIED F19628-84-C-0126 F/G 4/1 NL

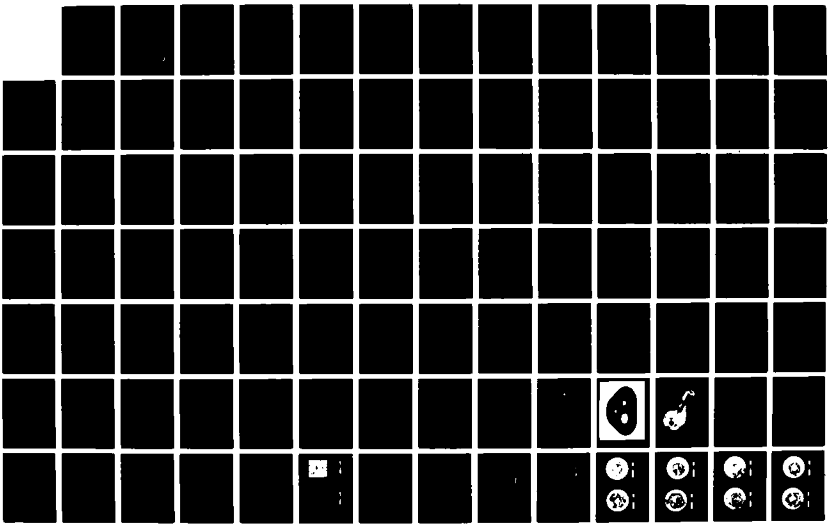


1.0
1.1
1.25
1.4
1.6
1.8
2.0
2.2
2.8
3.2
3.6
4.0

AFGL-TR-86-0233

A Study of Plasma Irregularities in the High-Latitude Region

D.R. Weimer
P.B. Anderson
M.E. Greenspan
E.M. Basinska-Lewin
J.H. James
J.M. Pelagatti

Regis College Research Center
235 Wellesley Street
Weston, MA 02193

27 October 1986

Final Report
19 June 1984 - 30 September 1986

APPROVED FOR PUBLIC RELEASE; DISTRIBUTION UNLIMITED

AIR FORCE GEOPHYSICS LABORATORY
AIR FORCE SYSTEMS COMMAND
UNITED STATES AIR FORCE
HANSCOM AIR FORCE BASE, MASSACHUSETTS 01731

" This technical report has been reviewed and is approved for publication"

FREDERICK J. RICH
Contract Manager

NELSON C. MAYNARD
Branch Chief

FOR THE COMMANDER

RITA C. SAGALYN
Division Director

This report has been reviewed by the ESD Public Affairs Office (PA) and is releasable to the National Technical Information Service (NTIS).

Qualified requestors may obtain additional copies from the Defense Technical Information Center. All others should apply to the National Technical Information Service.

If your address has changed, or if you wish to be removed from the mailing list, or if the addressee is no longer employed by your organization, please notify AFGL/DAA, Hanscom AFB, MA 01731. This will assist us in maintaining a current mailing list.

Do not return copies of this report unless contractual obligations or notices on a specific document requires that it be returned.

UNCLASSIFIED

SECURITY CLASSIFICATION OF THIS PAGE

REPORT DOCUMENTATION PAGE

1a. REPORT SECURITY CLASSIFICATION Unclassified	1b. RESTRICTIVE MARKINGS
2a. SECURITY CLASSIFICATION AUTHORITY	3. DISTRIBUTION/AVAILABILITY OF REPORT Approved for public release; distribution unlimited.
2b. DECLASSIFICATION/DOWNGRADING SCHEDULE	
4. PERFORMING ORGANIZATION REPORT NUMBER(S)	5. MONITORING ORGANIZATION REPORT NUMBER(S) AFGL-TR-86-0233
6a. NAME OF PERFORMING ORGANIZATION Regis College Research Ctr. / 6b. OFFICE SYMBOL (If applicable)	7a. NAME OF MONITORING ORGANIZATION Air Force Geophysics Laboratory
6c. ADDRESS (City, State, and ZIP Code) 235 Wellesley St., Weston, MA 02193	7b. ADDRESS (City, State, and ZIP Code) Hanscom AFB, MA 01731
8a. NAME OF FUNDING/SPONSORING ORGANIZATION / 8b. OFFICE SYMBOL (If applicable)	9. PROCUREMENT INSTRUMENT IDENTIFICATION NUMBER F19628-84-C-0126
8c. ADDRESS (City, State, and ZIP Code)	10. SOURCE OF FUNDING NUMBERS

PROGRAM ELEMENT NO.	PROJECT NO.	TASK NO.	WORK UNIT ACCESSION NO
61102F	2311	2311G2	2311G2GB

11. TITLE (Include Security Classification)
A STUDY OF PLASMA IRREGULARITIES IN THE HIGH-LATITUDE REGION.

12. PERSONAL AUTHOR(S) Weimer, D.R., Anderson, P.B., Greenspan, M.E., Basinska-Lewin, E.M., James, J.H., and Pelagatti, J.M.

13a. TYPE OF REPORT	13b. TIME COVERED	14. DATE OF REPORT (Year, Month, Day)	15. PAGE COUNT
Final	FROM 84JUNE19 TO 86SEPT30	86 OCT 27	104

16. SUPPLEMENTARY NOTATION

17. COSATI CODES			18. SUBJECT TERMS (Continue on reverse if necessary and identify by block number)
FIELD	GROUP	SUB-GROUP	Ionosphere, magnetosphere, auroral electrodynamics, plasma irregularities, DMSP, HILAT, SSIE, SSIES, SSIES-2, SSM, BERT, IMPS, CRRES, EISCAT, AMPTE, DE-1.

19. ABSTRACT (Continue on reverse if necessary and identify by block number) (cont'd on reverse side)
A summary is given of the work completed under contract F19628-84-C-0126; this work has included the engineering of space-qualified instruments, data processing services, and scientific study of high-latitude plasma irregularities and the physics of the aurora. Design work has been done on a series of plasma instruments for the Defense Meterorological Satellite Program (DMSP), the combined Release and Radiation Effects Satellite (CRRES), the Beam Ejection Rocket Technology (BERT) and Ejected Rocket Nosecone to measure induced Emissions (ERNIE) sounding rocket program, and the interactions Measurements Payload for Shuttle (IMPS). The function of the Special Sensor for Ions, Electrons, and Scintillations (SSIES) is described in detail. Computer programs have been written to process DMSP magnetometer data, and DMSP plasma density measurements have been processed to produce a model of the topside ionosphere. A scientific study has been conducted with HILAT data in order to produce an empirical description of high-latitude plasma irregularity production and transport. Data from HILAT has also been used to stud

20. DISTRIBUTION/AVAILABILITY OF ABSTRACT ☒ UNCLASSIFIED/UNLIMITED ☐ SAME AS RPT. ☐ DTIC USERS	21. ABSTRACT SECURITY CLASSIFICATION Unclassified
22a. NAME OF RESPONSIBLE INDIVIDUAL Frederick J. Rich	22b. TELEPHONE (Include Area Code) (617) 377-2431 / 22c. OFFICE SYMBOL AFGL/PHG

DD FORM 1473, 84 MAR — 83 APR edition may be used until exhausted. All other editions are obsolete.

SECURITY CLASSIFICATION OF THIS PAGE
UNCLASSIFIED

#19 Abstract (cont'd)

small-scale processes on the auroral dayside cusp region. Both HILAT and Dynamics Explorer 1 data have been used to study auroral electrodynamics in the ionosphere and above to auroral acceleration region. Research is in progress on a study of the coupling between the magnetotail and the auroral ionosphere using data from both the European Incoherent Scatter radar facility (EISCAT) and the Active Magnetoshere Particle Tracer Explorer Ion Release Module AMPTE IRM.

Table of Contents

1. INTRODUCTION

This report summarizes the work accomplished by Regis College under contract F19628-84-C-0126 with the Air Force Geophysics Laboratory. The stated objective of the work undertaken for this contract was to design space-qualified instruments, study high-latitude plasma irregularities, and develop global models of the topside ionosphere. Specific line items to be performed under this contract were:

a. Provide engineering resources and field services for the integration of the Special Sensor Ion, Electron, and Scintillation (SSIES) unit for DMSP flights F8, F9, and F10.

b. Upgrade the design of the SSIES unit for DMSP flights F11 through F14.

c. Provide the systems engineering support for integrating into a single system the Langmuir Probe, the Fluxgate Magnetometer, and the Passive Plasma Sounder experiments for the Combined Release and Radiation Effects Satellite.

d. Provide the engineering support for developing the electric field experiment to be flown on the BERT and ERNIE rocket.

e. Provide the engineering support necessary for refurbishing the existing Shuttle flight systems.

f. Study the global modelling of high-latitude plasma irregularities using plasma and particle data from current and future DMSP experiments.

g. Use current and future DMSP data to extend statistical models

of ionospheric thermal plasma developed from previous DMSP data.

h. Study the formation, production, and decay of high-latitude plasma irregularities using coordinated observation and measurement of the thermal plasma parameters, electric field, particle flux, and energy obtained from the HILAT satellite data, and from ground-based incoherent scatter radar data.

The remainder of this report consists of brief descriptions of the work done under this contract. The engineering work covering objectives (a) through (e) is detailed in Chapter 2. In addition to the engineering work on the SSIES unit, as specified in objective (a), Regis College has prepared a technical report on the SSIES instrument and has been preparing algorithms and software for processing the SSIES data after it is launched. An overview of this work is contained in Chapter 3. Regis College currently has not devoted much effort to the scientific analysis related to objective (f); instead there has been a considerable effort expended to develop software for processing DMSP data and in managing the DMSP data base, for use by AFGL and Regis College scientists. This processing of the DMSP data is described in Chapter 4. Similarly, Regis College developed the software to accomplish objective (g), although the final scientific analysis was done by AFGL. The development of this DMSP thermal plasma model is summarized in Chapter 5. The results of scientific studies related to objective (h) are summarized in Chapters 6 through 8.

A list of papers and publications generated as a result of work done in whole or part of this contract is contained in Chapter 9. In the cases where the results of work done on this contract have been

published, only brief summaries of the results are contained in this Final Report; the referenced publications should be consulted for specific details about the research. For the cases where the research results have not yet been published, more detailed accounts of the work are given in this report.

2. DESIGN OF SPACE-QUALIFIED INSTRUMENTS

2.1 Introduction

Regis College has provided engineering resources for the development of several AFGL satellite and rocket experiments. This work has included instrument design, evaluation, calibration, and spacecraft integration. Overviews of the various instruments' purpose and function are presented in the following sections, along with descriptions of the specific activities performed by Regis College personnel in the development of each instrument.

2.2 DMSP: SSIES, SSIES-2 & SSM

2.2.1.1 SSIES & SSIES-2 Overview

The purpose of the SSIES & SSIES-2 Plasma Monitor Systems is to obtain information about the characteristics of the space plasma (the electrically charged gas) above the peak (or maximum density region) of the F region of the ionosphere. This information is needed as part of the ionospheric specification required for efficient operational use of Air Force systems employing HF, VHF and UHF frequencies. The information will be obtained by four electrostatic probes to be flown on a series of satellites of the Defense Meteorological Satellite Program (DMSP).

The SSIES-2 system scheduled for launch on DMSP flights F11 - F14, is an upgraded design of the SSIES Plasma Monitor for flights F8 - F10.

The major improvement is the added capability for inflight block loading of the SSIES-2 main memory from the ground. This will significantly enhance in flight operation by allowing real time adjustment to processing algorithms in reaction to unexpected measurement situations. Other changes include new and upgraded component selection and improved noise reduction by moving the sensitive electrometer amplifiers from the main electronics packages to their individual sensor housings.

The major components of the SSIES-2 systems are: a) a microprocessor based Main Electronics Package (MEP), b) a Drift Scintillation Meter (DSM) Electronics Package, c) an Electron Electrometer Package, d) The Electron Sensor Assembly and e) an Ion Sensor Array Assembly as shown in Figure 2-1. The Ion Sensor Array Assembly consists of three cylindrical planar sensors, a triangular face plate (ground plane referenced to a bias) and a mounting bracket. This group of sensors includes the following: 1) Drift Meter Sensor, 2) Scintillation Meter Sensor and 3) Retarding Potential Analyzer (RPA). Each sensor is a cylinder with an aperture in the forward planar surface. An electrometer amplifier is mounted in the rear of each cylinder. The electron assembly consists of a boom mounted spherical electron sensor and an electron electrometer housing located near the base of the boom.

2.2.1.2 SSM Overview

The purpose of the SSM Triaxial Fluxgate Magnetometer is to obtain critical information about disturbances in the ionosphere and near-earth space environment which affect communication and surveillance systems.

One signature of such disturbances is a deflection of the geomagnetic field from its quiet-time position. These deflections are magnetic field vectors of 1 nano-Tesla (nT) to 1,500 nT which are approximately perpendicular to the main geomagnetic field. Such deflections will be measured by a triaxial, fluxgate magnetometer to be flown on the DMSP spacecraft S12, S13, S14 and S15. The main features of the SSM are shown in the block diagram, Figure 2-2. The electronics package interfaces with the spacecraft for primary power and analog monitors. The analog section of the electronics package provides drive signals to the sensor elements and detect the output signals from the sensor element. This sensor assembly is located on the exterior surface of the spacecraft. The electronics package also converts the analog signals to digital signals, manipulates the digital data and provides the interface with the DMSP Operation Linescan System (OLS) telemetry unit.

2.2.2.1 SSIES Activity

Engineering activities for the previously developed and delivered SSIES units on the DMSP S8, S9 and S10 spacecraft included interface specifications reports, integration support and field services. Provided SSIES-2 interface specifications and drawings to RCA for the spacecraft Interface Control Document (ICD). Also provided SSIES-2 interface specifications and drawings to Westinghouse (WEC) for the OLS document. Integration of the three spacecraft are being processed in the following order: S8, S10 and S9. During the course of integrating each spacecraft, flight units are repeatedly tested by a ground based computer system. All downlinked telemetry data from the spacecraft is

recorded on computer tape. For each of these tests RCA sends AFGL data from these computer tapes reproduced on stacks of printer paper. Engineering expertise was exercised in reviewing all of the above data. Integration of the S8 spacecraft has been completed and has been placed in storage at Vandenberg AFB for a future launch. Prior to shipping to Vandenberg, field service was provided in support of a Preship Verification Test at RCA. Integration of S10 and S9 spacecraft at RCA are both near completion.

2.2.2.2 SSIES-2 Activity

The SSIES-2 systems are to be flown on spacecraft S11, S12, S13 and S14. The MEP, DSM electronics package, Drift Meter Sensor, Scintillation Meter Sensor and Ion Sensor Array Assembly were all developed under other AFGL contracts. This contract was responsible for the design and development of the electron and RPA electrometers and the analog circuitry in the MEP unit. Other direct involvement included all levels of systems engineering and related support activities.

The electron and RPA electrometers were moved from the MEP to the sensor housings to reduce the triboelectric effect and reduce the stray capacitance across the input to the electrometers. In addition, the input operational amplifier was replaced with one having better radiation characteristics. Improved operational amplifiers and discrete components were selected for the analog circuitry in the MEP unit. Schematics of the three sections are shown in Figures 2-3, 2-4 and 2-5. Other engineering activities included the redesign of the RPA Sensor and

the design of the electron electrometer housing. Also designed an RPA (Ion) test chassis to facilitate testing the flight sensors during vacuum tests at University of Texas at Dallas (UTD). This chassis simulates the MEP unit by providing all the power supply voltages, sweeps, level shifting and telemetry signals. Another engineering activity included attending design meetings for implementing block loading (reprogrammability) capabilities on all future DMSP satellites (S11 and on). Block loading enables new or updated software programs to be uplinked from the ground to the satellite. The SSIES-2 system is the first unit to incorporate this new reprogrammability feature.

System level activities included providing engineering specifications and editing the Product Function Specification for the SSIES-2 system. Also provided to RCA specifications and engineering drawings for the new combined spacecraft and OLS Interface Control Document (ICD). Other activities included preparation of the Detailed Electrical Test / Functional Electrical Test (DET/FET) for WEC which will be used for initially testing each SSIES-2 system as delivered. Another test procedure written was for a Sensor Grid / Stimulation test for WEC which is part of the Sensor Clean and Cal Test. Also system calibration procedures were prepared.

Other system level activities included integration of the first SSIES-2 flight units, acceptance testing, thermal / burn-in tests and calibration. Calibration data was taken through the MEP unit's telemetry circuitry for the Electron and RPA Assemblies at +5 ^{o}C, +20 ^{o}C and

+35 ^{o}C. The MEP was also calibrated at the same above temperatures. As a part of the calibration activity, the RPA sensor was tested in a vacuum with an ion source at UTD.

2.2.2.3 SSM Activity

Systems engineering activities provided for the SSM system included reviewing and editing the technical specifications and the Product Function Specification. Also provided technical assistance at the Preliminary Design Review (PDR) and the Critical Design Review (CDR) at the NASA - Goddard Space Flight Center (GSFC).

2.3 CRRES-225: AFGL-701-13-1 & -13-2, AFGL-701-14 and AFGL-701-15

2.3.1 CRRES Overview

The purpose of the thirteen AFGL-701 instruments on the CRRES satellite is to determine the energetic particle fluxes throughout the earth's radiation belts and to determine the affect of energetic particles upon microelectronics. This goal will be achieved by a) measuring the particles' characteristics near the geomagnetic equator, b) measuring simultaneously the effects upon microelectronics, c) measuring those factors which cause changes in the energetic particle populations. Four of the thirteen instruments are combined to form a complement of experiments known as CRRES-225. These instruments are 1) AFGL-707-13-1, Fluxgate Magnetometer; 2) AFGL-701-13-2, Search Coil Magnetometer; 3) AFGL-701-14, Langmuir Probe; and 4) Passive Plasma Sounder. A block diagram of the above instruments is shown in Figure

2-6. AFGL has direct responsibility for the integration of all of these instruments.

2.3.1.1 AFGL-701-13-1 Overview

The purpose of the triaxial Fluxgate Magnetometer (AFGL-701-13-1) instrument is to obtain the ambient geomagnetic field and low frequency variations in that fields. This measurement will be used, 1) together with the look angles of the particle experiments to obtain pitch angles of the measured particles, 2) as a diagnostic of very low frequency waves in the ambient environment, and 4) to provide a secondary source of attitude information. The Fluxgate Magnetometer sensor is mounted on a rigid, 20 foot boom in order to get it far enough away from the spacecraft so that the total spacecraft generated magnetic field will be less than 2 nT. The electronics to operate the sensor is mounted inside the spacecraft with a link to the Langmuir Probe electronics which will provide power and telemetry. Each axis of the triaxial Fluxgate Magnetometer is sampled on two different ranges (+/-45,000 nT and +/-1,000 nT).

2.3.1.2 AFGL-701-13-2 Overview

The purpose of the Search Coil Magnetometer instrument is to obtain information on the plasma wave environment simultaneously with the Passive Plasma Sounder so that electric field fluctuations can be classified as due to electromagnetic or electrostatic waves and the plasma wave modes can be uniquely different. The Search Coil Magnetometer sensor is mounted on the same boom as the Fluxgate Magnetometer.

The output from the sensor is fed through a 14 channel filter bank in the Passive Plasma Sounder instrument.

2.3.1.3 AFGL-701-14 Overview

The purpose of the Langmuir Probe instrument is to obtain the characteristics of the thermal plasma which can interact with the energetic particles through wave-particle interaction. This instrument is capable of both current collection for density determination and voltage sensing for field measurements. The Langmuir Probe instrument consists of a pair spherical electron collectors mounted at the end of 50 meter wire booms. Each spherical collector contains a preamplifier and is connected to an electronics package for power, control and data processing. Interfaces are provided to two external cylinder wire boom preamplifiers and the Fluxgate Magnetometer. The electronics package supplies telemetry data to the spacecraft telemetry system and receives both serial and discrete commands from the spacecraft. Fluxgate Magnetometer digital data is made available on another external interface to the Low-Energy Plasma Analyzer (LEPA).

2.3.1.4 AFGL-701-15 Overview

The purpose of the Passive Plasma Sounder and Search Coil Magnetometer instruments, collectively known as the Plasma Wave experiment, is to measure the plasma wave environment in the earth's radiation belts and will also measure the electron number density. The Passive Plasma Sounder instrument consists of a 100 meter (tip to tip) cylinder wire boom (two 50 meter booms), two preamplifiers mounted near the base of

the booms and an electronics package. The electronics package receives power and commands from the spacecraft. It provides interfaces with the spacecraft for the digitized data and an external interface with the Langmuir Probe for Search Coil analog data.

2.3.2.1 CRRES-225 Activity

System level engineering was provided for integrating into a single system the Fluxgate Magnetometer, the Search Coil Magnetometer, Langmuir Probe and the Passive Plasma Sounder instruments which entailed many responsibilities. The system specifications were maintained in the form of an Interface Control Document (ICD). This is document controlled by the CRRES Prime Contractor, Ball Aerospace Systems Division (BASD), which contains specifications on all instruments, and was continually updated. A document for the Spacecraft Integration Test Plans was compiled and when released by BASD it was reviewed for AFGL's approval. Prior to delivery of the CRRES-225 compliment of instruments, an ICD Compliance Package was compiled, written and delivered to Space Division. From this document, Space Division gave a certificate of approval for delivering the instruments to BASD.

Other activities included the responsibility of integrating the prototype instruments at AFGL and later integrating the flight instruments also at AFGL. Other instrument activity included coordinating the acceptance tests which included Electromagnetic Compatibility Testing (EMC), vibration and thermal/vacuum testing. In preparation for thermal/vacuum testing, a complete test configuration was designed.

This setup enabled all thirteen flight packages to operate in the thermal/vacuum chamber while being controlled by ground support equipment (GSE) outside the chamber. The last level of integration was done at BASD for the incoming delivery Bench Test. This test was executed in accordance with the above Spacecraft Integration Test Plan.

2.3.2.2 AFGL-701-13-1 Activity

Engineering support was provide for the testing, calibration and integration of the Fluxgate Magnetometer manufactured by Schonstedt Instrument Company. Support was provided in calibrating the Fluxgate Magnetometer analog outputs at Schonstedt. Support was also provided at NASA - GSFC on two different occasions in calibrating the instrument through the Langmuir Probe instrument. Other support included acceptance and life thermal testing with the Langmuir Probe instrument. Technical support was provided in the setup of a magnetometer test facility.

2.3.2.3 AFGL-701-14 Activity

The Langmuir Probe instrument consists of five units which are as follows: 1) Electronics Package, AFGL-701-14A; 2) DC Preamplifier, AFGL-701-14B; 3) DC Preamplifier, AFGL-701-14C; 4) Wire Boom Assembly, AFGL-701-14D; and 5) Wire Boom Assembly, AFGL-701-14E. The preamplifiers were fabricated by NASA - GSFC and the wire booms were fabricated by Weitzmann Consulting. The development of AFGL-701-14A Electronics Package hardware was the primary CRRES-225 responsibility of this contract. Software for the package was done under another AFGL contract

at the University of California at Berkeley (UCB). Development responsibility included debugging and breadboard testing at UCB. After the breadboard stage, design review meetings were attended to establish specifications for the prototype and flight units. After the prototype unit fabrication, assistance was provided in debugging the prototype unit at UCB. At the prototype stage, several analog and digital circuit design changes were completed before fabricating the flight unit. Testing support was provided at UCB for the flight unit after it was fabricated. Other engineering support was provided during acceptance testing and burn-in at AFGL. Final calibration of the AFGL-701-14 instrument was supported at UCB.

2.4 BERT-I

2.4.1 Overview

The purpose of the BERT-I program (Beamed Emission Rocket Test) was to study the VLF wave spectra detected by a separable payload during continuous electron beam emissions from a launched vehicle. The observations included broadband turbulence attributed to a plasma cloud formed through beam ionization of ambient neutrals; electrostatic waves that vary with plasma density with frequency separations of approximately twice the hydrogen gyrofrequency; and electromagnetic modes near even harmonics of the hydrogen cyclotron frequency. The vehicle used for the study was a rocket which consisted of two separate payloads. The main body of the rocket, BERT, contained the electron beam emitter, and a separable nosecone, ERNIE (Ejected Rocket Nosecone to measure Induced Emission), was instrumented plasma diagnostics. The ERNIE payload

hardware consisted of an electric field instrument which used a 3 meter tip-to-tip dipole antenna, a search coil magnetometer and a Langmuir Probe instrument.

2.4.2 Activity

Provided engineering for design, development, calibration, integration and field support of a Langmuir Probe instrument for the ERNIE payload. Also supported the electric field instrument at integration and launch. The Langmuir Probe instrument was designed to operate in two modes, a swept bias mode to obtain measurements of plasma density and temperature, and vehicle potential, and a fixed bias mode to measure electron density fluctuations from 50 H_z to 7 kH_z. This instrument consists of two parts: 1) Electron Probe and 2) Electronics Package. Figure 2-7 is a block diagram of the Langmuir Probe instrument and it also shows an outline of the two modes (sweep and fixed bias). The Electron Sensor consisted of an outer gridded sphere with an inner solid sphere. When the outer grid was swept, this enabled the inner sphere to collect electrons for determining electron density and temperature, and vehicle potential. In the fixed bias mode, the electrons were used for determining the electron density irregularities. The Electron Sensor current was fed into data processing circuits in the Electronics Package. The Electronics Package was divided into two separate sections: 1) analog circuitry and 2) digital circuitry. The analog design consisted of an log electrometer, level shifter, sweep generator and monitor circuits as shown in Figure 2-8. The digital design consisted of a sequence timer and sweep control circuits as shown in Figure 2-9.

After the Langmuir Probe design was completed and the engineering drawings were drawn, AFGL fabricated the flight hardware. The flight instrument was then debugged and tested to design specifications. Following this, the instrument was burned-in and calibrated at AFGL. Engineering support was provided during integration at AFGL, at NASA's thermal/vacuum facility in Houston and at White Sands Missile Range (WSMR). Support was also provided at WSMR at launch which was 14 JUN 85.

2.5 Shuttle - IMPS

2.5.1 IMPS Overview

The Interactions Measurement Payload for Shuttle (IMPS), part of the AFGL Space Systems Environmental Interactions Technology Program, is conceived as a series of integrated payloads to be carried on low-altitude, high-inclination space shuttle flights. Each IMPS mission will measure environmental interactions and their effect on candidate elements of planned Air Force space systems. As a part of the above payload, there will be a Field and Plasma experiment whose purpose is to investigate the shuttle/environment interactions and provide background data.

2.5.2 Activity

Provided engineering support for the conceptual design of the Plasmas and Fields experiment in Figure 2-10. The block diagram is subdivided into two sections: 1) PFE and 2) PFI. The PFI section will

consist of three subsystems: 1) Langmuir Probe, 2) Spherical Probe, and 3) Search Coil Magnetometer. Hardware for the Langmuir Probe to used will be a flight spare from the ERNIE payload described in the BERT-I program section (2.3). A refurbished Spherical Probe system will be used which has previously been flown on an earlier shuttle mission which is shown in Figure 2-11. The Search Coil will be similar to the one flown on the ERNIE payload. Other engineering activities included redesigning the telemetry and command interfaces with Jet Propulsion Laboratory.

3. THE SPECIAL SENSOR FOR IONS, ELECTRONS, AND SCINTILLATION

Regis College has played a major role in the development of the Special Sensor for Ions, Electrons, and Scintillation (SSIES) for the Defense Meteorological Satellite Program (DMSP) spacecraft S8, S9, and S10. Development of SSIES began in 1979. The first DMSP satellite to carry the instrument probably will be launched in 1987. The design, fabrication, and testing of SSIES has been a joint project of the Air Force Geophysics Laboratory, Analytyx Electronics, Inc., Regis College, and the University of Texas, Dallas. Data reduction software has been developed by the Air Force Geophysics Laboratory, Bedford Research Associates, and Regis College. Regis has contributed to SSIES design and systems engineering as well as to the development of data reduction software. In addition, Regis personnel have written a technical report which will serve as a handbook for users of SSIES data.

The purpose of the SSIES is to monitor ionospheric thermal plasma parameters which can be used to predict conditions which affect Air Force communications and operations. Parameters to be measured include in situ thermal plasma densities and scale heights, plasma density fluctuations, and bulk motions of the ionospheric plasma. These parameters will be combined with other data and used as input to models which predict ionospheric effects on radio transmissions and satellite orbits.

SSIES will be flown on the Block 5D-2 Defense Meteorological

Satellite Program (DMSP) spacecraft S8 through S10. These spacecraft travel in sun-synchronous, circular polar orbits at 832 km altitude in the topside ionosphere. The SSIES instrument has three planar ion sensors which share a common ground plane, a retarding potential analyzer (RPA), a drift meter, and a total ion density trap. The instrument also includes a spherical electron Langmuir probe on a three foot boom and associated electronics for all the sensors. Figure 3-1 shows the sensors in position on a DMSP spacecraft. The ion sensor ground plane and the apertures of the three ion detectors are shown in Figure 3-2, and the Langmuir probe in Figure 3-3. Figure 3-4 is a block diagram of the instrument. It shows the four sensors and the electronics used to bias the various sensor grids, collectors, and ion sensor aperture plane.

The SSIES is designed to operate in an environment with three ion species, O^+, H^+, and He^+. O^+ predominates. At mid-latitudes, night time ion temperatures usually are of order 1000° (.086 eV) and daytime ion temperatures of order 3000° (0.26 eV). Nighttime electron temperatures are of order 1200° (0.10 eV) and daytime electron temperatures of order 3500° (0.30 eV). Typical densities range between 10^3 and 10^6 cm^{-3}. Ion and electron temperatures and densities depend on local time, latitude, and magnetospheric activity. For temperatures in the normal range, the instrument requires densities in the range 10^3 to 10^6 cm^{-3} to operate well. A density of 10^3 cm^{-3} is necessary to provide ion currents large enough to be measured by the three ion sensors, and to shield the ion apertures and the Langmuir probe from electric fields due

to spacecraft charging. Densities greater than 10^6 cause saturation of the instrument electronics. Another environmental problem is energetic electron fluxes which may reach intensities great enough to contaminate SSIES ion measurements in the auroral zone.

The SSIES is an improvement over its predecessor, the Special Sensor for Ions and Electrons (SSIE) in several respects. Unlike SSIE, SSIES will sense differences between the spacecraft potential and the plasma potential and will keep the reference potential for the Langmuir probe and the ion detector apertures close to the plasma potential. This will allow the measurement of ion and electron temperatures under a wide range of spacecraft conditions. Two of the sensors of the SSIES instrument, the drift meter and the total ion density trap or scintillation meter, are new to the DMSP satellites. SSIES, unlike SSIE, is microprocessor controlled. The microprocessor will perform onboard data reduction including calculation of the plasma potential. Because the instrument is microprocessor controlled, it has a wide selection of operating modes appropriate to different ionospheric and spacecraft conditions.

The data from the different SSIES sensors are used to determine different plasma parameters. The RPA measures ion current as a function of retarding voltage. RPA measurements are used to determine the densities and temperatures of different ion species, the downrange plasma drift velocity, and the spacecraft potential. The drift meter determines the ion currents to the four quadrants of its collector

plate. The differences in the magnitudes of these currents can be used to determine the components of the plasma drift velocity perpendicular to the ram direction. The drift meter has a special operating mode in which the drift velocities of light ions can be distinguished from the drift velocity of O^+, the predominant species. The scintillation meter or total ion density trap uses rapid measurements of ion current to measure small scale fluctuations of the plasma density. The Langmuir probe measures electron current as a function of voltage. Langmuir probe data are used to determine electron density and temperature and spacecraft potential.

The plasma parameters determined from SSIES data will serve as inputs for analyses of phase shifts and scintillation of radio signals and of joule heating of the atmosphere. The in situ plasma density and scale height determined from SSIES data, together with other data sources which describe the lower ionosphere, will be used to determine total ionospheric electron content (TEC) on an operational basis. The TEC determines the phase delay of radio signals. Density fluctuations near the peak density regions of the E and F layers cause scintillation of radio signals. SSIES measurements of density fluctuations at 832 km altitude can be related to these fluctuations at lower altitudes. Joule heating of the atmosphere causes increased drag on satellites. The volume rate of joule heating is a function of the electric field and ionospheric conductivity. The electric field is proportional to the ion drift velocity, measured by SSIES. Electrostatic analyzer measurements of precipitating particle fluxes made by another DMSP sensor, the SSJ/4,

will be used as inputs to conductivity models. Thus, the SSIES and SSJ/4 measurements will be combined to calculate the rate of Joule heating of the lower ionosphere by currents driven by forces from the magnetosphere.

SSIES data will be received at Air Force Global Weather Central (AFGWC), Offutt AFB, NE, within minutes of being transmitted from a DMSP satellite to a remote tracking site. AFGWC will process the raw data and will routinely use the resulting information to support Air Force operations. Once a day the raw data received by AFGWC will be dumped to magnetic tape for shipment to the Air Force Geophysics Laboratory (AFGL) for climatological and scientific studies. AFGL processing of the raw data will take place in two phases: In Phase I the raw data will be read, sorted by satellite, time-ordered, and copied onto local magnetic tapes. In Phase II the edited raw data will be read from the local tapes and data from each sensor analyzed to find the geophysical parameters described above. Figure 3-5 contains a diagram of the data processing steps, from the receipt of the data tapes to the final output.

The geophysical parameters calculated from the SSIES raw data in Phase II of the processing will be accumulated to form a scientific database of ionospheric plasma parameters stored on magnetic tape. These parameters will be plotted on microfiche on a routine basis. Quantities to be plotted include: From the drift meter, the components of the drift velocity perpendicular to the satellite's velocity, and an

initial computation of the electric fields and along-track potential from the drifts. From the scintillation meter, total ion density and power from the various filters. From the RPA, density of the different ion species, ion temperature, aperture potential, spacecraft potential, and downrange drift velocity. From the Langmuir probe, electron temperature and density and spacecraft potential. In addition, the perpendicular components of the drift velocity and electric field and the integrated cross-polar cap potential will be plotted in geomagnetic polar coordinates. An interactive, menu-driven analysis program will be available so that short periods of the SSIES database can be examined in more detail. A summary of the Phase II processing is shown in Figure 3-6. The algorithms used are described in two reports prepared under this contract (Publications 1 and 12).

Data from the SSIES data base and a technical report which explains the SSIES instrument and data will be available to investigators outside AFGL (Publication 12). Thus the SSIES data set will be a valuable resource for the community of scientists studying the ionosphere.

4. DMSP DATA REDUCTION

Regis College has developed software for the processing of DMSP science data as a part of the work done on this contract. Additionally, Regis College personnel managed the routine processing of the DMSP data through production runs. A significant fraction of the resources allocated to this contract is required just for this routine processing of the DMSP data. A brief description of this work is contained in this section.

Production data reduction runs were done on Ion/Electron data from DMSP satellites F6 and F7, using software provided by Bedford Research Associates. Raw data were merged onto tapes DM1200 through DM1460, with the exception of Phase I files (15 days worth) which were saved onto tapes DM1275 through DM1322 and DM1467 through DM1538. These single-file tapes are also backed up on multiple-file CC tapes.

Programs have been written to process the DMSP F7 magnetometer data. The main magnetometer program, called SSMPLOT, began as a very basic program which did interactive screen plots. It has been expanded into a large program with many functions, through many updates, revisions, and enhancements.

The basic SSMPLOT program was initially coded so that the output could be directed to the CRT screen, onto paper, or onto microfiche. This program processed all latitudes and plotted uncorrected data, which shows interference to the magnetic field measurements from the spacecraft transmitter and the electric motors on the gyro wheels.

The following routines were then added to the main program (described in the approximate order in which they were written and tested):

1. Logic to remove "gyro" jumps. The subroutine is called JMPLGC. These jumps can be detected because of their large size, in the range of +/- 1500 nT. Figure 4-1 shows a plot of magnetometer data with gyro jumps and Figure 4-2 shows the same data with the jumps removed.

2. Code to process polar data only. This is not controlled by a switch. The code resides in the main driver and it reduces all input to data that crosses the poles from +/- 47.0 degrees. NOTE: The Bedford Research program which prepares data as input to the plotting program has a switch on it so that it prepares all latitudes (if switch = 0) or selects out polar latitudes (if switch = 1).

3. A routine called ROTATE, to rotate from Spacecraft coordinates into geomagnetic coordinates.

4. A routine to plot the magnitude of $\sqrt{dB_y^2 + dB_z^2}$ on a rectangular frame (if IFLGCR = 0) or plot the same information with a circular representation (if IFLGCR = 1), which shows the path of the satellite across the pole.

5. Code to save the frame information on a file called TAPE1.

This is on a switch called IFILESW. The files were saved beginning with January, 1984, after it was felt that the routines which correct the interference were working fairly well.

6. A routine called CALCSZA, to calculate the time where the satellite goes from dark to sunlight or from sunlight to dark. A Z is plotted at the correct time on the baseline of the plot to represent the change in solar zenith angle.

7. Subroutine PICK, which takes the data (TAPE8) as received from the Bedford Research Associates routines and prepares it for the more important calculations in the program. Dr. Robert Langel (NASA/GSFC) contributed information on an accurate spacecraft background magnetic field and matrix rotation. PICK works as follows:
   a. Fills in missing seconds of data if there are less than 60 per minute.
   b. Puts it through a matrix conversion to take out the tendency of the data to "bow".
   c. Removes the spacecraft background for each vector.

8. A subroutine called SMOOTH which brings back into line the anomalies created when a certain spacecraft transmitter goes on. These jumps are in the range of 100 to 300 nT, and up until now have always occurred in the northern hemisphere.

9. A subroutine called SMOOY, which handles small but consistent anomalies which occur regularly in the northern hemisphere. The code pulls 3 to 5 minutes of Y-vector back into line. Figures 4-3 and 4-4 show an example of the magnetometer measurements before and after the corrections which are made by the subroutines SMOOTH and SMOOY.

The normal output from the routine processing of DMSP magnetometer data consists of files which are written using an unformatted write. However, requests for the data are often received from other installations. For that contingency there is a small program called CONVERT which takes an unformatted file as input and writes it as formatted output. The data which are converted are as follows:

```
A. IE     -  NUMBER OF EPHEMERIS FOR THAT RECORD

B. IDAY   -  JULIAN DAY

C. IYR    -  YEAR

D. DBR    -  AN ARRAY WITH THE STRUCTURE DBR(I,J,K)
             WHERE I VARIES WITH THE X,Y,Z COMPONENT
             WHERE J IS THE 60 SECONDS PER MINUTE
             WHERE K IS THE MINUTE ( 1 THROUGH 25 )

E. EPHH   -  NAMED COMMON, CONTAINING THE "IE" OF THE FOLLOWING:
             IETIME  - TIME IN SEC OF THAT MINUTE
             GLAT    - GEOGRAPHIC LATITUDE
             GLONG   - GEOGRAPHIC LONGITUDE
             GMLAT   - CORRECTED GEOMAGNETIC LATITUDE
                       TRACED FROM SATELLITE TO 110 KM. ALT
             GMLONG  - GEOMAGNETIC LONGITUDE
             XMLT    - LOCAL TIME
             NS      - NUMBER OF SECONDS OF DATA IN EACH MIN
             TIME    - IETIME IN SECONDS (ONLY REAL)
             ALT     - ALTITUDE
```

F. BMS - MODEL FIELD FOR EACH MINUTE

There are other programs associated with the magnetometer data which use as input the unformatted output files from the initial processing and plot it in different ways. FITGAP is a color plotting program which uses the output data from one day produce two plots. All northern hemisphere polar passes and all southern hemisphere polar passes from the one day are shown on each of the two graphs. The data for individual passes are lined up from left to right in the correct time column. The data points are detrended and then averaged five at a time. A color index is assigned to each five-point average and it is plotted as a solid horizontal line. Figure 4-5 shows an example of FITGAP output, using data from June 28, 1984.

CIRPLT is another color plotting program which uses the pre-processed data as input. This program has an option to select the pass or passes contained on one plot by entering the time span. The output consists of color-coded magnetic field measurements plotted on the spacecraft's path in polar coordinates. An example is shown in Figure 4-6.

5. DMSP TOPSIDE IONOSPHERE PLASMA DENSITY MODEL

Ground-based studies of the ionospheric density have been frequent over the past half century. However, such studies are inherently limited to altitudes below the layer of maximum electron density (characterized by plasma frequency f_0F_2) at approximately 325 to 475 km. Higher altitudes are best studied through the use of satellite data and incoherent scatter radar. Existing empirical models of plasma density are biased towards ground measurements. These yield an adequate description of the bottomside ionosphere. However, though there are a number of papers describing satellite measurements of plasma density in the topside ionosphere, there was a need for a comprehensive study of plasma density structures in this region for wide spans of latitude, longitude, and season.

Using data from the topside ionosphere plasma monitor (SSIE) on the Defense Meteorological Satellite Program (DMSP) F2 and F4 spacecraft, it was decided by AFGL to do a statistical study of plasma density covering all latitudes, longitudes, and seasons for 1979. Regis College developed the software and processed the data for this statistical study. A summary of this work is contained here.

Density data were compiled for the period from January 1 to December 31, 1979. This represents 12 months of F2 data and 6 months of F4 data. The database consists of log base 10 of the density averaged over each 5-second period and the root-mean-square of the density for the same period. This data along with time and ephemeris information

were saved on tape for further processing. Due to problems with the spacecraft being driven to negative potentials, most of the electron data was not usable. (Ion density measurements are not affected by spacecraft potential.) 322 of the 365 possible days were in a form suitable for use in this survey.

The data currently exists on 8 tapes: M1536, M1538, M1540, M1542, M1544, M1546, M1548, and M1739. These are nine-track, 1600 bpi tapes saved under the Control Data Corporation NOS-2 operating system. Each tape consists of multiple files - one file contains one day of data. Each file contains a series of records beginning with a header record followed by a data record. This sequence continues until an EOF mark is reached. A header consists of the following CDC INTEGER values:

(a) satellite number,

(b) revolution number,

(c) day of the month,

(d) month,

(e) year,

and (f) number of data sets in the upcoming data record. A data record contains a series of 7-item data sets. The items are stored as CDC REAL numbers and represent:

(a) universal time (UT),

(b) log base 10 of the density,

(c) magnetic local time,

(d) magnetic latitude,

(e) geographic latitude,

(f) geographic longitude,

and (g) root-mean-square (rms) of log base 10 of the density. Geographic coordinates correspond to the subsatellite point; magnetic coordinates are given in the corrected geomagnetic coordinate system of Gustafsson[1], referred to the sub-satellite point.

A set of statistical bins were then created from these tapes. Only data items with rms less than a given value were placed into the bins. The data were originally sorted into bins representing (a) 3 degrees of latitude, (b) 60 degrees of longitude, (c) 3 months of the year, (d) 0.25 hours magnetic local time, and (e) each satellite. This resulted in 60 by 6 by 4 by 96 by 2 bins. Afterwards, it was concluded that magnetic local time did not vary enough to justify 96 divisions, while 4 divisions were not enough to adequately describe the seasonal variation. Thus, we repeated our survey using bins representing (a) 30 degrees of latitude, (b) 60 degrees of longitude, (c) 9 or 10 days, (d) AM or PM magnetic local time, and (e) each satellite, resulting in 60 by 6 by 40 by 2 by 2 bins.

To study median plasma density, the following criteria were used to decide whether a value should be placed in a bin:

rms $\leq$ 0.02 for -30 to +30 degrees latitude,

rms $\leq$ 0.10 for -60 to -30 and
+30 to +60 degrees latitude,

and rms $\leq$ 0.50 for -90 to -60 and
+60 to +90 degrees latitude.

---

[1]Gustafsson, G., A revised corrected geomagnetic coordinate system, Arkiv fur Geophysik, 5, 595-616, 1970.

Various operations were then performed on the binned data. First, contour plots and color plots were produced displaying the average density as a function of: latitude and longitude, latitude and season, and season and longitude. These were done for both AM and PM magnetic local time. In each case the other parameters were simply summed. It was concluded that variations in longitude were not significant, leaving us with the 2 plots represented by Figures 5-1 and 5-2. Next, the measured median density was compared with the density from previous models. Finally, the large matrices of numbers used to generate Figures 5-1 and 5-2 were fitted to a polynomial in order to give a statistical model of plasma density based on this data. The results of this polynomial fit are contained in a report published by AFGL[2].

To study low and mid-latitude plasma density irregularities the criteria of the rms being greater than 0.02 was used. This yielded a collection of "irregular" plasma measurements which were then arranged by season, geographic longitude, and magnetic latitude. This basically shows the probability of encountering irregular plasma at any given time and location. The irregular plasma can in turn be related to degradation of radio propagation.

---

[2]Rich, F. J. and M. Smiddy, Plasma Densities and Irregularities at 830 km altitude based on observations during 1979, AFGL-TR-86-0121, ERP No. 955, ADA172118, 1986.

6. HILAT MEASUREMENTS OF PLASMA IRREGULARITIES

6.1 Introduction

The objective of this research was to study high-latitude plasma irregularities using measurements of physical parameters obtained from the High Latitude (HILAT) satellite. Topics to be studied were the production, transport, and lifetime of plasma irregularities.

HILAT was launched on June 27, 1983 with a complement of five experiments, with the intent to probe irregularities in the ionospheric plasma which produce radio wave scintillation. The five instruments are a coherent radio beacon, plasma monitor, vector magnetometer, electron spectrometer, and auroral ionospheric mapper. The satellite orbit is nearly circular at an altitude of 820 km and 82° inclination. Data are collected by means of real-time transmissions to high-latitude ground stations. The three primary stations are located at Tromso, Norway; Sondre Stromfjord, Greenland; and Churchill, Manitoba.

The work done on this contract has been focused primarily on the data from the plasma monitor, which includes measurements of plasma density from a Retarding Potential Analyzer (RPA) and measurements of plasma drift velocity (due to electric fields) from an Ion Drift Meter (IDM). The results of this work are described in the following two sections. In the first section the description of the work is rather detailed, as this work currently has not been published elsewhere.

6.2 Large-Scale Plasma Density Irregularities

6.2.1 Overview

Irregularities in the Earth's ionospheric plasma occur on scales ranging from hundreds of kilometers down to centimeters. At intermediate (kilometer) and small (meter) scales plasma instability processes are assumed to be responsible for creating the structure in the plasma perpendicular to magnetic field lines. At large scales (tens to hundreds of kilometers) the variations are governed by plasma production, decay, and transport processes. Although the small-scale structure is responsible for radio wave scintillations, the plasma instabilities which occur on large-scale plasma gradients couple the different scale-length regimes.

In order to understand the high-latitude F-region plasma structure on a global basis it is necessary to determine when and where the irregularities are produced, how long they last, and how they are transported by plasma convection.[3] An example of a theoretical study on this topic is the paper by Kelley et al.[4], in which production, decay, and convection models are combined to produce a map of irregularity amplitudes. The intent of the work described here is to provide experimental observations to complement the theoretical works.

---

[3]Vickrey, J.F., On the Morphology of Plasma Density Irregularities in the Auroral F-Region, topical report for period 15 Jan 1981 - 15 Mar 1982, contract DNA001-81-C-0076, SRI International, Menlo Park, CA, 1982.

[4]Kelley, M. C., J. F. Vickrey, C. W. Carlson, and R. Torbert, On the Origin and Spatial Extent of High-Latitude F Region Irregularities, J. Geophys. Res., 87, 4469-4475, 1982.

6.2.2 Experimental Procedure

Plasma ion densities are measured by the RPA on HILAT at a frequency of 1.5 Hz, or one sample every 2/3 second. This corresponds to a spatial sampling interval of about 5 km, so due to instrumental constraints the small-scale density structure cannot be probed directly with HILAT. We concentrate, instead, on the large-scale ionization enhancements, referred to loosely as "blobs".

The first step in the analysis was to filter the data into three frequency bands. Figure 6-1 is an example of the result of this filtering. The top graph shows the original density measurements; the bottom three traces show the signals which are output from a low-pass filter, a medium-frequency band-pass filter, and a high-pass filter. To serve as a frame of reference, measurements of plasma drift velocity from the IDM are similarly filtered, as shown in Figure 6-2. Although the drift velocity is originally sampled at a much higher rate (32 Hz and 16 Hz) than the density measurements, for the purpose of this comparison the data had been averaged and decimated to obtain a signal which is sampled at a frequency of 2 Hz.

The filtering of the RPA and IDM data was accomplished by a Fourier transform, followed by a multiplication by a window function in the frequency domain and an inverse Fourier transform back to the time domain. Hanning-type window functions were used for the filtering since rectangular windows, which have sharp cut-offs, result in distortion and "ringing" in the filtered signal. For the low-pass filter the amplitude response is :

$$A_1(f) = \frac{1}{2}\left\{1 + \cos\frac{\pi f}{2f_1}\right\} \qquad 0 \leq f \leq 2f_1$$

$$A_1(f) = 0 \qquad 2f_1 \leq f \leq f_N$$

where f_1 is the "cut-off" frequency where the amplitude response is 1/2 and f_N is the Nyquist frequency (one-half the sample frequency). The high-pass filter amplitude response is:

$$A_3(f) = 0 \qquad 0 \leq f \leq f_2$$

$$A_3(f) = \frac{1}{2}\left\{1 - \cos\frac{\pi(f-f_2)}{2(f_3-f_2)}\right\} \qquad f_2 \leq f \leq (2f_3 - f_2)$$

$$A_3(f) = 1 \qquad (2f_3 - f_2) \leq f \leq f_N$$

where f_3 is the high-pass cut-off frequency. The medium-frequency band-pass filter is the complement of the other two filters:

$$A_2(f) = \frac{1}{2}\left\{1 - \cos\frac{\pi f}{2f_1}\right\} \qquad 0 \leq f \leq 2f_1$$

$$A_2(f) = 1 \qquad 2f_1 \leq f \leq f_2$$

$$A_2(f) = \frac{1}{2}\left\{1 + \cos\frac{\pi(f-f_2)}{2(f_3-f_2)}\right\} \qquad f_2 \leq f \leq (2f_3 - f_2)$$

$$A_2(f) = 0 \qquad (2f_3 - f_2) \leq f \leq f_N$$

Frequencies of 0.03 Hz, 0.06 Hz, and 0.15 Hz were used for f_1, f_2, and f_3. The time periods for the lower and upper cut-offs are 33.33 and 6.66 seconds, corresponding to spatial wavelengths of 250 km and 50 km. This choice of frequencies appears to separate the data into phenomenally distinct regimes.

Following the digital filtering, the medium-frequency signals were

used in a statistical survey of plasma "blob" formation and transport. A simple computer program was used to count density enhancements. The medium-frequency signals, which have a zero baseline, were scanned to find negative to positive zero-crossings which mark the beginning of blobs, and the next positive to negative transitions which mark the ends. The separation between these points indicates the size, and the largest point in between indicates the magnitude.

For every blob detected a record was made of it's size, magnitude, magnetic local time, invariant latitude, and the magnetic activity index (K_p) for the time of the data record. For the last three parameters only integer "bin" indices were actually recorded. The magnetic local time is separated into 24 bins, each an hour wide and centered on the hour. The invariant latitude is divided into 16 bins, each 2.5° wide, spanning the range from 50° to 90°. The magnetic activity is divided into only two bins: low activity (K_p=0 to 3+) and high activity (K_p= 4- to 9).

For this study the HILAT RPA density measurements and the IDM drift velocity measurements were both processed in this manner; the drift velocity variations serve as a reference for the density variations, as they indicate where there are electric fields and current fluctuations. The analysis was conducted on all data from the Sondre Stromfjord and Tromso stations, for the period in 1984 from the spring equinox to the fall equinox (days 121 to 225). At other times of the year the night-time plasma density may drop below 10^3 cm^{-3}, at which point the plasma instrument data are unreliable. In all, 1583 station passes were analyzed, each containing 8 to 12 minutes of data.

The distributions of the data in MLT-invariant latitude for low and high activity are illustrated in Figures 6-3 and 6-4. The scale indicates the total number of density data samples which were obtained in each bin. For instance, there were 8203 samples (the largest) taken in one bin, corresponding to about 91 minutes. There was considerably less data obtained under conditions of high activity; the bin with the most counts had only 2987 samples, or 33 minutes. A few bins below 60^{o} latitude had no data, as indicated in black.

The total number of density enhancements which were counted was 42,149 for low activity and 15,104 for high activity. Plots of the distribution of all enhancements, however, result in a somewhat random distribution with a tendency for a higher number at the low-latitude dayside and less in the nightside. But if only the enhancements with a magnitude greater than 10^3 cm^{-3} are counted (reducing the numbers to 17,704 and 7,877) then definite patterns emerge, as shown in Figures 6-5 and 6-6. These data had been normalized by dividing the blob counts for each bin by the total time spent by HILAT in that bin and multiplying by the largest bin time. The bin with the most samples has the lowest normalization factor, equal to one. The resulting scale is an indication of the number of density enhancements counted per 91 minutes of data.

The practice of selecting blobs on the basis of magnitude tends to favor those on the dayside where the background density is higher. As an alternative to measuring the absolute magnitude of the density enhancements, the relative magnitude ($\delta n/n_o$) may be measured instead. The same procedure as before was followed in which the enhancements were

counted by detecting the zero-crossings of the medium-frequency filter output. But the peak magnitudes were then divided by the background plasma density, as determined from the low-pass filter output. (As DC offsets and linear trends were subtracted from the signals before doing the initial Fourier transforms, these offsets were added back on to the low-frequency data to get the background density.) Figures 6-7 and 6-8 show the results of selecting enhancements with $\delta n/n_0$ greater than 0.1. The total number selected by this criteria was 5,073 for low activity and 2,883 for high activity.

The reference plots with the maps of drift velocity fluctuations are shown in Figures 6-9 and 6-10. Only velocity fluctuations with magnitudes greater than 0.05 km/sec were selected for these plots. At the typical HILAT altitude and auroral latitude this corresponds to electric field variations greater than 2 mV/m.

6.2.3 Discussion of Results

The data shown here confirm the generally held belief that large-scale plasma enhancements are created in the auroral zone and are transported away from the production zone by convection. In Figures 6-5 and 6-6 there are seen distinct areas where "blobs" are produced on the dayside between 8 and 19 hours MLT. The cusp regions are especially prominent. In the high and low activity cases the low-latitude boundary of the blobs is co-located with the low-latitude boundary of the velocity fluctuations in the corresponding figures (6-10 and 6-11). However, whereas the velocity (electric field) fluctuations show a well-defined auroral oval, the density variations extend into the polar cap

where there are no corresponding electric field fluctuations. The pattern of the enhancements in the polar cap and towards the nightside is consistent with the transport of the plasma by the conventional two-cell plasma convection pattern, with anti-sunward flow over the polar cap.

The nightside auroral zone does not appear very prominently on Figures 6-5 and 6-6, in which the data were selected according to the absolute magnitude of the plasma enhancements. However, in Figures 6-7 and 6-8, where the data were selected by relative magnitude, the variations in the nightside are more prominent. Figure 6-7 shows a particularly interesting band, from 23 to 4 hours MLT, which is located on the southern edge of a similar band shown in Figure 6-9. There is a definite tendency to find more blobs in the midnight to dawn region than in the pre-midnight region. The data below 60° latitude must be treated with some suspicion due to lower sampling times. Further analysis on these data is currently in progress in order to produce a paper for publication.

6.3 Small-scale Drift Velocity Variations

The Ion Drift Meter has the capability to measure cross-track ion drifts (north-south electric fields) at a sampling rate of 32 Hz. This corresponds to a spatial scale-size of about 0.45 km. Unfortunately HILAT does not have the capability to measure in situ plasma density at a similar scale, although plasma below HILAT structured on a much smaller scale can be probed with the radio beacon.

Computer software was developed in order to do spectral analysis of

the IDM data, using the Maximum Entropy Method (MEM). Each spectrum would cover four seconds of data (128 points), as this is the period for which the IDM does a continuous measurement of the cross-track ion velocity at the full 32 Hz rate. The spectra are spaced apart in time by eight seconds. From each MEM spectrum the integrated power and spectral slope are calculated. Figure 6-11 shows the power and spectral slope as a function of time for a satellite pass on day 71 of 1984. For reference, half-second averages of the drift velocity and its slope are shown in Figure 6-12.

These are were used in collaboration with other researchers working on the HILAT project but on other contracts at other institutions. In Publication 5 it is shown that there are intense radio scintillations associated with the regions of structured velocity shown in Figures 6-11 and 6-12. At the same time large-scale density gradients were not present. Thus it was concluded that there are classes of scintillation-producing irregularities which are associated with velocity shears rather than the more traditional gradient-drift instability.

6.4 Dayside Cusp Processes

The regions near the dayside cusp are characterized by rather complex physical processes. From a dynamic point of view, the cusp is the focal point for the solar wind/magnetosphere coupling. Within the cusp/cleft region the latitudinal overlaps of the evening and morning convection cells produce a channeling effect in the appearance of the flow pattern. Not only does the noon sector contain part of the large-scale Region 1/Region 2 field-aligned current (FAC) systems, but it also

contains a distinctive cusp FAC[5]. Intense small-scale variations are observed in cusp electron precipitation[6,7], electric fields[8] and FAC's[9]. Each of these sources may provide free energy for generating the density irregularities in the F layer of the ionosphere that give rise to radio scintillations.

The results of a study of plasma and field measurements made with the instruments on board the HILAT satellite while the satellite was crossing the northern polar cusp region on December 2, 1983 are presented in Publication 10. Figure 6-13 presents the overview of large scale measurements: the ion density of ambient plasma, the east-west component of the ion drift velocity and deflections in the east-west component of the magnetic field due to the field aligned currents. During the time period of these measurements we observed an increase in scintillations of radio signals and strongly variable fluxes of precipitating low-energy electrons. In the region corresponding to the highest level of

---

[5]Iijima, T. and T. A. Potemra, Field-aligned currents in the dayside cusp observed by Triad, J. Geophys. Res., 81, 5971, 1976.

[6]Gussenhoven, M.S., D. A. Hardy, and R. L. Carovillano, Average electron precipitation in the polar cusps, cleft and polar cap, in The Polar Cusp, ed. by J.A. Holtet and A. Egeland, Reidel Publ. Co., Dordrecht, p. 85-97, 1985.

[7]Hardy, D.A., M. S. Gussenhoven, and E. Holeman, A statistical model of auroral particle precipitation, J. Geophys. Res., 90, 4229, 1985.

[8]Maynard, N.C., Structure in the DC and AC electric fields associated with the dayside cusp region, in The Polar Cusp, ed. by J.A. Holtet and E. Egeland, D. Reidel Publishing Co., Dordrecht, p. 305-322, 1985.

[9]Doyle, M.A., F. J. Rich, W. J. Burke, and M. Smiddy, Field aligned currents and electric fields observed in the region of the dayside cusp, J. Geophys. Res., 86, 5656, 1981.

radio scintillations we also detected fluctuations in electron fluxes on a time scale of half a second superimposed on a low-energy inverted-V event. The analysis of these measurements which provide information on both large and small scale dynamics of the dayside cusp led to the following conclusions: (1) the large scale convection pattern is characteristic for the northern hemisphere high latitude ionosphere when the interplanetary magnetic field has negative Y and Z components; (2) the most intense scintillations and the cusp field aligned currents occur on recently opened magnetic field lines; (3) plasma created by increased fluxes of precipitating low-energy electrons convects antisunward with a velocity of about 0.5 km/sec (local maxima in the ion density measured at 830 km and in the total electron content (TEC) estimated from the dispersion of radio signals are shifted relative to each other by approximately 2 degrees in invariant latitude - see Figure 6-14); (4) enhanced chemical reactions due to the Joule heating associated with large electric fields maximize at the equatorward edge of the cusp leading to the net depletion in TEC and plasma density (see Figure 6-13 and 6-14); (5) plasma irregularities throughout the F region are formed due to the combined effect of structured soft electron precipitation and current-convective instabilities; (6) if the sub-second fluctuations of the ion drift measurements, coincident with similar modulations of electron fluxes (see Figure 6-15), are due to static variations in the ambient electric field, there are potential drops of a few tens of volts between the altitude of the satellite (approximately 830 km) and the lower ionosphere.

The coincident appearance of 2 and 4 Hz modulations in data from the electron spectrometer and the ion drift meter raise the problem of the possible contamination of the ion measurements by the high electron fluxes. In our case after careful examination of data from both instruments we concluded that the electron contamination alone cannot explain variations of the signal seen by the ion drift meter and thus the modulations in the ion flow reflect changes in the geophysical environment. However, one should be careful in interpretation of data obtained with this instrument, especially under conditions of high electron fluxes and low ion density.

7. AURORAL ELECTRODYNAMICS

During the course of this contract, Regis College has conducted research in the area of auroral electrodynamics. This subject deals with the relationships between auroral currents, electric fields, and the conducting ionosphere. An understanding of the basic physical processes is useful in order to understand the production of large-scale plasma irregularities in the auroral zone. The primary justification for this effort, however, is that the Air Force has recently become interested in calculating the rate of joule heating in the ionosphere due to auroral currents.

In a paper by Doyle et al. (Publication 7), HILAT data were used in order to compare measured values of the electric field (as determined from IDM data) with calculated values. The calculated values were obtained from a mathematical model which took as input the field-aligned current and the ionospheric conductivity, which were estimated from HILAT measurements of the magnetic field and electron precipitation. Figure 7-1 shows the result of this comparison. In the top panel of this figure the measured electric field (solid line) is overlaid with the calculated values (dashed line), where the calculation was done by a step-wise numerical technique. The second panel shows the same type of comparison, but this time the calculation was based on functional representations of the magnetic field and ionospheric conductivity. The difference between the measured values and the functional representations are shown in the bottom two panels.

The results shown in Figure 7-1 indicate that the large-scale

features are well mapped, while the small-scale features equatorward of the primary precipitation zone are underestimated. The total ionospheric joule heating calculated along the satellite trajectory was found to exceed the particle energy deposition by a factor of 2.6. Further details about this study may be found in Publication 7.

At altitudes above the auroral acceleration region the relationship between the electric and magnetic fields takes a form which is entirely different from that found just above the ionosphere. This is the topic of a study published by Weimer et al. (Publications 6 and 9), using data from the Dynamics Explorer 1 (DE-1) satellite. At small spatial scale-lengths the high-altitude electric field is determined by the gradient of the high-altitude potential, which is proportional to the field-aligned current density. The verification for this is shown in Figure 7-2. The top panel shows the north-south electric field measured on DE-1, which was moving in the north-south direction. The second panel shows the potential derived by integration of the electric field. This potential is assumed to be proportional to the field-aligned current, which when integrated and multiplied by the appropriate constants results in a model of the magnetic field, shown in the third panel. There is a very close match with the measured magnetic field, shown in the bottom panel.

To summarize, at high altitude the second integral of the north-south electric field is proportional to the east-west magnetic field deviation. In contrast, at the ionosphere the electric field is directly proportional to the magnetic field (in regions of constant conductivity). Details of this theory and additional examples can be

found in Publication 9 (part of this work was funded by a NASA Grant to the University of Iowa for DE-1 data analysis). In addition, a simple numerical model has been developed which calculates and plots low- and high-altitude electric fields, given the current density as an input. This model can also handle the cases of non-uniform ionospheric conductivity and non-linear field-aligned current-voltage relations; these cases do not have simple analytic solutions. D. Weimer has written a description and shows results from this numerical model in Publication 11.

8. EISCAT/AMPTE OBSERVATIONS

During a 1 year stay at the Max-Planck Institute for Extraterrestrial Physics in Garching, West Germany Ewa Basinska-Lewin participated in the observational campaign involving the European Incoherent Radar Facility EISCAT and the AMPTE IRM (Active Magnetosphere Particle Tracer Explorer - Ion Release Module) satellite. Comprehensive descriptions of AMPTE are contained in IEEE Trans. Geosci. Remote Sensing, vol. GE-23, No. 3, May 1985; EISCAT has been described by Folkestad et al.[10]. This work was done in collaboration with Drs. Gerhard Haerendel, Wolfgang Baumjohann, Stephan Buchert of MPE and Drs. Cesar La Hoz and Peter Collis of EISCAT.

The orbital apogee (18 R_e) of the German IRM satellite, which was launched in August, 1984, precessed to the magnetotail region in the spring of 1985. The satellite measurements include a comprehensive set of particle and field parameters. When combined with simultaneous ionospheric measurements made by EISCAT the data offer a valuable opportunity to study ionospheric-magnetospheric coupling; in particular the mapping of magnetotail, plasma sheet, and plasma sheet boundary dynamics to ionospheric altitudes.

The EISCAT/AMPTE observations were performed in March/April and

[10]Folkestad, K., T. Hagfors, and S. Westerlund, EISCAT: an updated description of technical characteristics and operational capabilities, Radio Sci., 18, 867, 1983.

June/July 1985. The EISCAT measurements provided over 200 hours of incoherent scatter radar observations of the high-latitude ionosphere covering a broad range of local times from evening through midnight till morning. Approximately 80 hours of IRM measurements were taken in the near Earth magnetotail and the high latitude magnetospheric boundary layer.

While the comprehensive data analysis is still in progress, we have focused our attention on the so-called dipolarization events detected in the magnetotail by the IRM and their relationship to the existing simultaneous data sets. Dipolarization refers to the change in the direction of the magnetic field from tail-like towards a more dipolar structure. The selected data sets were obtained on March 28[11] and April 10[12], 1985. Figure 8-1 displays tracks of the IRM satellite projected down the magnetic field lines down to an altitude of 350 km for both observational periods. The ellipse corresponds to the EISCAT radar field of view, and full dots represent the locations of the EISCAT Magnetometer Cross sites. Although interpretation of the simultaneous measurements obtained during these times is not completed yet, it is evident in both data sets that dipolarizations of the magnetic field in the near-Earth magnetotail are associated with an increase of ionospheric activity observed by ground magnetometers and radars. One

[11]Luhr, H., Baumjohann, W. and Lui, A.T.Y., 1986, Dipolarizations: 28 March 1985 event, in <u>Material for AMPTE Workshop</u> to be held at MPE Garching 25 - 27 June, 1986, part I.

[12]Buchert, S., 1986, AMPTE/IRM EISCAT Correlations, in <u>Minutes of the AMPTE JSWG Meeting</u> held at MPE Garching, W. Germany, June 25 - 27, 1986.

example of such a relation is shown in the Figure 8-2. The data presented here were measured on March 28, 1985 between 20:30 and 21 hours UT. During that time there was a clear anticorrelation between satellite measurements of B_x (the magnetic field component parallel to the tail axis) and the northward component (X) of the magnetic field measured at the ground station north of Tromso. B_x is an approximate measure of the cross-field electric current, and X is proportional to the strength of the ionospheric electrojet. An anticorrelation between these two quantities indicates that a decrease of the cross-tail current is associated with an increase of the electrojet current in the ionosphere. Although there are gaps in the radar measurements during this period, one could see a clear increase in the integrated Pedersen an Hall conductivities during one of these events.

The existing IRM and EISCAT data can be compared with measurements obtained by the low orbiting satellites (HILAT and DMSP). In the preliminary examination of the HILAT data and DMSP images taken during times that EISCAT/AMPTE observations were made, several interesting passes were found. Analysis of the corresponding data sets could elucidate magnetospheric sources (based on the results of the IRM measurements) for high-latitude plasma structures and irregularities in the topside ionosphere. EISCAT incoherent scatter radar observations provide independent measurements of plasma density, electric fields, currents and precipitating particles characteristics that can be compared with the quantities provided by the instruments on board the HILAT and DMSP satellites. Furthermore the experience of working with

9. PUBLICATIONS

The following papers and publications were done in whole or part on contract FY19628-84-C-0126:

(1) Basinska, E. M., F. J. Rich, Development of software for the analysis of plasma measurements using the retarding potential analyzer, Scientific Report, Contract FY19628-84-C-0126, AFGL-TR-84-0327, 1984.

(2) Basinska, E. M., W. J. Burke, and P. F. Fougere, HILAT observations of plasma irregularities in the cusp, EOS, 65, 1040, Nov. 1984.

(3) Bythrow, P. F., M. A. Doyle, C. I. Meng, R. E. Huffman, D. A. Hardy, F. J. Rich, T. A. Potemra, and L. J. Zanetti, The Kelvin Helmholtz instability at the BPS/CPS interface: A source of small-scale Birkeland currents and auroral arcs, EOS, 65, 45, 1040, Nov. 1984.

(4) Weimer, D. R., F. J. Rich, and R. A. Heelis, Correlations between high latitude plasma drift velocity and density structures, EOS, 66, 46, 1004, Nov. 1985.

(5) Basu, S., S. Basu, C. Senior, D. Weimer, E. Nielson, and P. F. Fougere, Velocity shears and sub-km scale irregularities in the nighttime auroral F-region, Geophys. Res. Lett., 13, 1, 101-104, 1986.

(6) Weimer, D. R., D. A. Gurnett, and C. K. Goertz, The conductance of auroral magnetic field lines, in Ion Acceleration in the Magnetosphere and Ionosphere, Geophysics monograph series, Vol. 38, edited by T. Chang, p. 108-113, AGU, Washington, D.C., 1986.

(7) Doyle, M. A., W. J. Burke, D. A. Hardy, P. F. Fougere, F. J. Rich, and T. A. Potemra, A simple model of auroral electrodynamics compared with HILAT measurements, J. Geophys. Res., 91, 6979-6985, 1986.

(8) Bythrow, P. F., M. A. Doyle, T. A. Potemra, L. J. Zanetti, R. E. Huffman, C. I. Meng, D. A. Hardy, F. J. Rich, and R. A. Heelis, Multiple auroral arcs and Birkeland currents: evidence for plasma sheet boundary waves, Geophys. Res. Lett., 13, 8, 805-808, 1986.

(9) Weimer, D. R., C. K. Goertz, D. A. Gurnett, J. D. Menietti, J. L. Burch, and M. Sugiura, The current-voltage relationship in auroral current sheets, J. Geophys. Res., paper 6A8528, 1986.

(10) Basinska, E. M., W. J. Burke, S. Basu, F. J. Rich, and P. F. Fougere, Low frequency modulation of plasma and soft electron precipitation near the dayside cusp, accepted by J. Geophys. Res., 1986.

(11) Weimer, D. R., Calculation of auroral zone electric fields, submitted to J. Geophys. Res., 1986.

(12) Greenspan, M. E., P. B. Anderson, and J. M. Pelegatti, Characteristics of the Thermal Plasma Monitor (SSIES) for the Defense Meterological Satellite Program (DMSP) spacecraft S8 through S10, Scientific Report, Contract FY19628-84-C-0126, AFGL-TR-86-0227, 1986.

10. FIGURE CAPTIONS AND FIGURES

Figure 6-8 Distribution of plasma density "blobs" with $\delta n/n_o$ greater than 0.1, high activity.

Figure 6-9 Distribution of drift velocity fluctuations with magnitude greater than 0.05 km/sec, low activity.

Figure 6-10 Distribution of drift velocity fluctuations with magnitude greater than 0.05 km/sec, high activity.

Figure 6-11 Plot of integrated power and spectral slope vs. time, calculated from HILAT IDM data using Maximum Entropy Method.

Figure 6-12 Plot of HILAT IDM data for same time period as in Figure 6-11.

Figure 6-13 The HILAT satellite trajectory on December 2, 1983 presented in magnetic local time and invariant magnetic latitude. The satellite was moving towards the South. The solid line corresponds to the path of the satellite orbit, the broken line to the intersect of the HILAT beacon signal received at Sondre Stromfjord with the F region at an altitude of 350 km. The individual panels present deviation in the east-west component of the magnetic field in nT, the east-west component of the ion

drift velocity (averaged over 1 second) and the ion density (sampled every 2 seconds by the IDM).

Figure 6-14 Ion density n in ions/cm^3 (open circles) measured at 830 km and averaged over 15 seconds, total electron content TEC in units of 10^{16} electrons/m^2 (full dots) and the intensity scintillation index S_4 at 137 MHz (crosses) versus invariant latitude. Horizontal bars correspond to the range of invariant latitudes where satellite measurements indicate eastward flow of thermal plasma, increased precipitation of low-energy electrons and field-aligned currents. Total electron content is corrected for the slant angle at an altitude of 350 km and both TEC and S_4 are plotted vs invariant latitude of the F region penetration point. The location of the inverted-V structure observed by the satellite is marked by the shaded area at invariant latitudes between 76.7° and 76°. Scintillation measurements for the antenna elevation angle less than 20° are unreliable.

Figure 6-15 Three upper panels present counts detected in three energy channels of the electron spectrometer during a low-energy inverted-V event. The east-west component of the ion drift velocity is shown at the bottom panel.

Figure 7-1 Comparison of calculated and observed values of E_x when the inputs to the calculation are (top panel) measured values of ΔB_y and conductivity every 0.5 s and (second panel) functional forms of ΔB_y and conductivity. Vertical lines mark the region of the bright auroral form. The third and bottom panels compare the measured and functional forms of ΔB_y and conductivity, respectively, used in the calculation of E_x shown in the second panel.

Figure 7-2 Top graph is north-south electric field measured in the orbit plane of DE-1 on day 292 of 1981. The dark blocks above the time axis indicate where data gaps have been filled in. The second graph shows the potential obtained by integrating this electric field, and the third graph shows a model of the east-west magnetic field obtained with a second integration. At the bottom is shown the measured magnetic field.

Figure 8-1 Location of the IRM magnetic conjugate points, EISCAT Magnetometer Cross sites and EISCAT radar field of view for March 28 and April 10, 1985. Positions of the IRM footprint were calculated using Mead-Fairfield model for $K_p = 3$.

Figure 8-2 The EISCAT/IRM observations on March 28, 1985 between 20:30 and 21 hours UT. The upper panel presents satellite measurements of B_x - magnetic field component along the magnetotail axis. The northward component of the magnetic field measured by the ground station north of Tromso is shown at the second panel. Pedersen and Hall conductivities based on the radar measurements are shown at the third and fourth panel respectively.

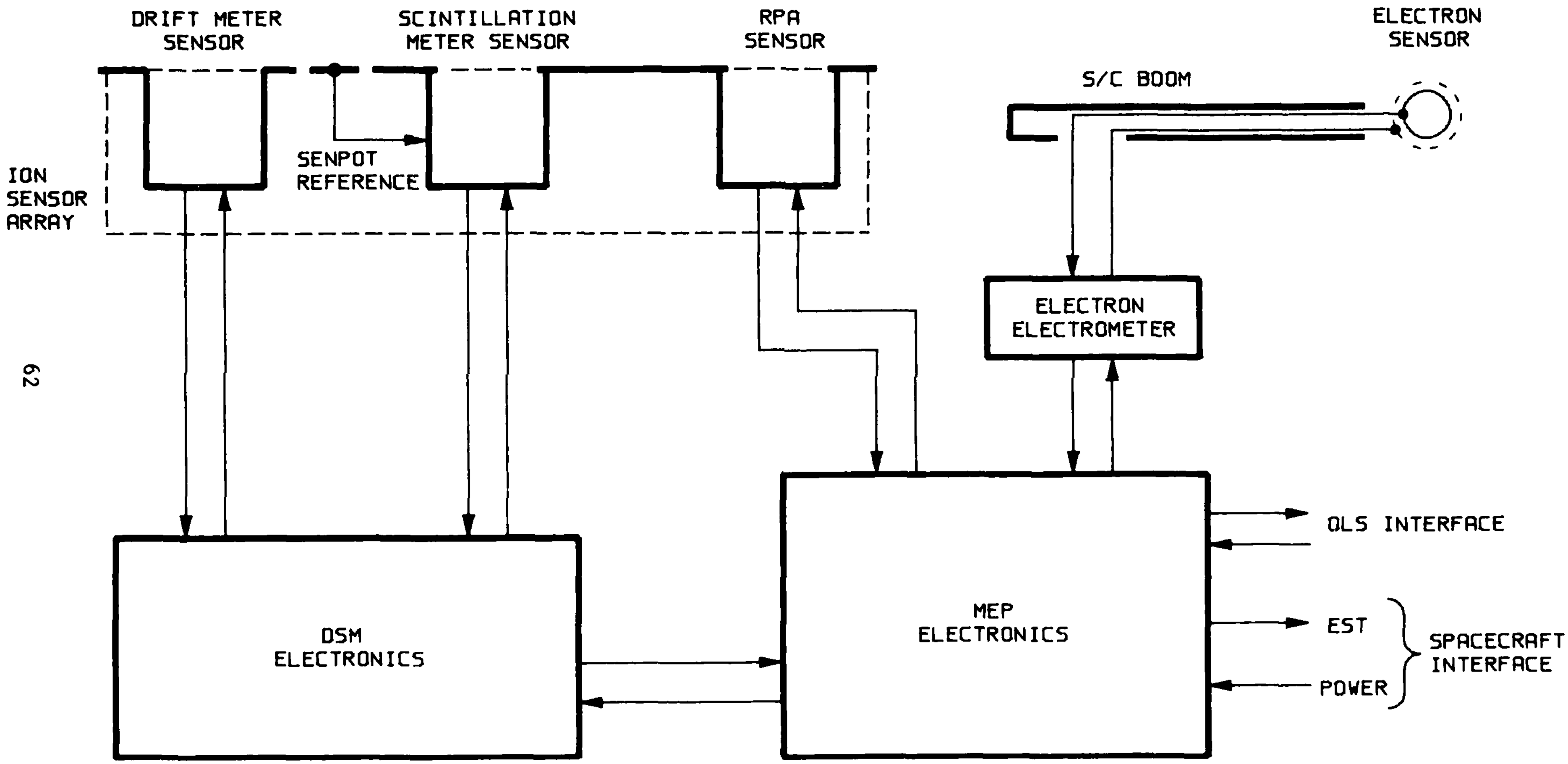

Figure 2-1
SSIES-2 MAJOR COMPONENTS

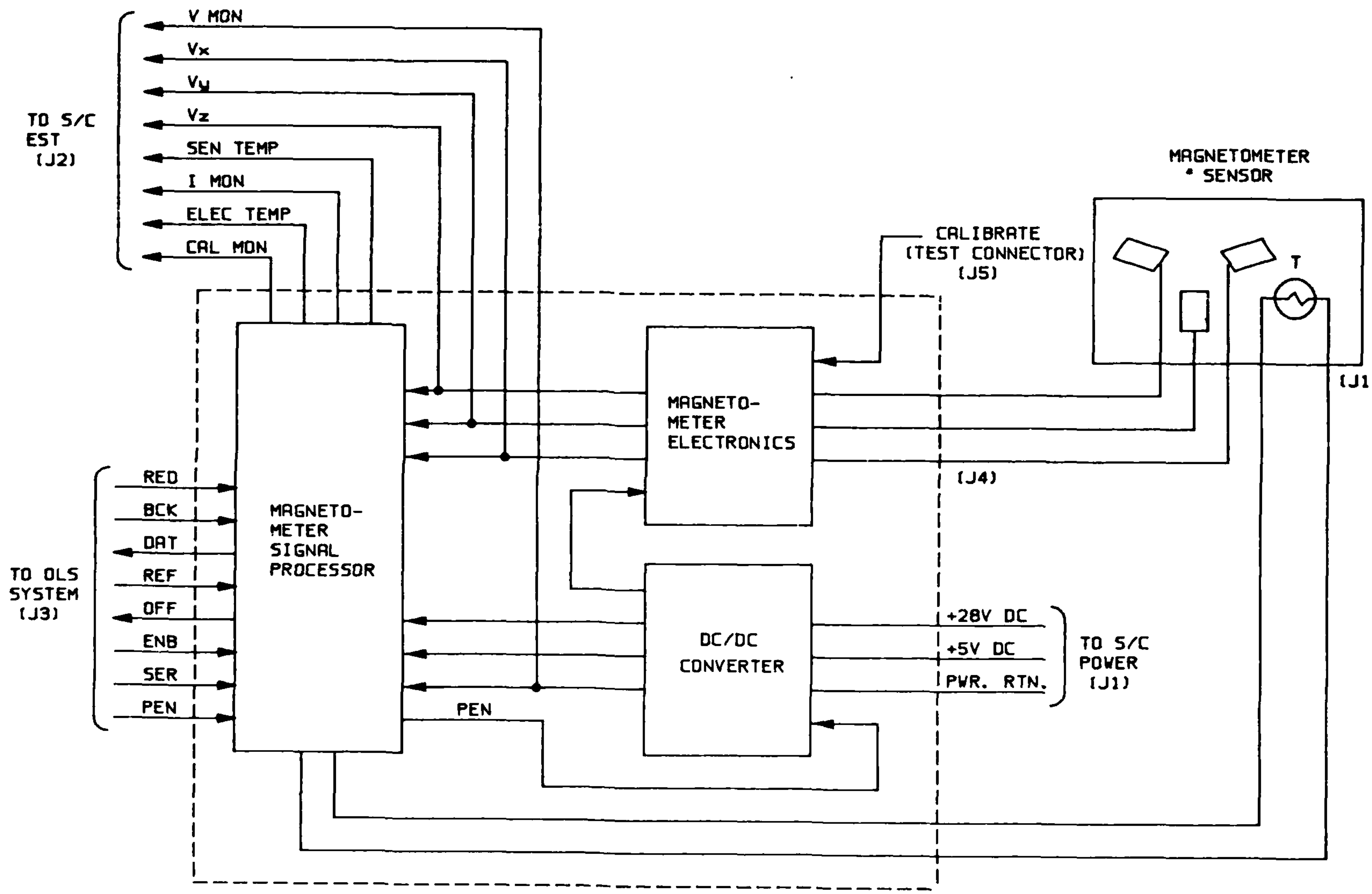

FIGURE 2-2 SSM SYSTEM BLOCK DIAGRAM

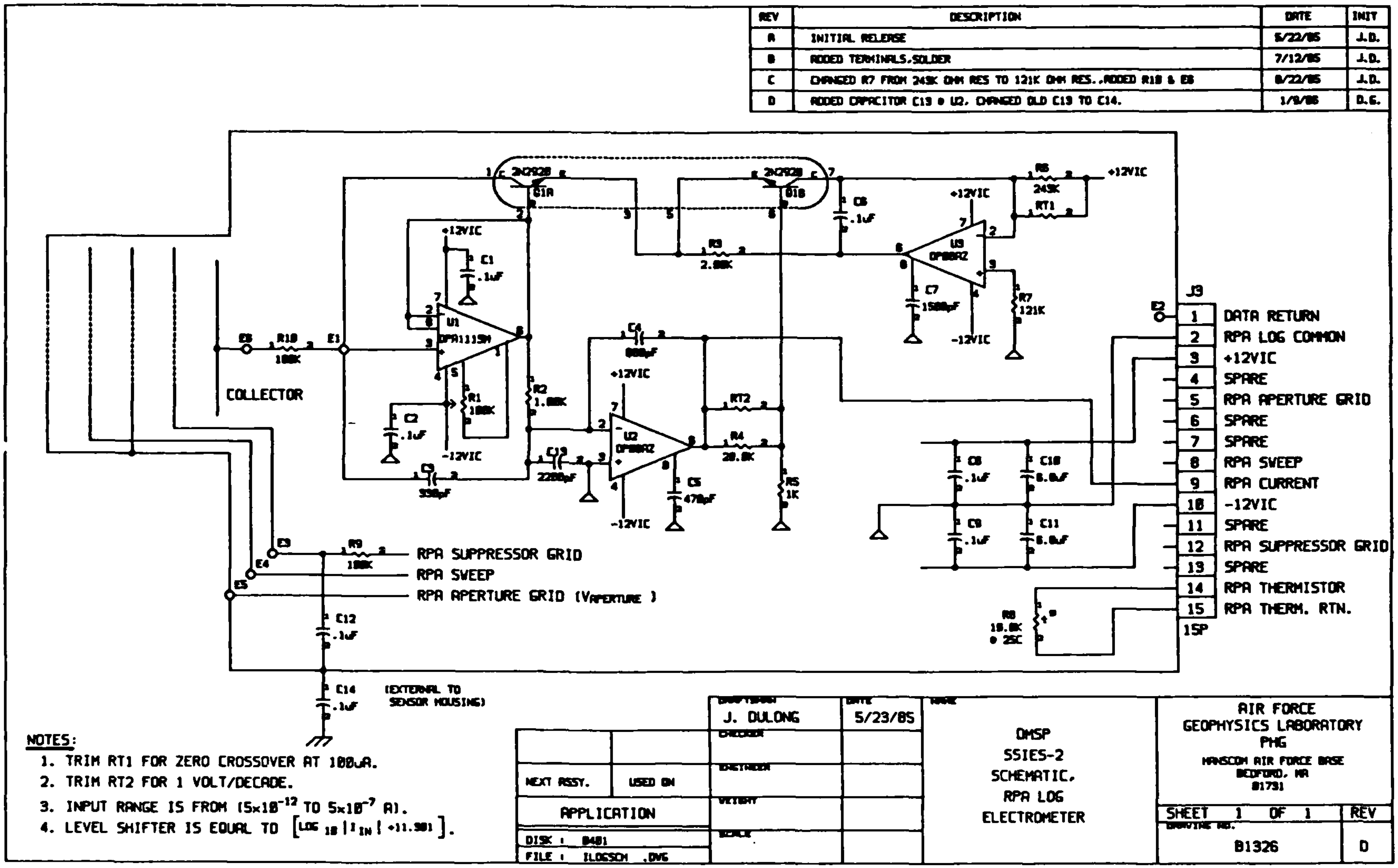
REV
DESCRIPTION
DATE
INIT
A
INITIAL RELEASE
5/22/85
J.D.
B
ADDED TERMINALS,SOLDER
7/12/85
J.D.
C
CHANGED R7 FROM 243K OHM RES TO 121K OHM RES.,ADDED R10 & E6
8/22/85
J.D.
D
ADDED CAPACITOR C13 @ U2, CHANGED OLD C13 TO C14.
1/9/86
D.G.
COLLECTOR
RPA SUPPRESSOR GRID
RPA SWEEP
RPA APERTURE GRID (VAPERTURE)
(EXTERNAL TO SENSOR HOUSING)
J3
DATA RETURN
RPA LOG COMMON
+12VIC
SPARE
RPA APERTURE GRID
SPARE
SPARE
RPA SWEEP
RPA CURRENT
-12VIC
SPARE
RPA SUPPRESSOR GRID
SPARE
RPA THERMISTOR
RPA THERM. RTN.
NOTES:
1. TRIM RT1 FOR ZERO CROSSOVER AT 100uA.
2. TRIM RT2 FOR 1 VOLT/DECADE.
3. INPUT RANGE IS FROM (5x10^-12 TO 5x10^-7 A).
4. LEVEL SHIFTER IS EQUAL TO [LOG 10 | I IN | +11.301].
J. DULONG
5/23/85
NEXT ASSY.
USED ON
APPLICATION
DISK : 0481
FILE : ILOGSCH .DWG
DMSP
SSIES-2
SCHEMATIC,
RPA LOG
ELECTROMETER
AIR FORCE
GEOPHYSICS LABORATORY
PHG
HANSCOM AIR FORCE BASE
BEDFORD, MA
01731
SHEET 1 OF 1
REV
B1326
D

Figure 2-3

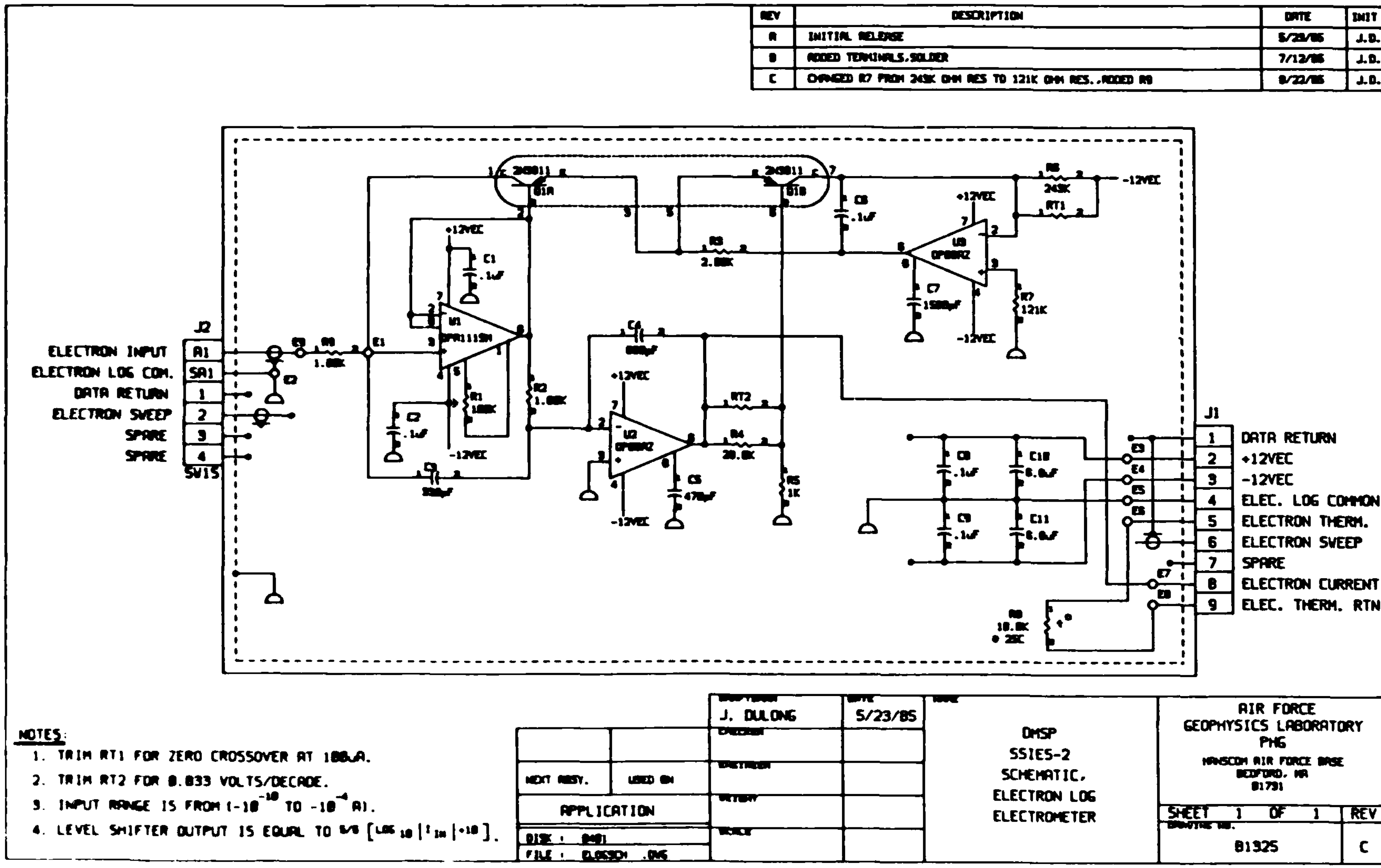

REV | DESCRIPTION | DATE | INIT
A | INITIAL RELEASE | 5/23/85 | J.D.
B | ADDED TERMINALS,SOLDER | 7/12/85 | J.D.
C | CHANGED R7 FROM 243K OHM RES TO 121K OHM RES.,ADDED R9 | 8/22/85 | J.D.
J2
ELECTRON INPUT
ELECTRON LOG COM.
DATA RETURN
ELECTRON SWEEP
SPARE
SPARE
J1
DATA RETURN
+12VEC
-12VEC
ELEC. LOG COMMON
ELECTRON THERM.
ELECTRON SWEEP
SPARE
ELECTRON CURRENT
ELEC. THERM. RTN.
NOTES:
1. TRIM RT1 FOR ZERO CROSSOVER AT 100µA.
2. TRIM RT2 FOR 0.833 VOLTS/DECADE.
3. INPUT RANGE IS FROM (-10^-10 TO -10^-4 A).
4. LEVEL SHIFTER OUTPUT IS EQUAL TO 5/6 [LOG10 |IIN| +10].
J. DULONG
5/23/85
NEXT ASSY.
USED ON
APPLICATION
DMSP
SSIES-2
SCHEMATIC,
ELECTRON LOG
ELECTROMETER
AIR FORCE
GEOPHYSICS LABORATORY
PHG
HANSCOM AIR FORCE BASE
BEDFORD, MA
01731
SHEET 1 OF 1
REV
81325
C

Figure 2-4

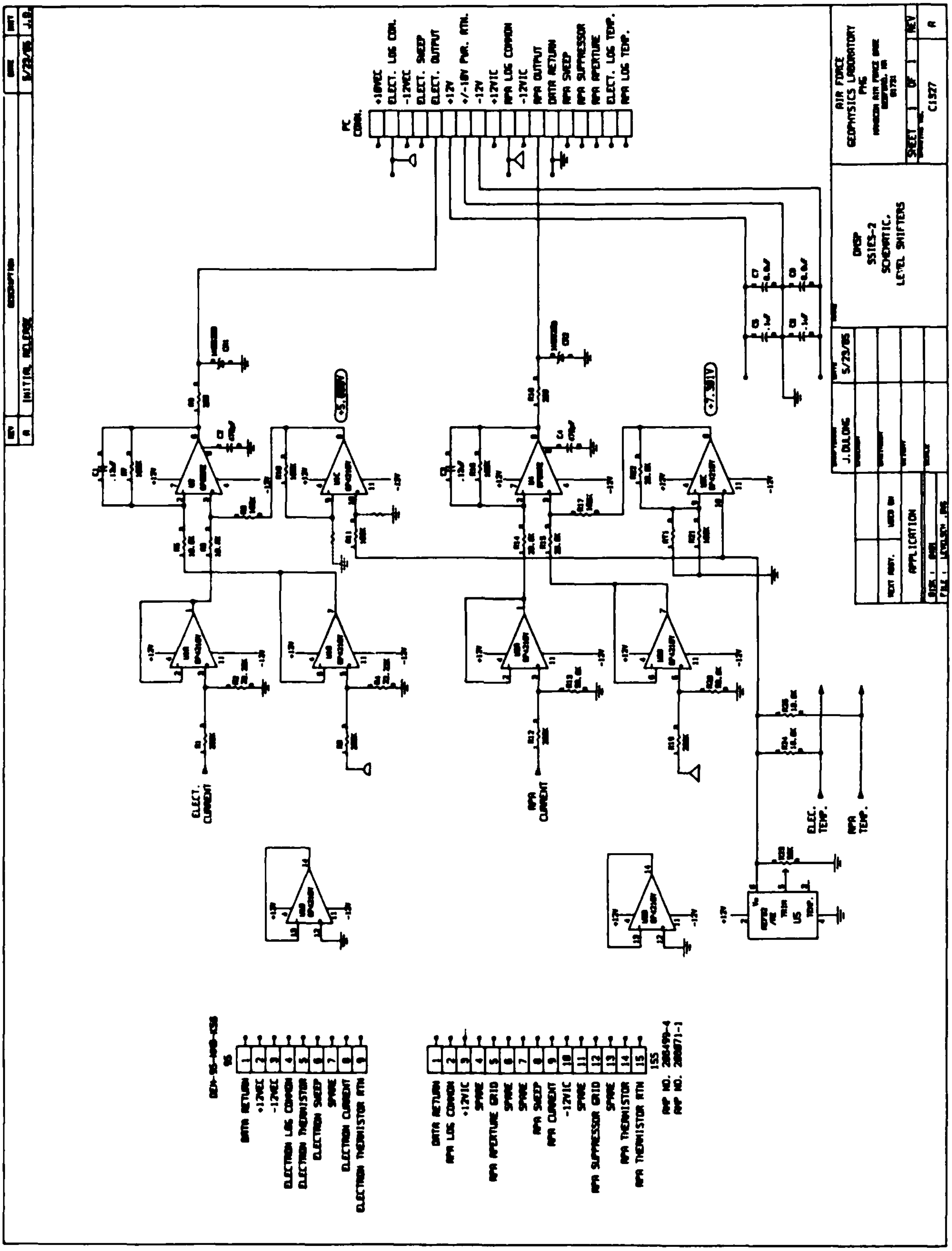

INITIAL RELEASE
AIR FORCE
GEOPHYSICS LABORATORY
DMSP
SSIES-2
SCHEMATIC,
LEVEL SHIFTERS
J.DULONG
5/29/85
APPLICATION
C1327
ELECT.
CURRENT
RPA
CURRENT
ELEC.
TEMP.
RPA
TEMP.

Figure 2-5

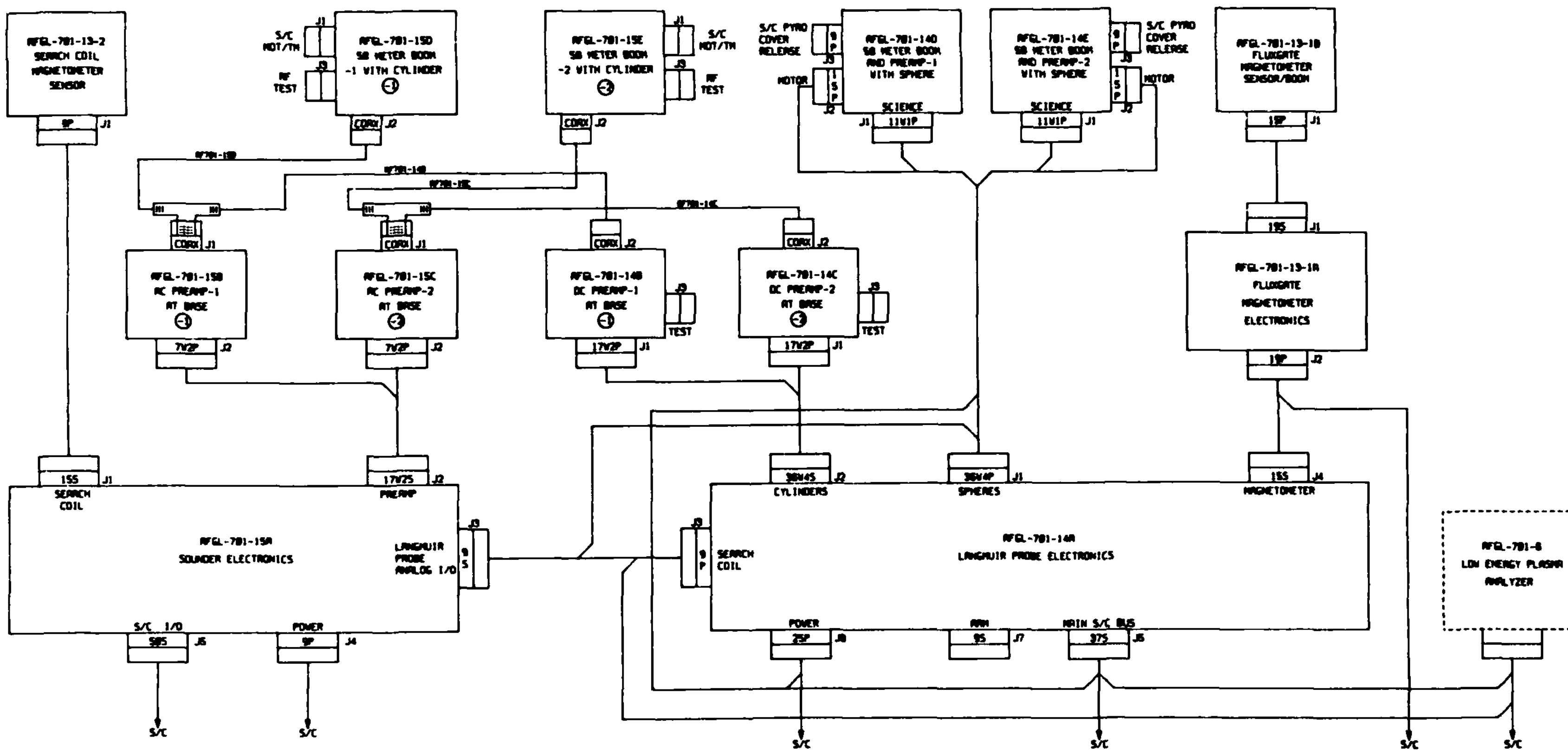
AFGL-701-13-2
SEARCH COIL
MAGNETOMETER
SENSOR
AFGL-701-15D
SB METER BOOM
-1 WITH CYLINDER
AFGL-701-15E
SB METER BOOM
-2 WITH CYLINDER
AFGL-701-14D
SB METER BOOM
AND PREAMP-1
WITH SPHERE
AFGL-701-14E
SB METER BOOM
AND PREAMP-2
WITH SPHERE
AFGL-701-13-1B
FLUXGATE
MAGNETOMETER
SENSOR/BOOM
S/C PYRO
COVER
RELEASE
MOTOR
SCIENCE
S/C
MOT/TM
RF
TEST
AFGL-701-15B
AC PREAMP-1
AT BASE
AFGL-701-15C
AC PREAMP-2
AT BASE
AFGL-701-14B
DC PREAMP-1
AT BASE
AFGL-701-14C
DC PREAMP-2
AT BASE
TEST
AFGL-701-13-1A
FLUXGATE
MAGNETOMETER
ELECTRONICS
AFGL-701-15A
SOUNDER ELECTRONICS
SEARCH
COIL
PREAMP
LANGMUIR
PROBE
ANALOG I/O
S/C I/O
POWER
AFGL-701-14A
LANGMUIR PROBE ELECTRONICS
CYLINDERS
SPHERES
MAGNETOMETER
SEARCH
COIL
POWER
ARM
MAIN S/C BUS
AFGL-701-6
LOW ENERGY PLASMA
ANALYZER
S/C

Figure 2-6

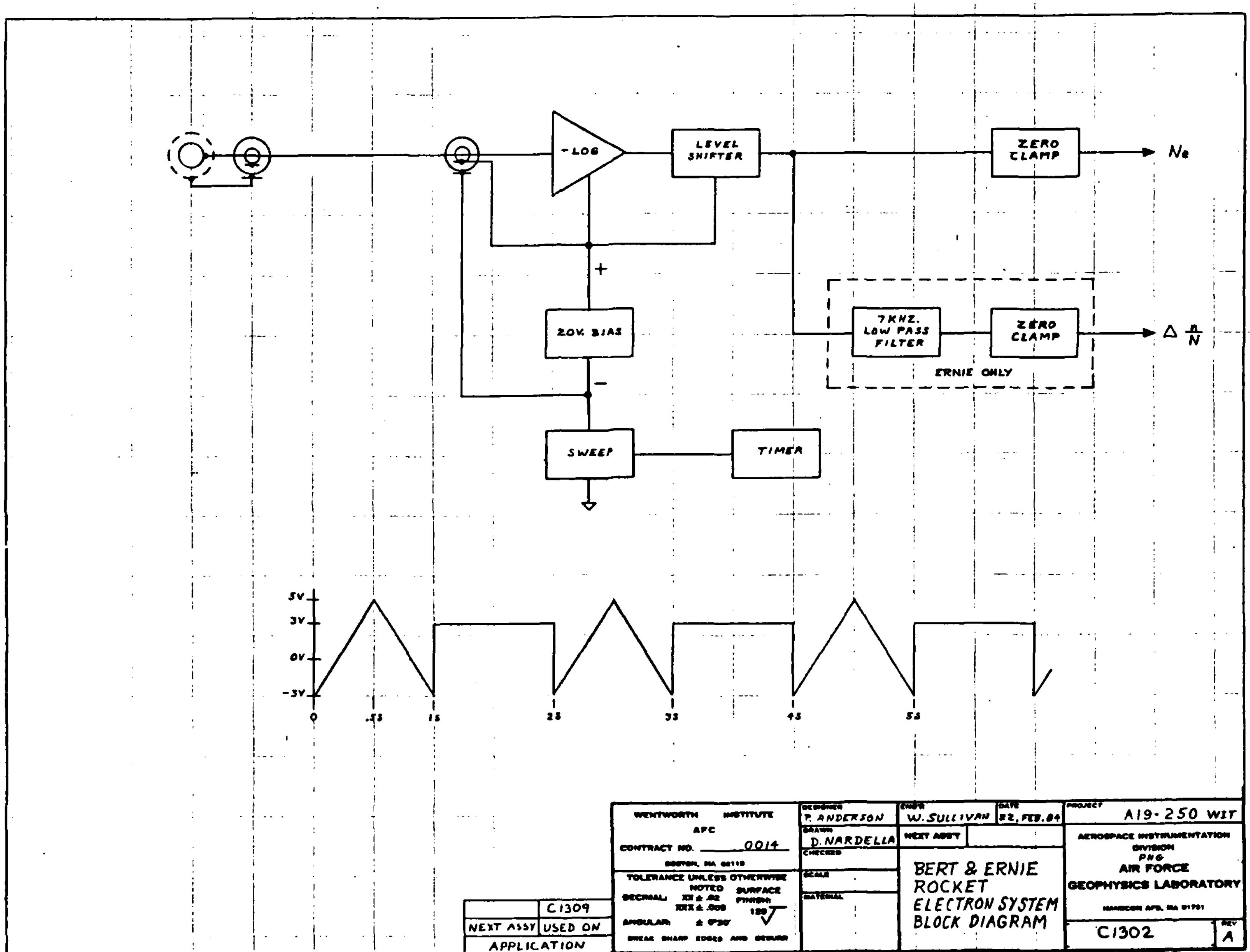
-LOG
LEVEL SHIFTER
ZERO CLAMP
Ne
+
20V. BIAS
-
7KHZ. LOW PASS FILTER
ZERO CLAMP
ERNIE ONLY
SWEEP
TIMER
5V
3V
0V
-3V
0
.75
1.5
2.5
3.5
4.5
5.5
WENTWORTH INSTITUTE
AFC
CONTRACT NO. 0014
BOSTON, MA 02115
TOLERANCE UNLESS OTHERWISE NOTED
DECIMAL: XX ± .02 XXX ± .005
ANGULAR: ± 0°30'
SURFACE FINISH
BREAK SHARP EDGES AND BURRS
DESIGNER P. ANDERSON
DRAWN D. NARDELLA
CHECKED
SCALE
MATERIAL
ENGR W. SULLIVAN
DATE 22, FEB. 84
NEXT ASSY
BERT & ERNIE ROCKET ELECTRON SYSTEM BLOCK DIAGRAM
PROJECT A19-250 WIT
AEROSPACE INSTRUMENTATION DIVISION
PHG
AIR FORCE GEOPHYSICS LABORATORY
HANSCOM AFB, MA 01731
C1302
REV A
C1309
NEXT ASSY
USED ON
APPLICATION

Figure 2-7

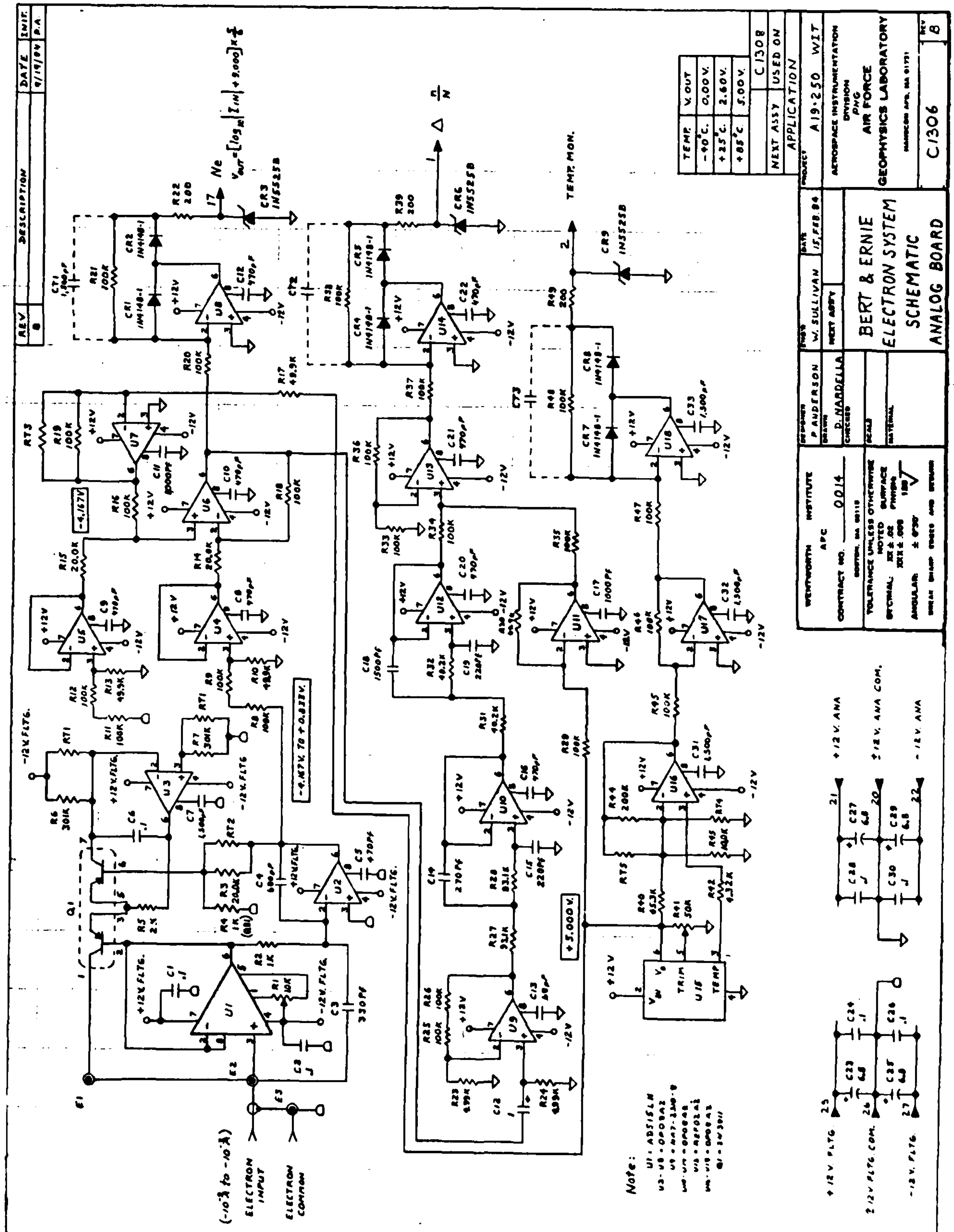
BERT & ERNIE
ELECTRON SYSTEM
SCHEMATIC
ANALOG BOARD
C1306
AIR FORCE
GEOPHYSICS LABORATORY
A19-250 WIT
TEMP. MON.
ELECTRON INPUT
ELECTRON COMMON

Figure 2-8

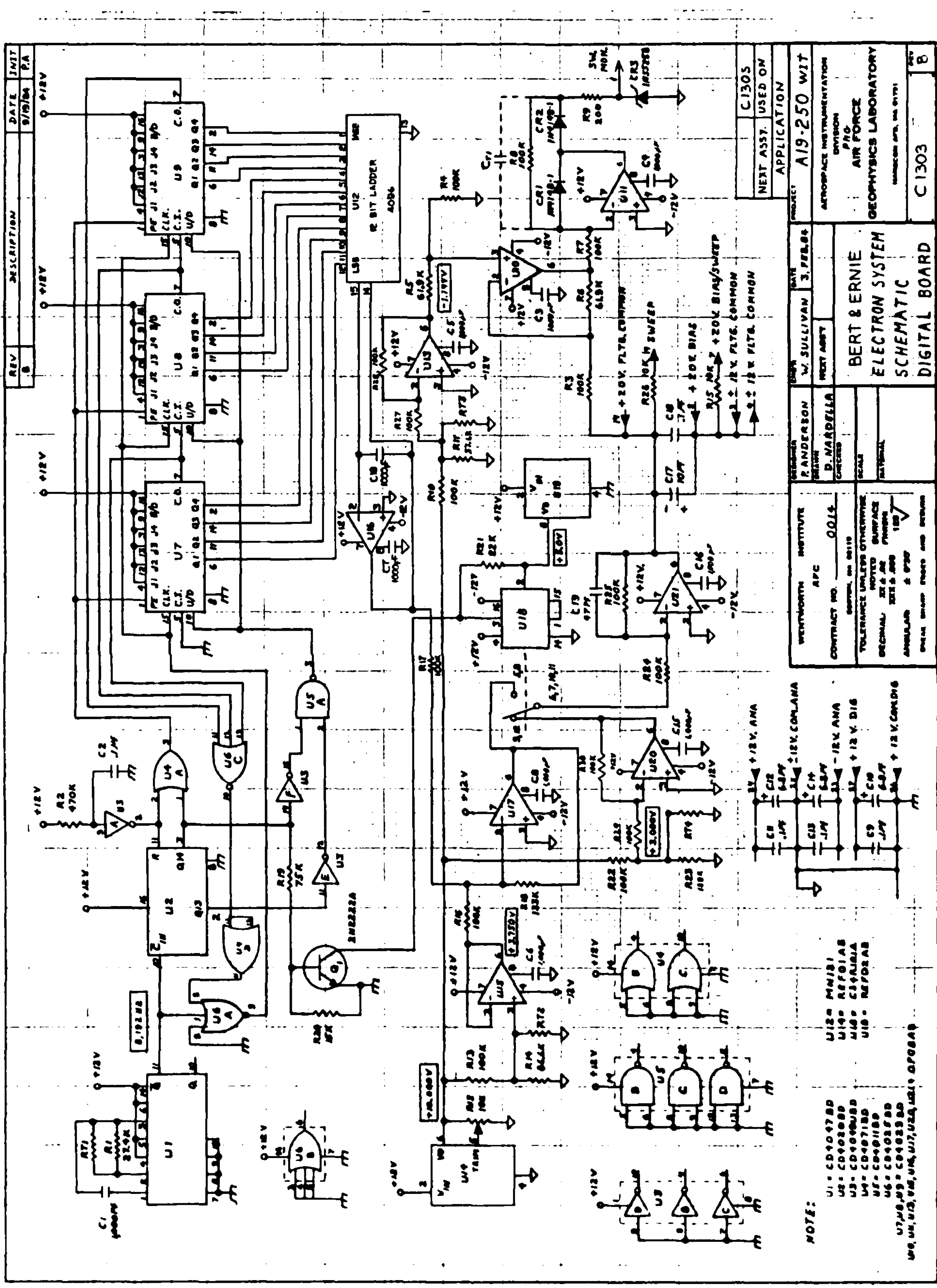

Figure 2-9

PLASMAS AND FIELDS EXPERIMENT (PAF)
BLOCK DIAGRAM

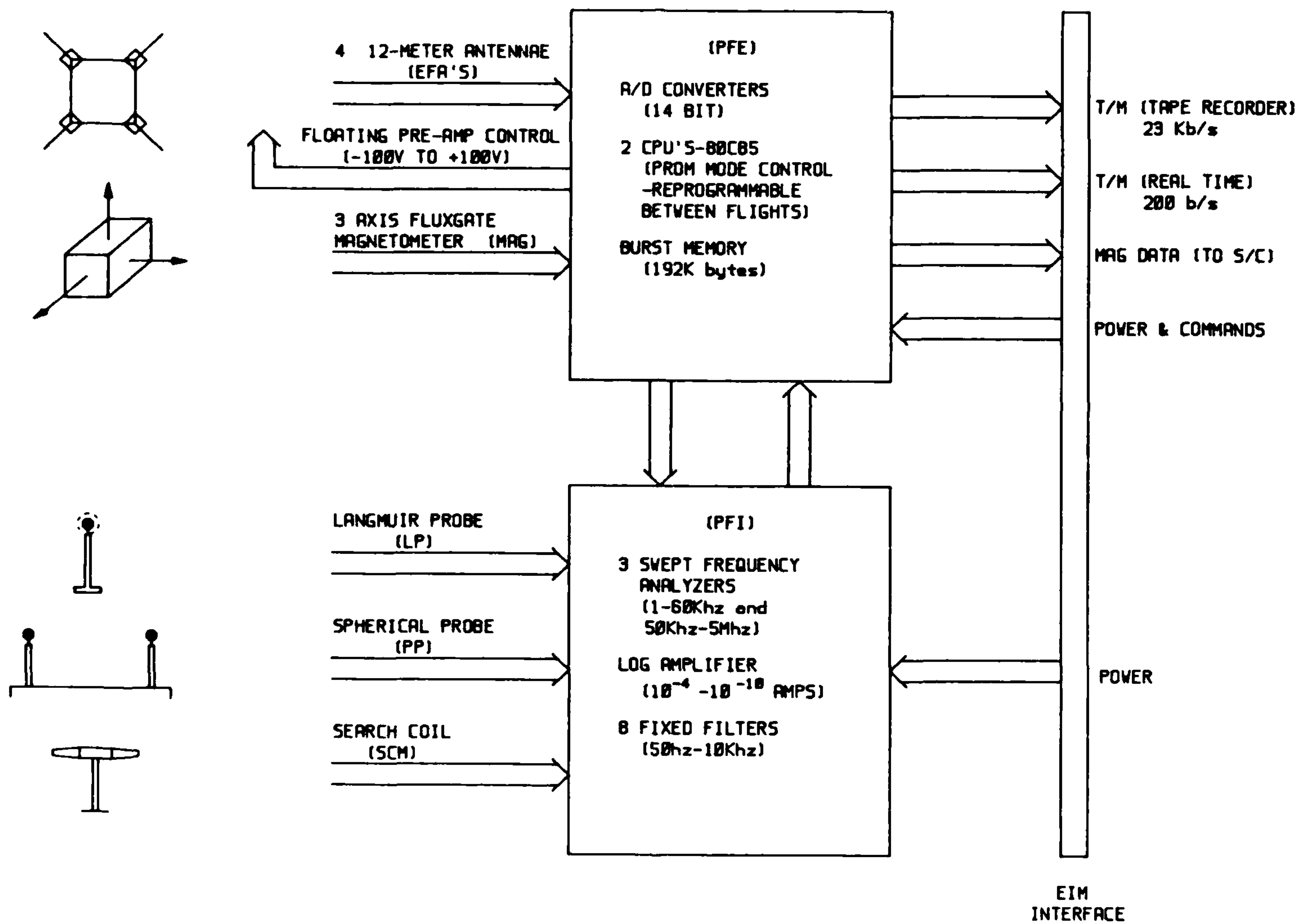

Figure 2-10

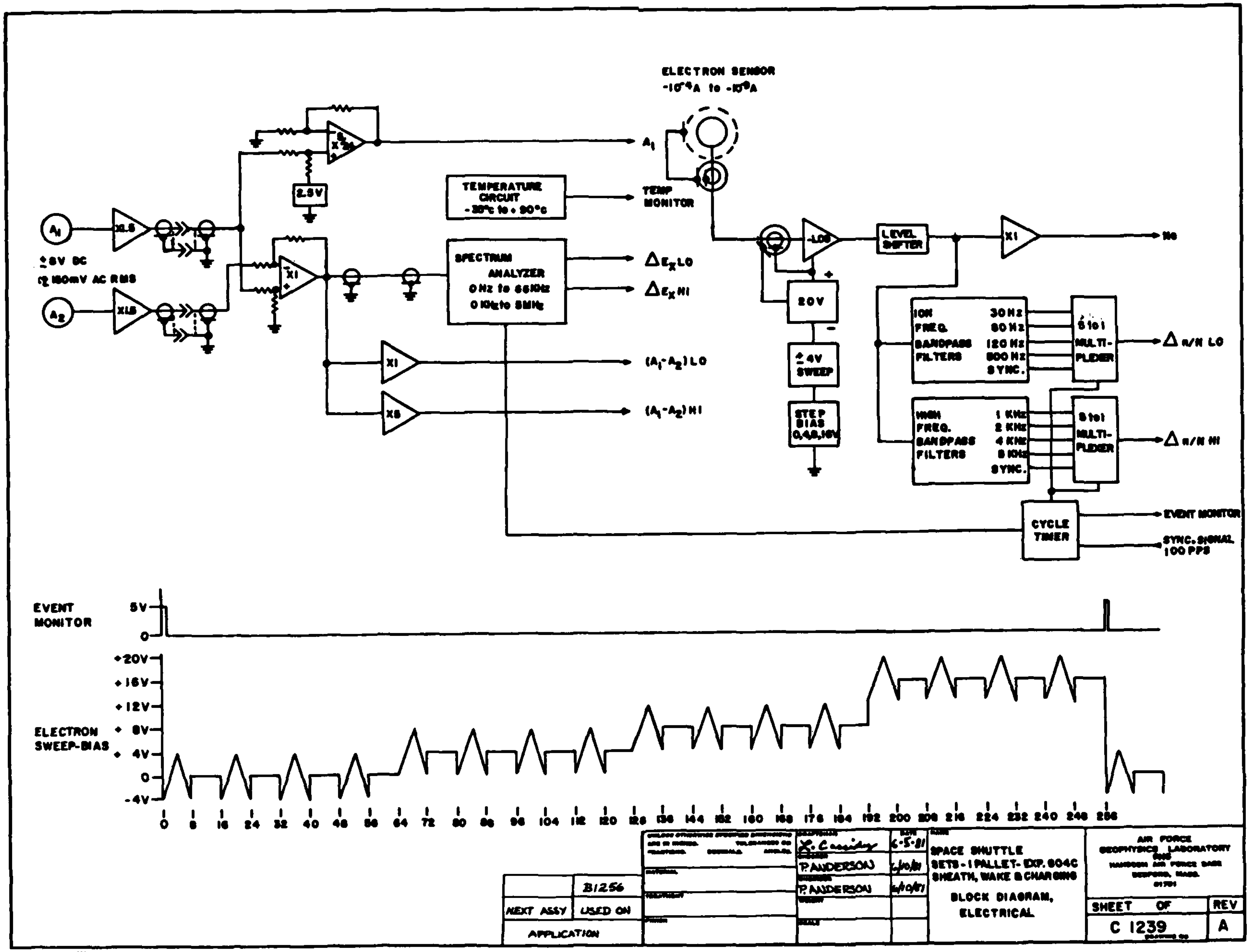
ELECTRON SENSOR
-10^{-6}A to -10^{-9}A
A_1
TEMPERATURE CIRCUIT -20°c to +90°c
TEMP MONITOR
2.5V
SPECTRUM ANALYZER
0 Hz to 65 KHz
0 KHz to 5MHz
ΔE_x LO
ΔE_x HI
$\pm$8V DC
180mV AC RMS
(A_1-A_2) LO
(A_1-A_2) HI
LEVEL SHIFTER
Ne
20V
$\pm$4V SWEEP
STEP BIAS
LOW FREQ. BANDPASS FILTERS
30 Hz
60 Hz
120 Hz
800 Hz
SYNC.
HIGH FREQ. BANDPASS FILTERS
1 KHz
2 KHz
4 KHz
8 KHz
SYNC.
5 to 1 MULTI-PLEXER
Δ n/N LO
Δ n/N HI
CYCLE TIMER
EVENT MONITOR
SYNC. SIGNAL 100 PPS
EVENT MONITOR
5V
0
ELECTRON SWEEP-BIAS
+20V
+16V
+12V
+8V
+4V
0
-4V
0 8 16 24 32 40 48 56 64 72 80 88 96 104 112 120 128 136 144 152 160 168 176 184 192 200 208 216 224 232 240 248 256
B1256
NEXT ASSY
USED ON
APPLICATION
P. ANDERSON
P. ANDERSON
6-5-81
SPACE SHUTTLE
SETS-1 PALLET-EXP. 804C
SHEATH, WAKE & CHARGING
BLOCK DIAGRAM, ELECTRICAL
AIR FORCE GEOPHYSICS LABORATORY
SHEET
OF
REV
C 1239
A

Figure 2-11

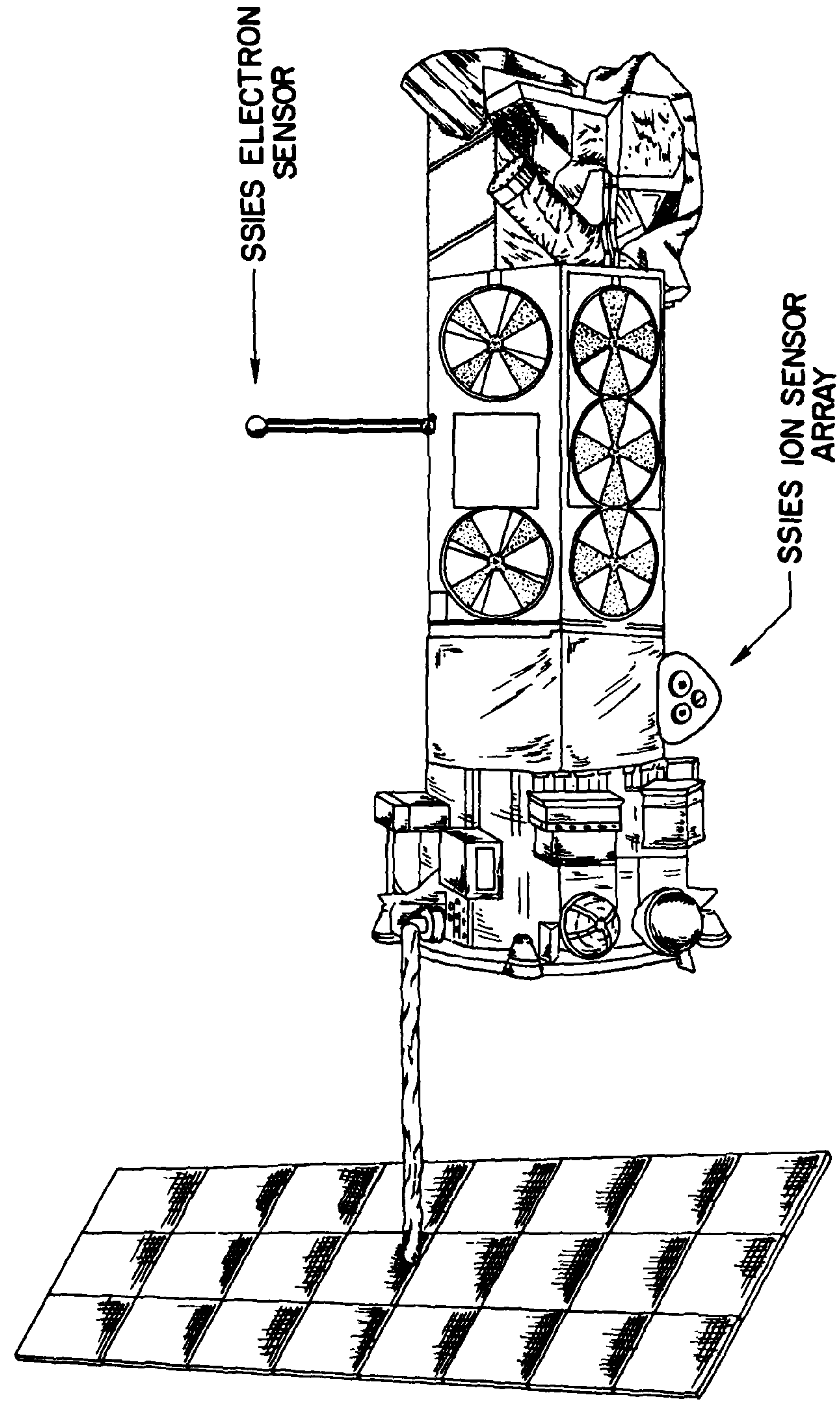

Figure 3-1

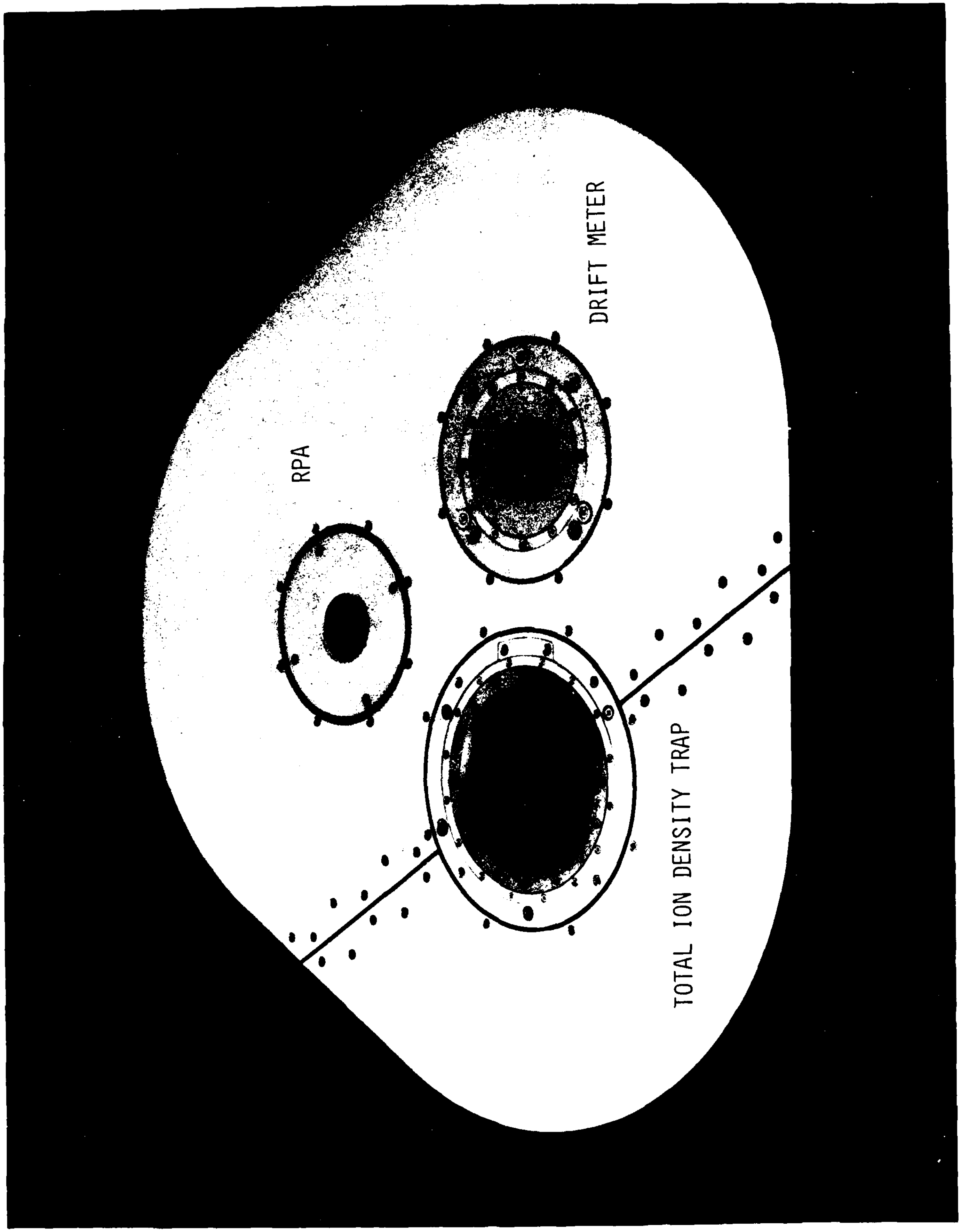

Figure 3-2

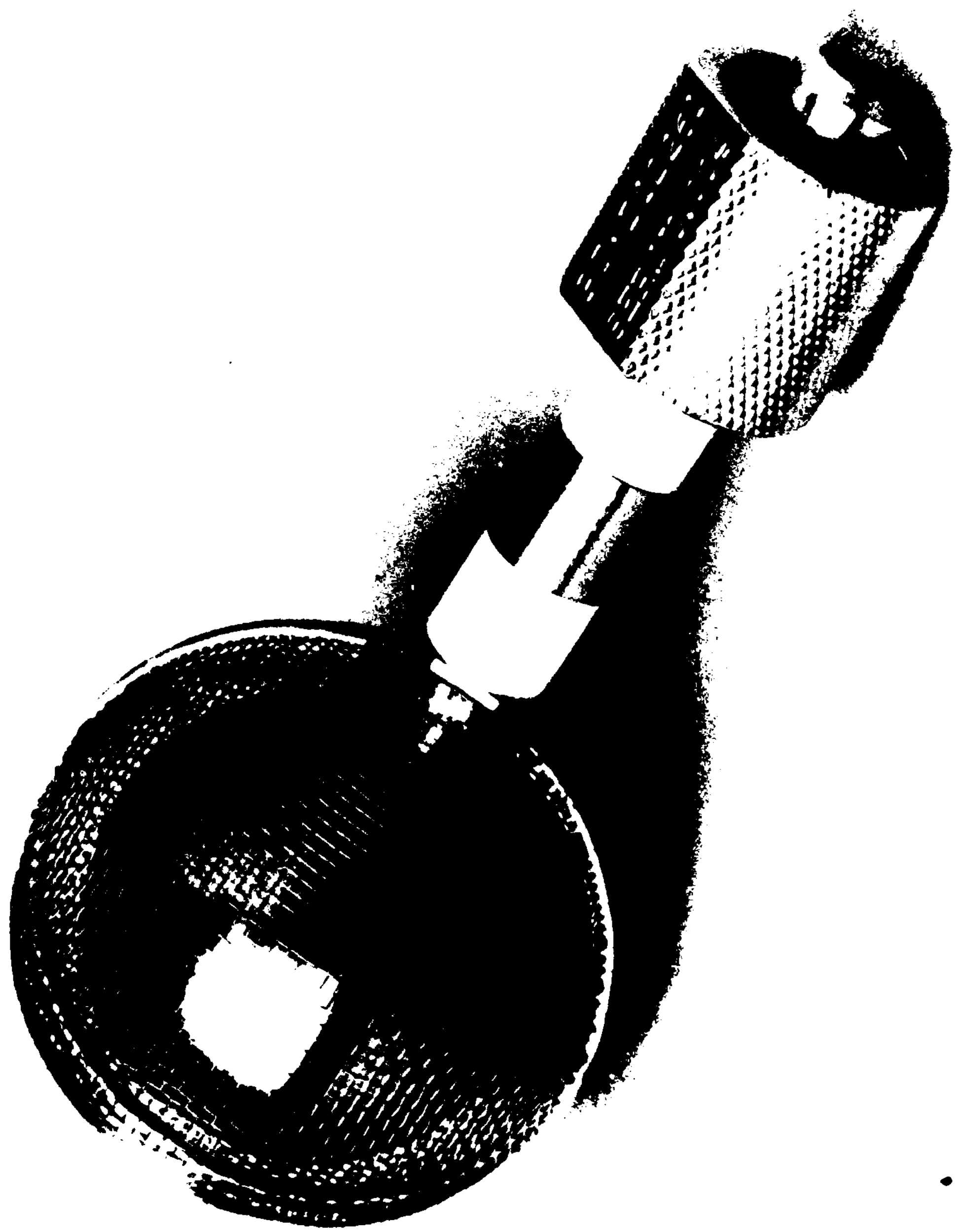

Figure 3-3

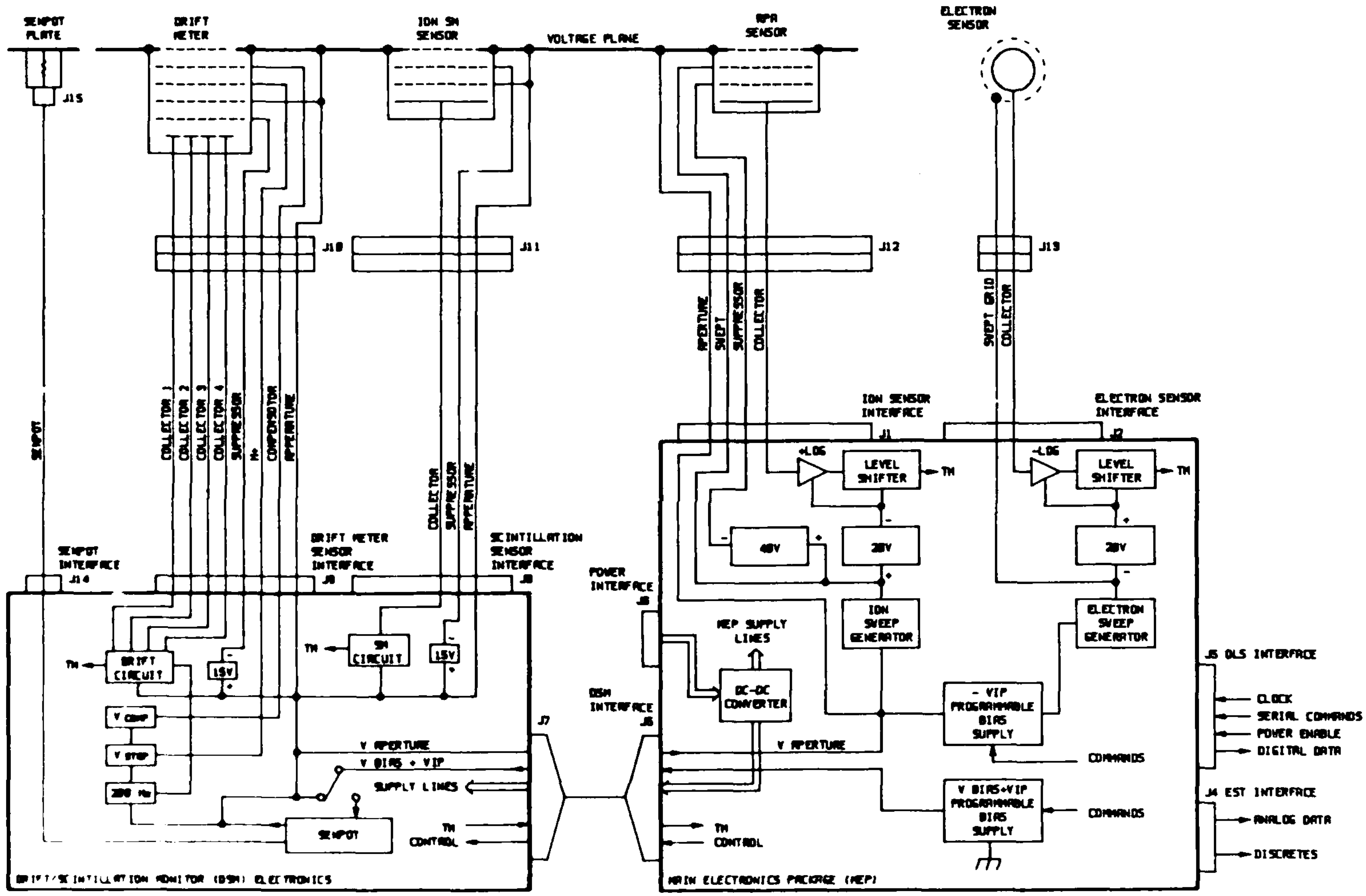

SSIES/S9 AND S10
FUNCTIONAL / ELECTRICAL
SYSTEM BLOCK DIAGRAM

Figure 3-4

SSIES DATA ANALYSIS PLAN

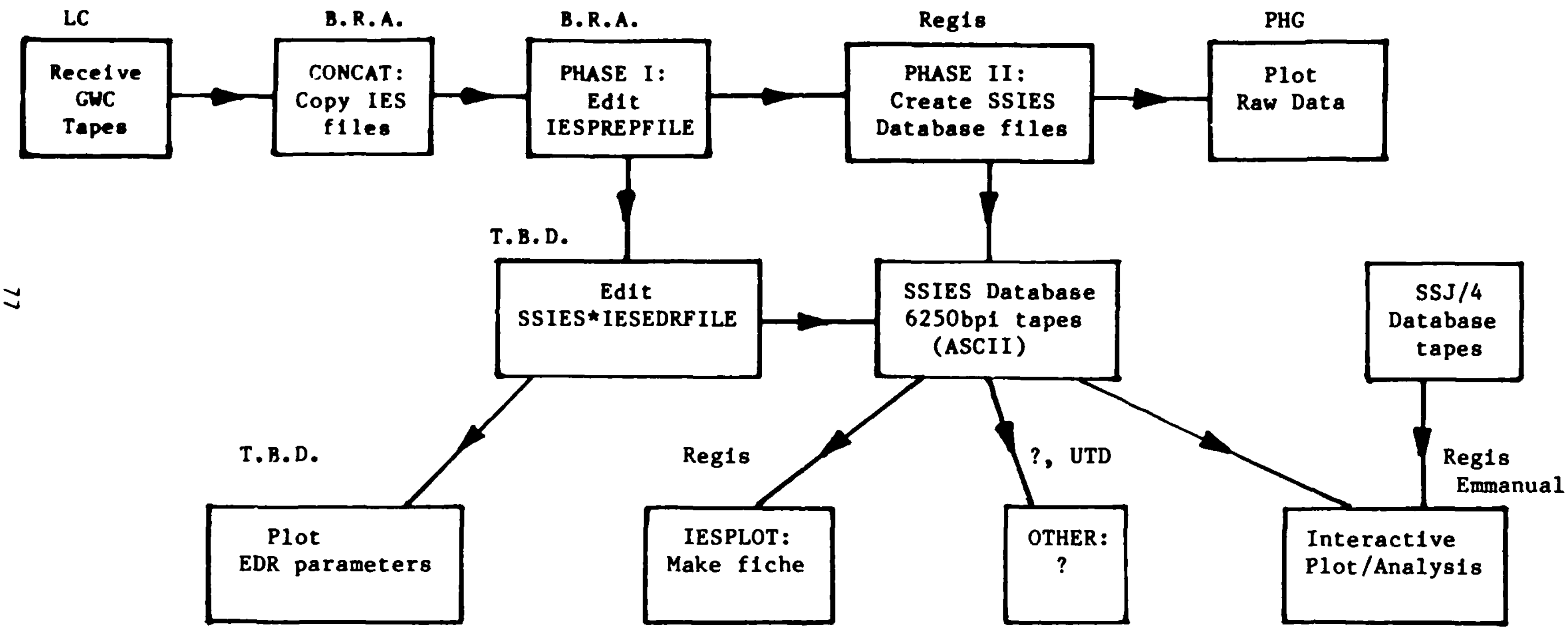

Figure 3-5

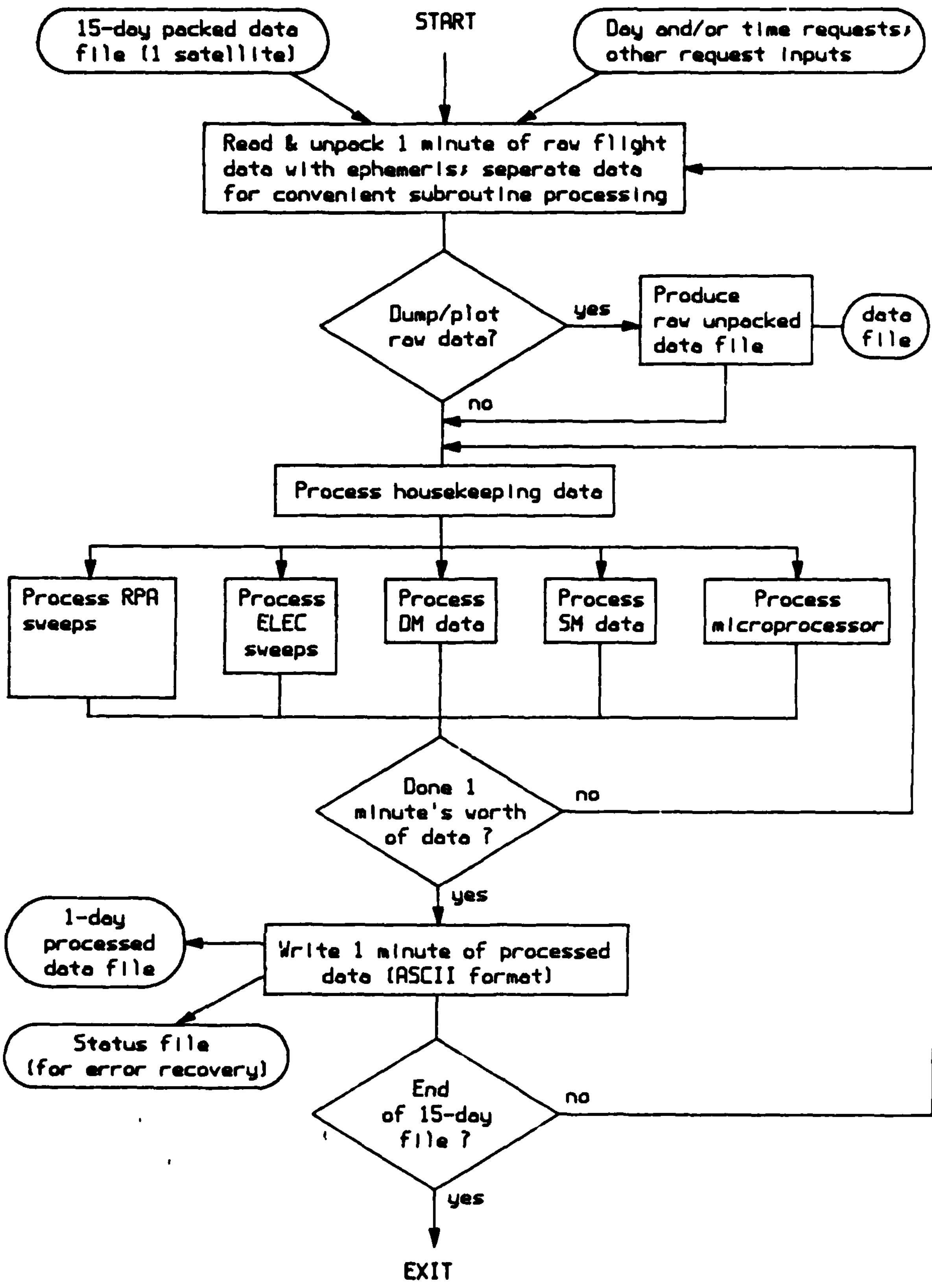
15-day packed data file (1 satellite)
START
Day and/or time requests; other request inputs
Read & unpack 1 minute of raw flight data with ephemeris; seperate data for convenient subroutine processing
Dump/plot raw data?
yes
Produce raw unpacked data file
data file
no
Process housekeeping data
Process RPA sweeps
Process ELEC sweeps
Process DM data
Process SM data
Process microprocessor
Done 1 minute's worth of data ?
no
yes
1-day processed data file
Write 1 minute of processed data (ASCII format)
Status file (for error recovery)
End of 15-day file ?
no
yes
EXIT

Figure 3-6

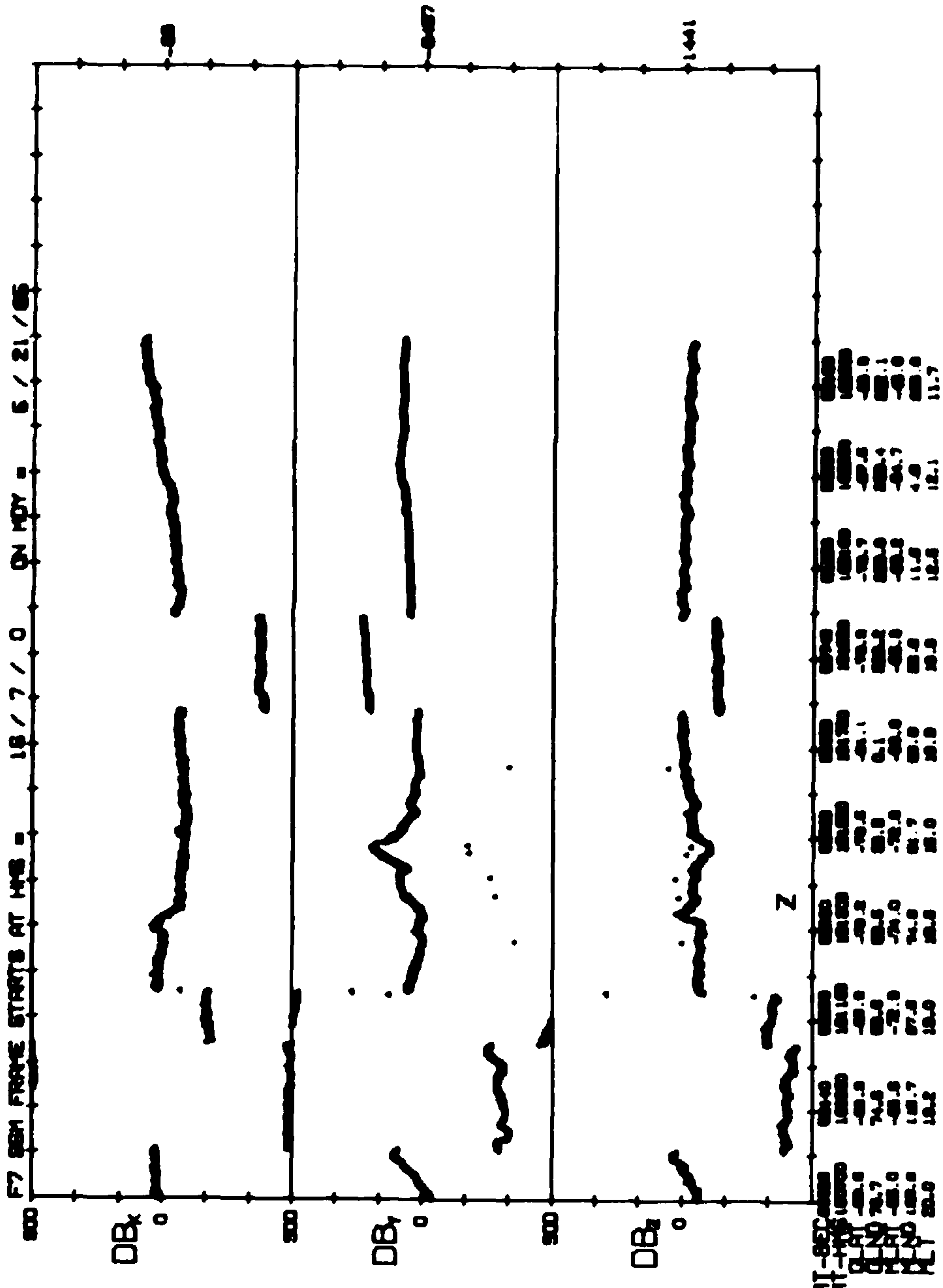

Figure 4-1

Figure 4-2

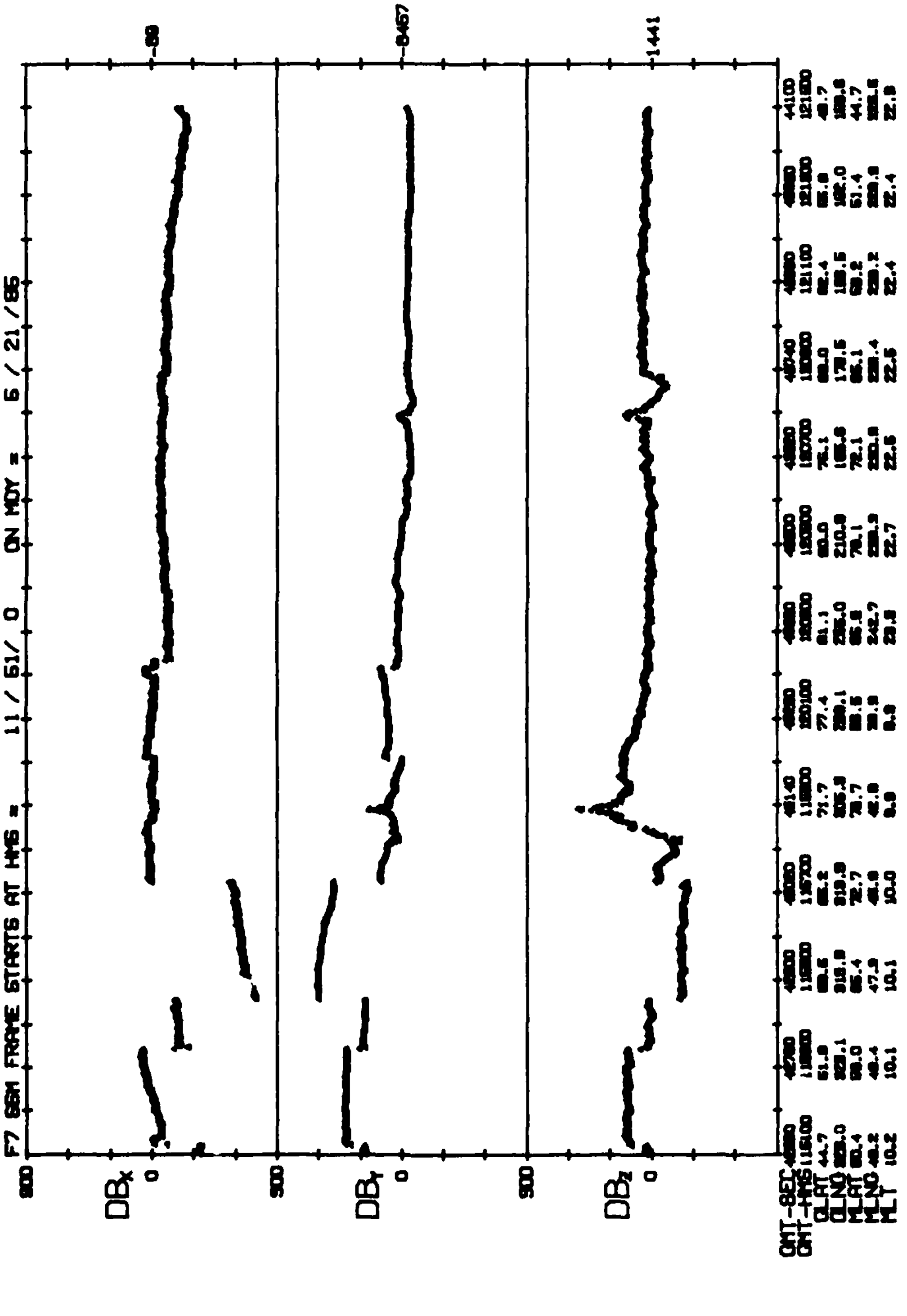
F7 SSM FRAME STARTS AT HMS = 11 / 51 / 0 ON MDY = 5 / 21 / 85
DBx
DBy
DBz
GMT-SEC
GMT-HMS
GLAT
GLNG
MLAT
MLNG
MLT

Figure 4-3

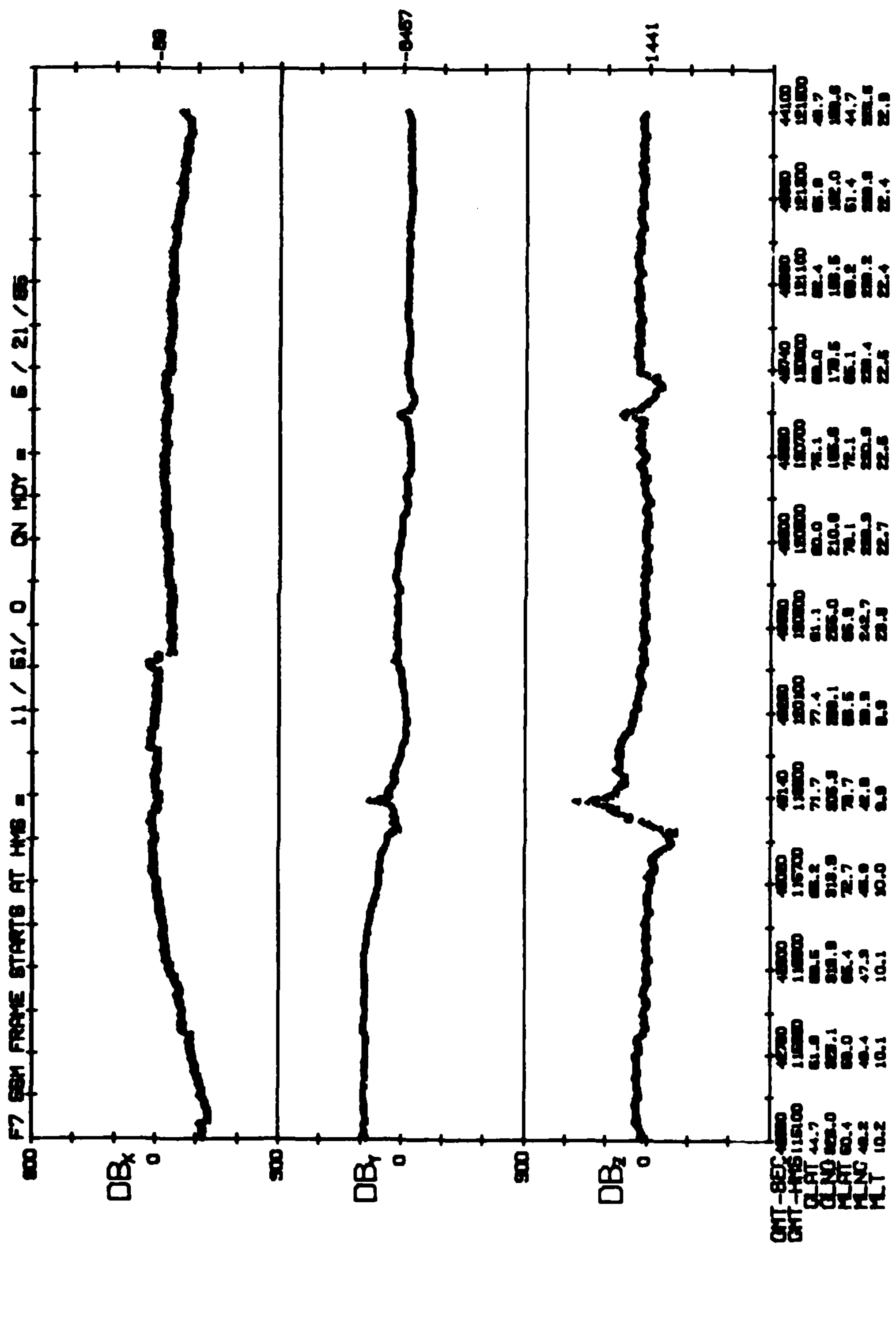

Figure 4-4

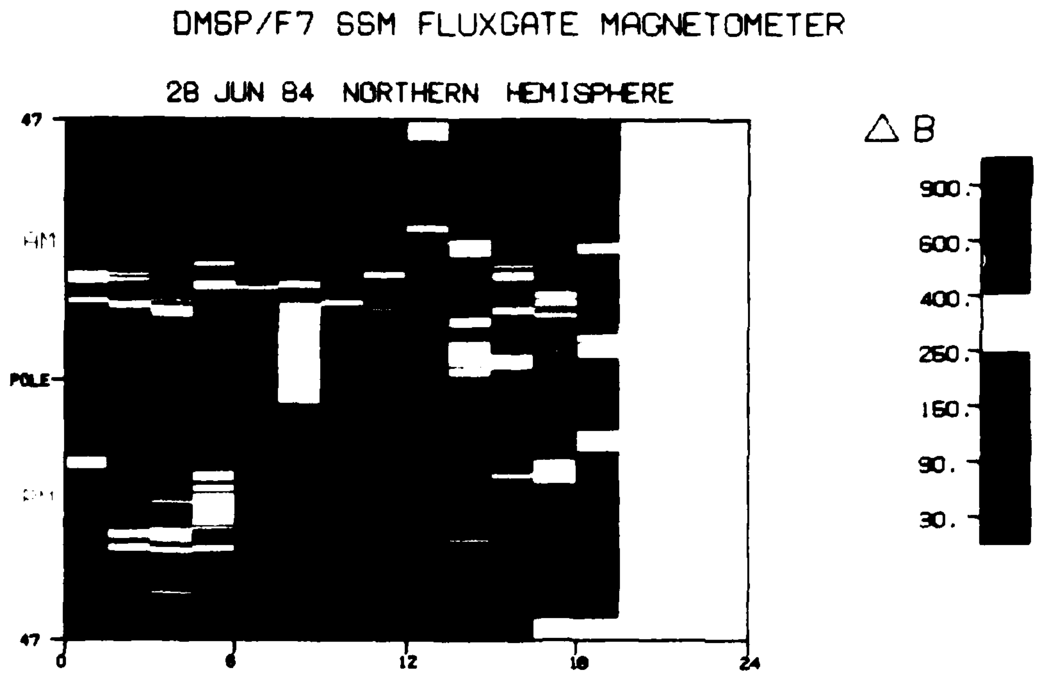

Figure 4-5

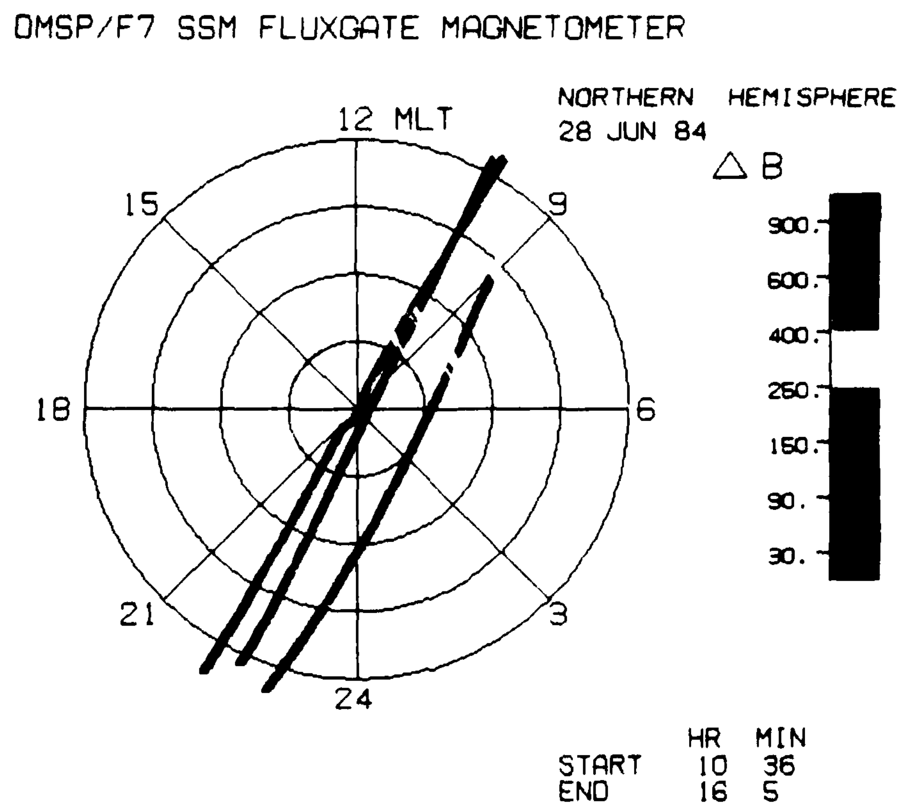

Figure 4-6

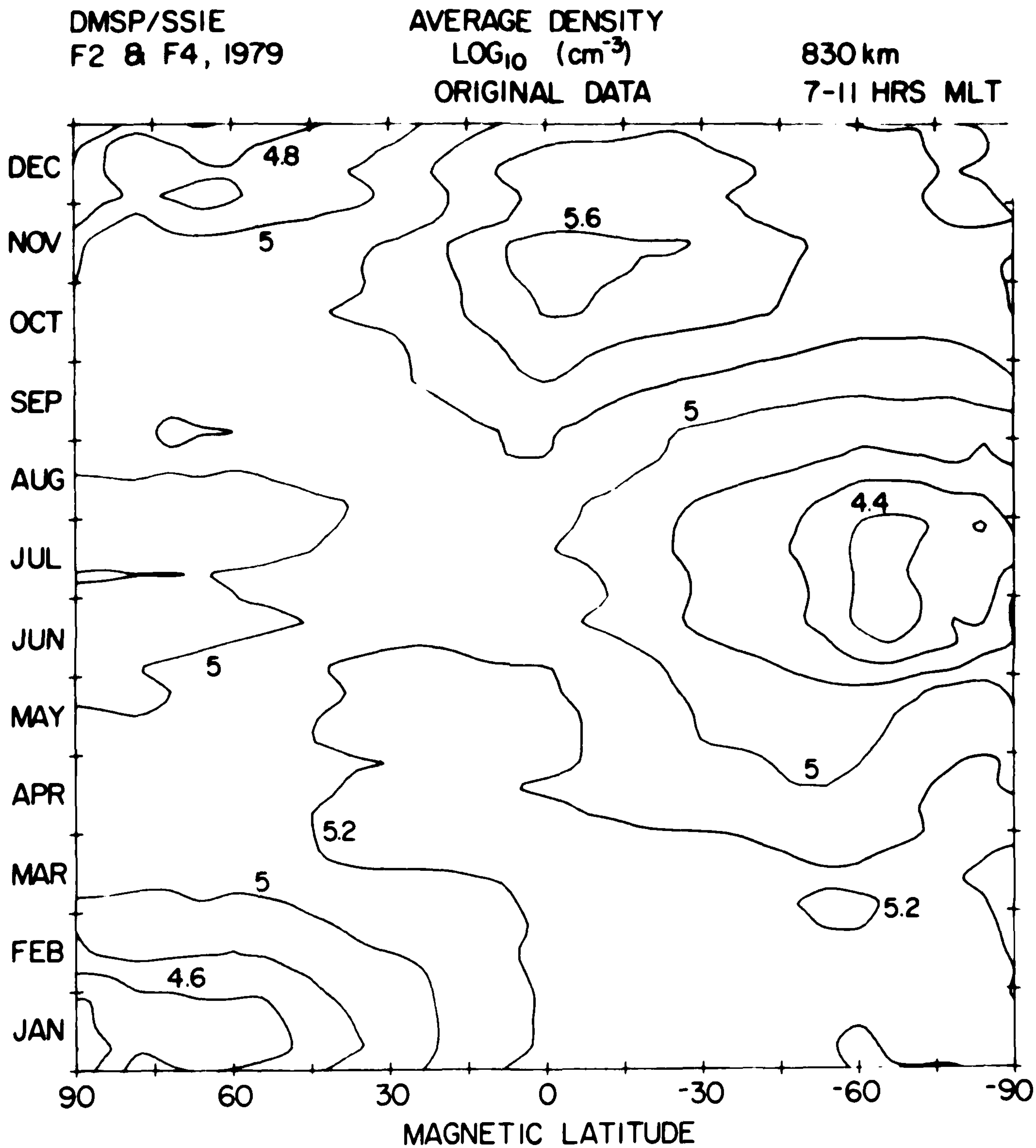
DMSP/SSIE
F2 & F4, 1979
AVERAGE DENSITY
LOG10 (cm-3)
ORIGINAL DATA
830 km
7-11 HRS MLT
DEC
NOV
OCT
SEP
AUG
JUL
JUN
MAY
APR
MAR
FEB
JAN
4.8
5.6
5
5
4.4
5
5
5.2
5
5.2
4.6
90
60
30
0
-30
-60
-90
MAGNETIC LATITUDE

Figure 5-1

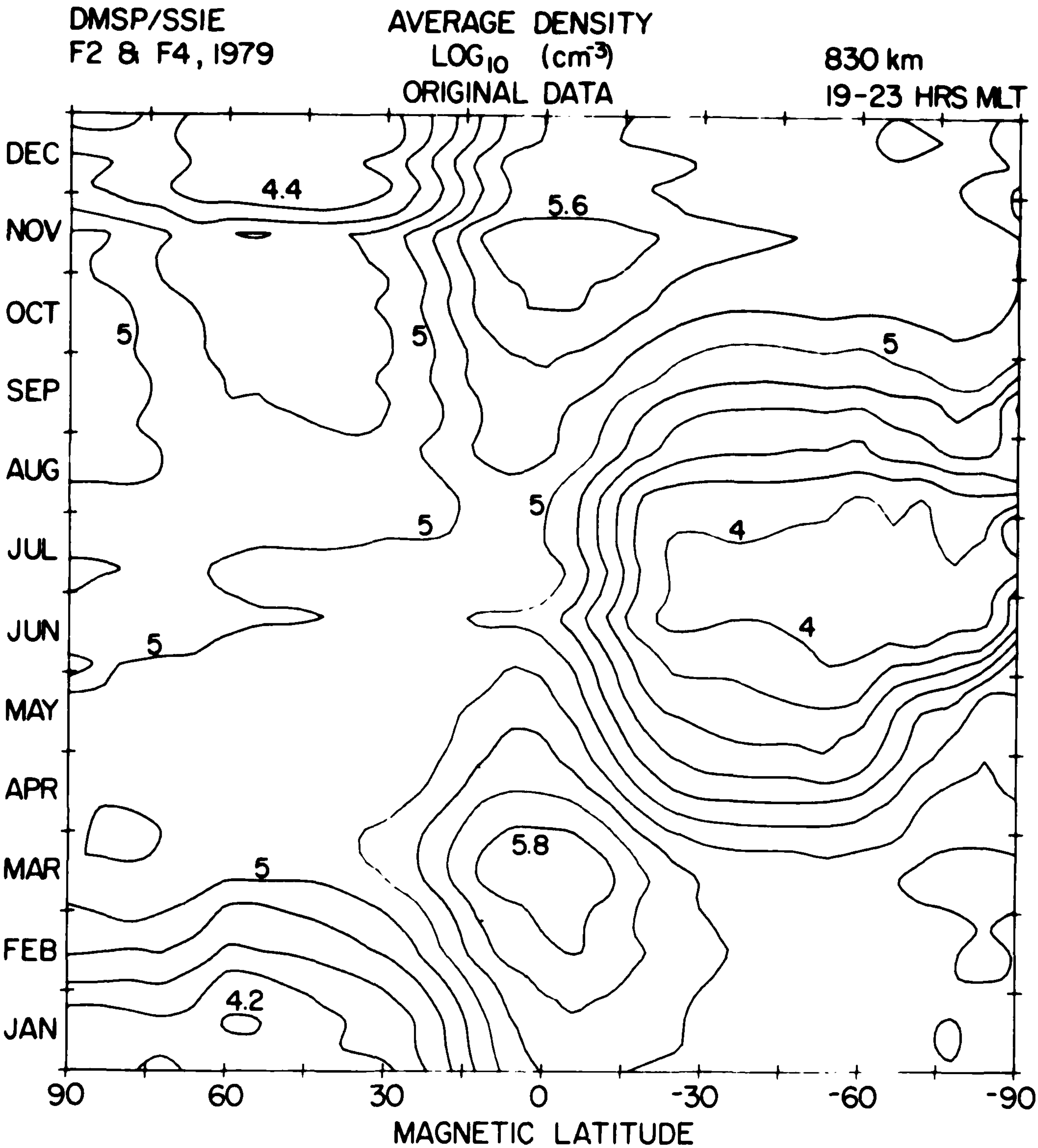
DMSP/SSIE
F2 & F4, 1979
AVERAGE DENSITY
LOG10 (cm-3)
ORIGINAL DATA
830 km
19-23 HRS MLT
DEC
NOV
OCT
SEP
AUG
JUL
JUN
MAY
APR
MAR
FEB
JAN
4.4
5.6
5
5
5
5
5
4
4
5
5.8
5
4.2
90
60
30
0
-30
-60
-90
MAGNETIC LATITUDE

Figure 5-2

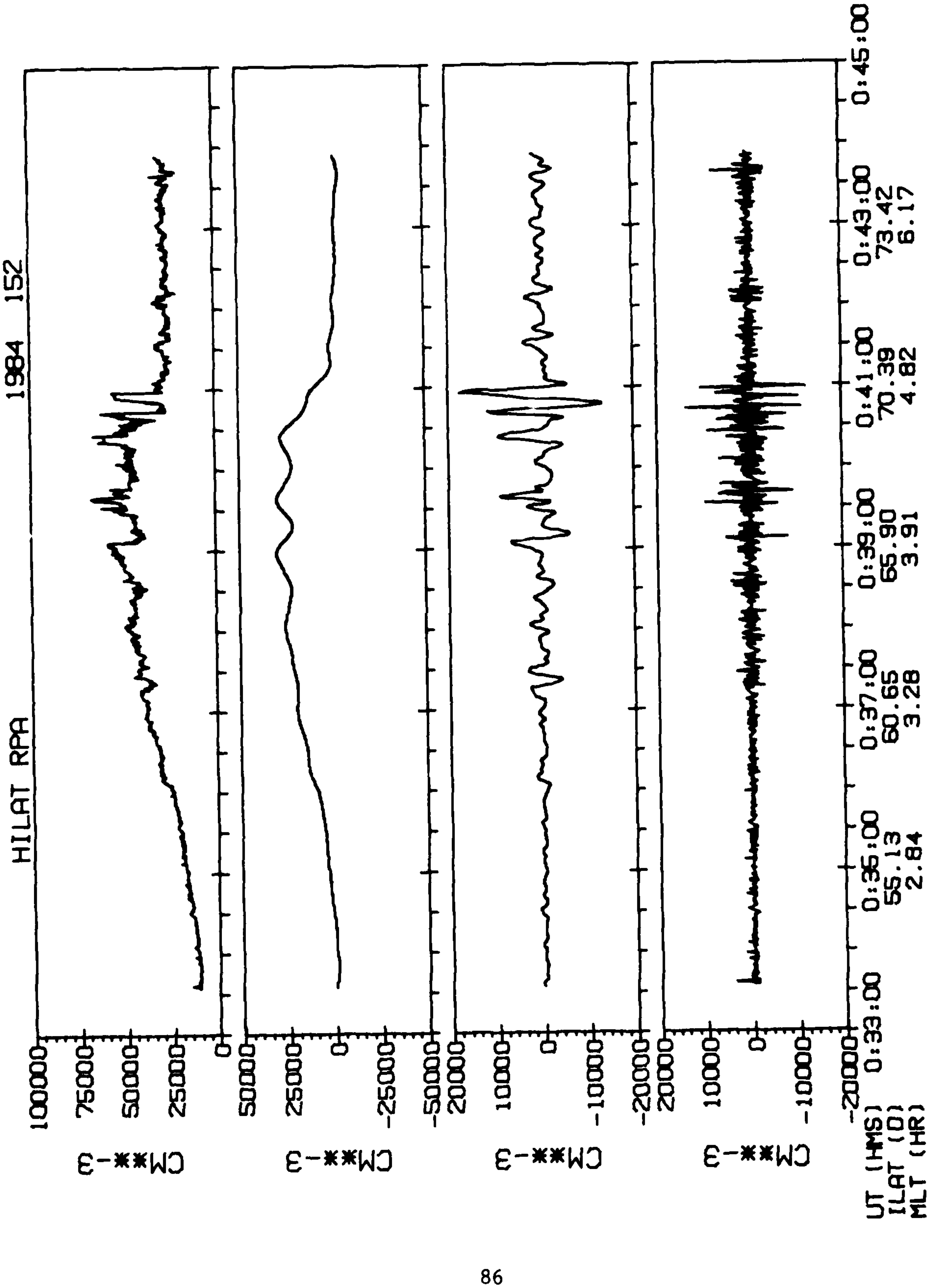
HILAT RPA
1984 152
CM**-3
CM**-3
CM**-3
CM**-3
100000
75000
50000
25000
0
50000
25000
0
-25000
-50000
20000
10000
0
-10000
-20000
20000
10000
0
-10000
-20000
UT (HMS)
ILAT (D)
MLT (HR)
0:33:00
0:35:00
55.13
2.84
0:37:00
60.65
3.28
0:39:00
65.90
3.91
0:41:00
70.39
4.82
0:43:00
73.42
6.17
0:45:00

Figure 6-1

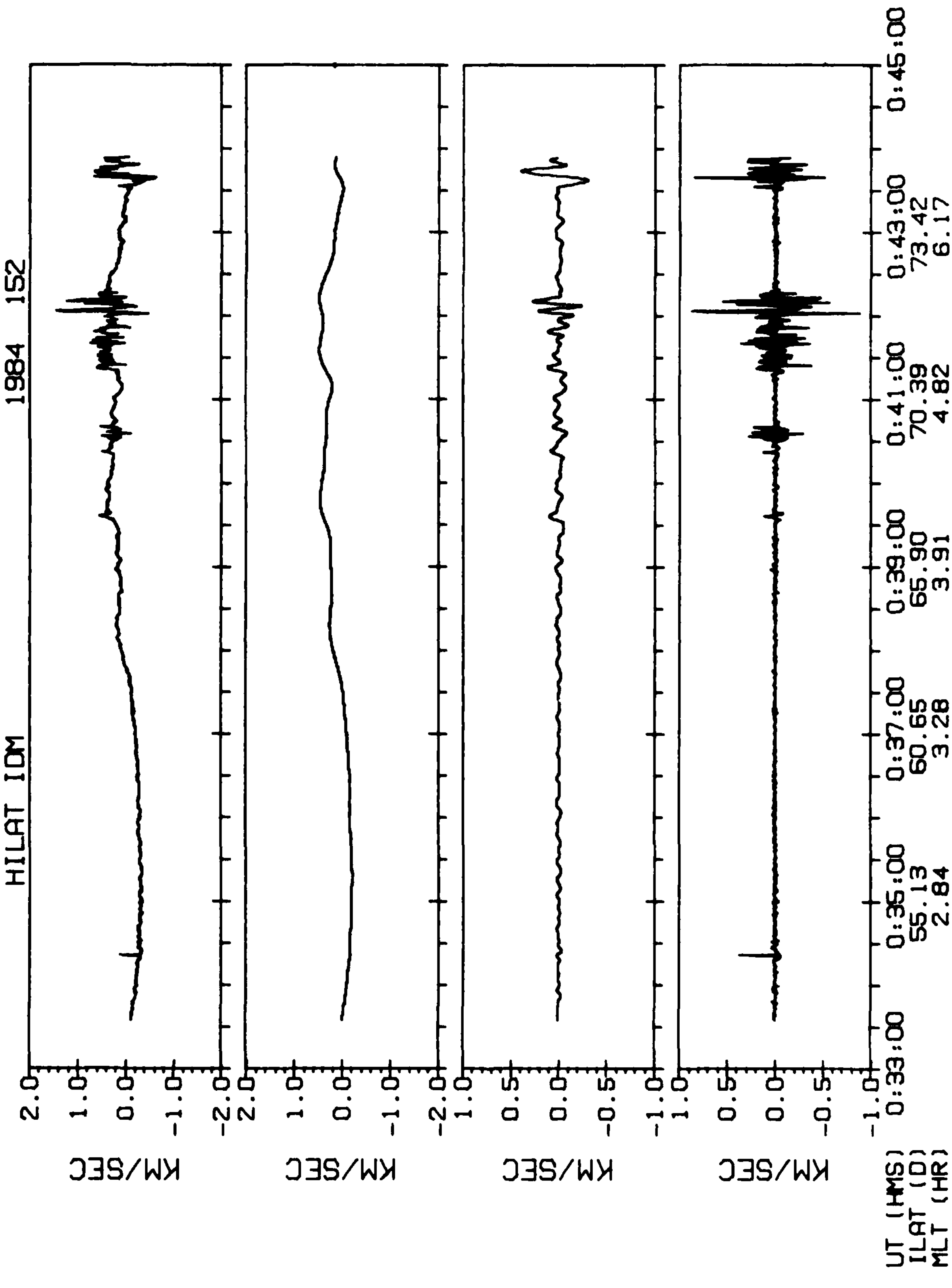

HILAT IDM
1984 152
KM/SEC
KM/SEC
KM/SEC
KM/SEC
2.0
1.0
0.0
-1.0
-2.0
0.5
-0.5
UT (HMS)
ILAT (D)
MLT (HR)
0:33:00
0:35:00
55.13
2.84
0:37:00
60.65
3.28
0:39:00
65.90
3.91
0:41:00
70.39
4.82
0:43:00
73.42
6.17
0:45:00

Figure 6-2

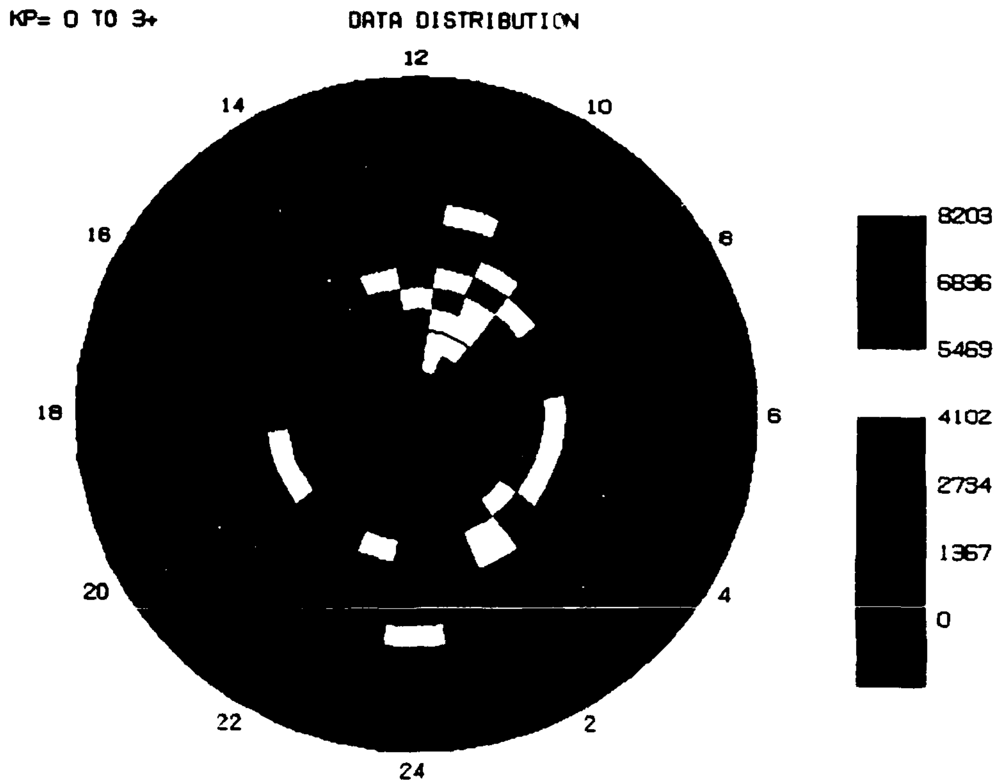

Figure 6-3

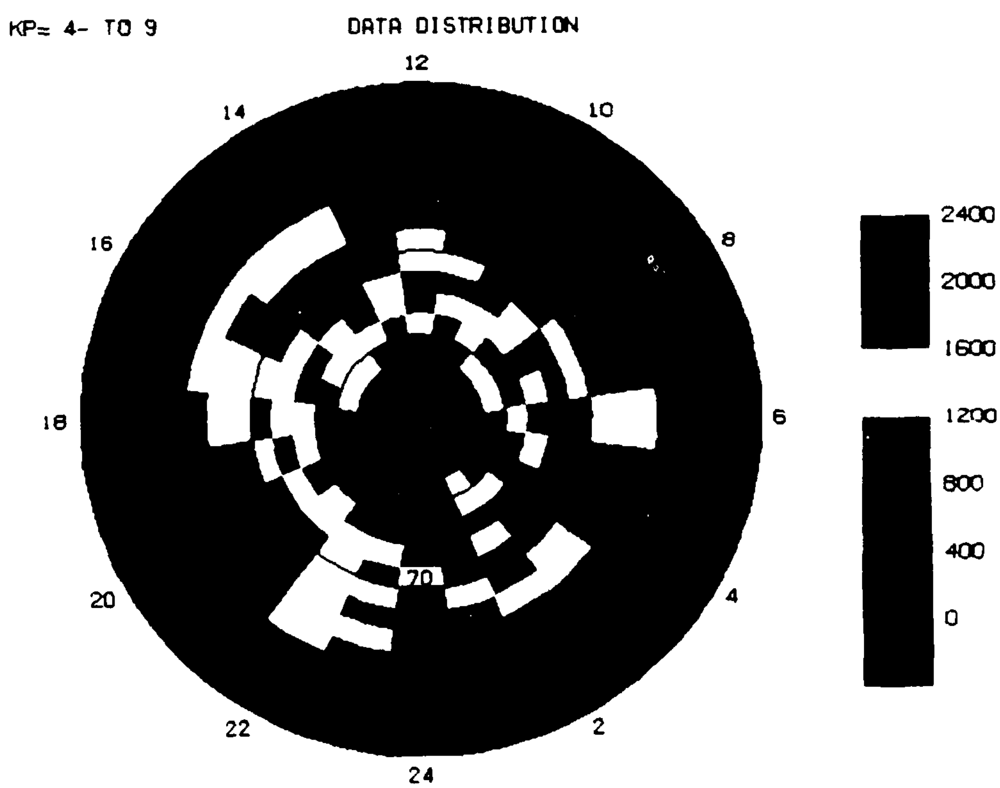

Figure 6-4

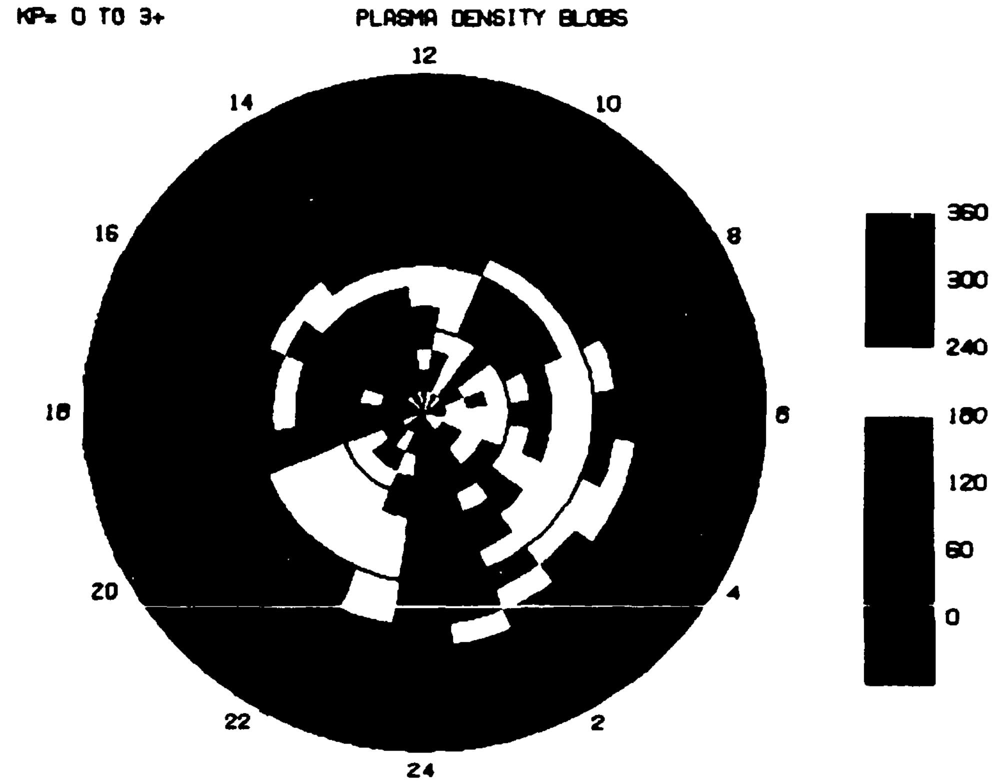

Figure 6-5

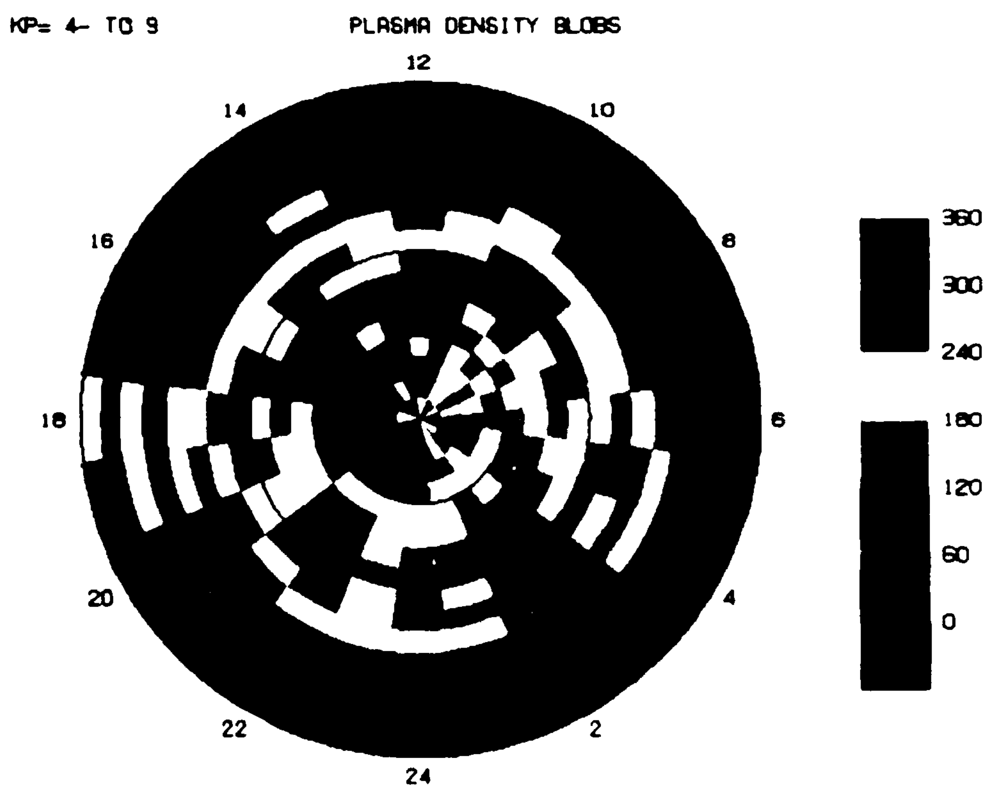

Figure 6-6

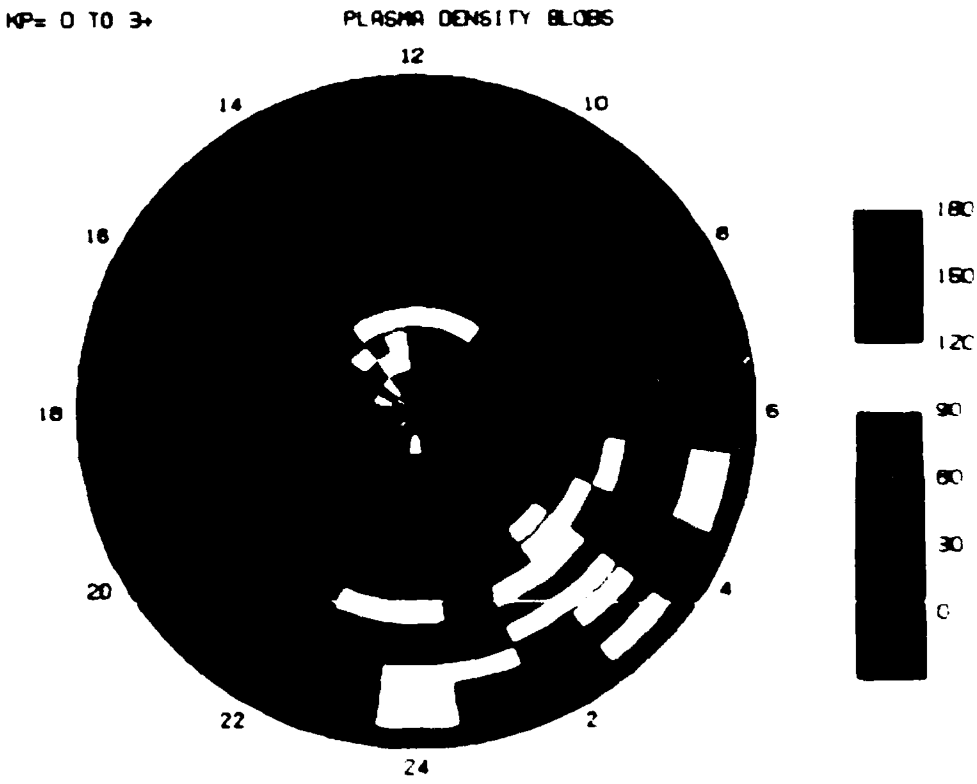

Figure 6-7

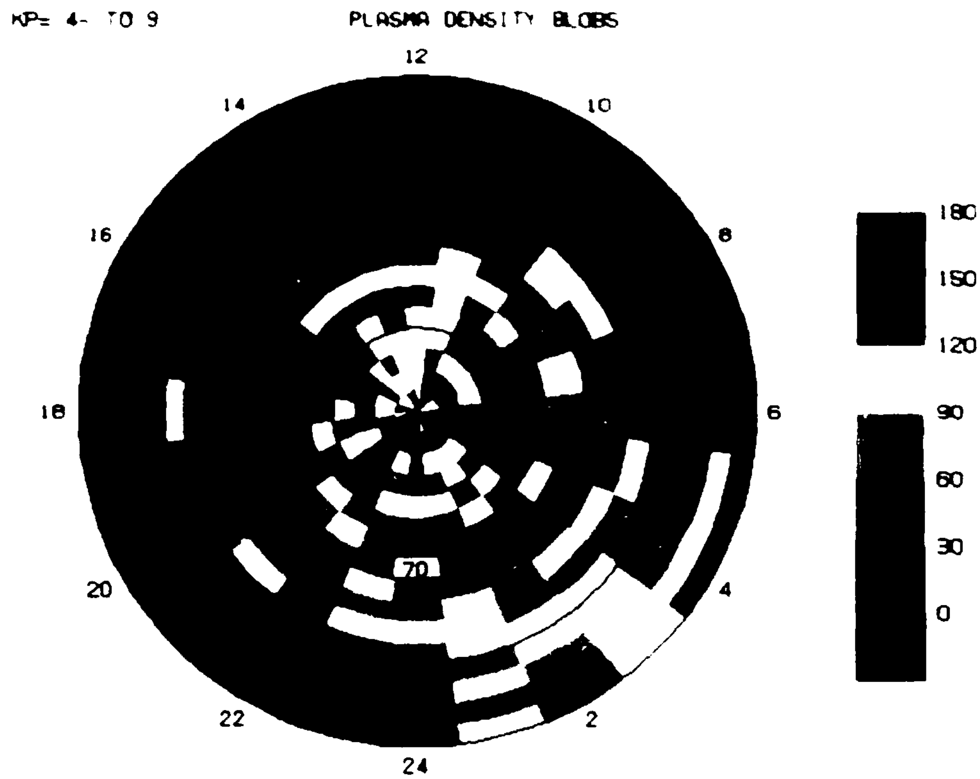

Figure 6-8

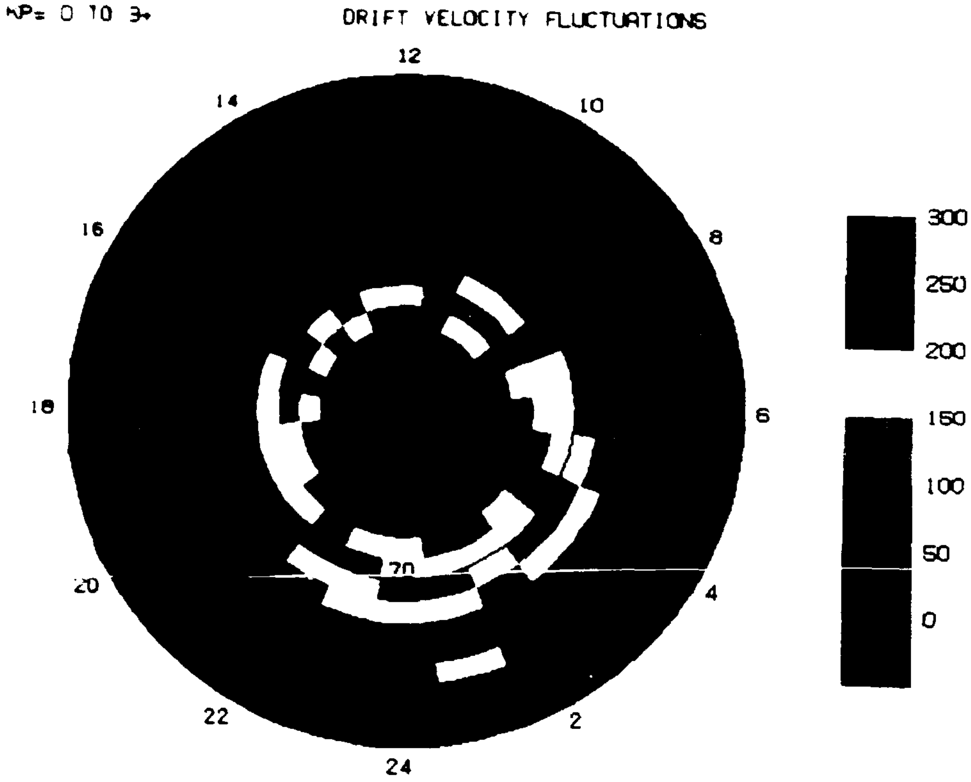

Figure 6-9

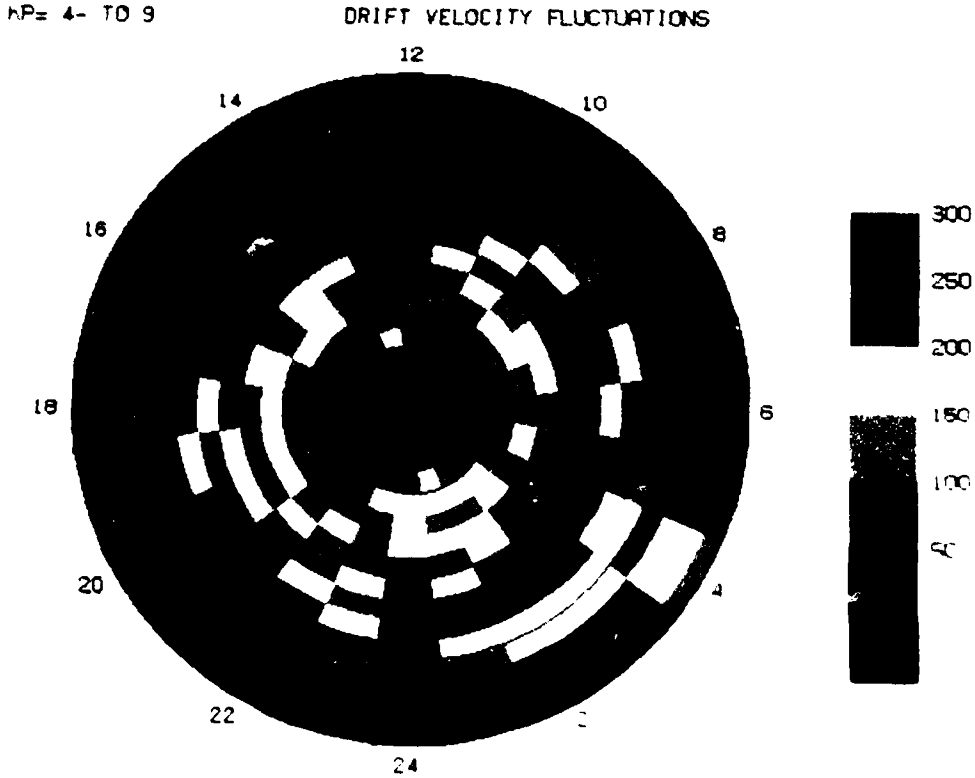

Figure

AD-A179 910 A STUDY OF PLASMA IRREGULARITIES IN THE HIGH-LATITUDE REGION(U) REGIS COLL RESEARCH CENTER WESTON MA D R WEIMER ET AL. 27 OCT 86 AFGL-TR-86-0233 2/2

UNCLASSIFIED F19628-84-C-0126 F/G 4/1 NL

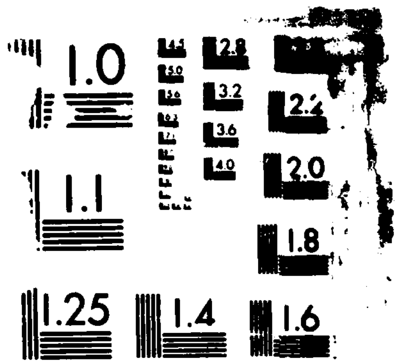
1.0
2.8
3.2
3.6
4.0
2.0
1.1
1.8
1.25
1.4
1.6

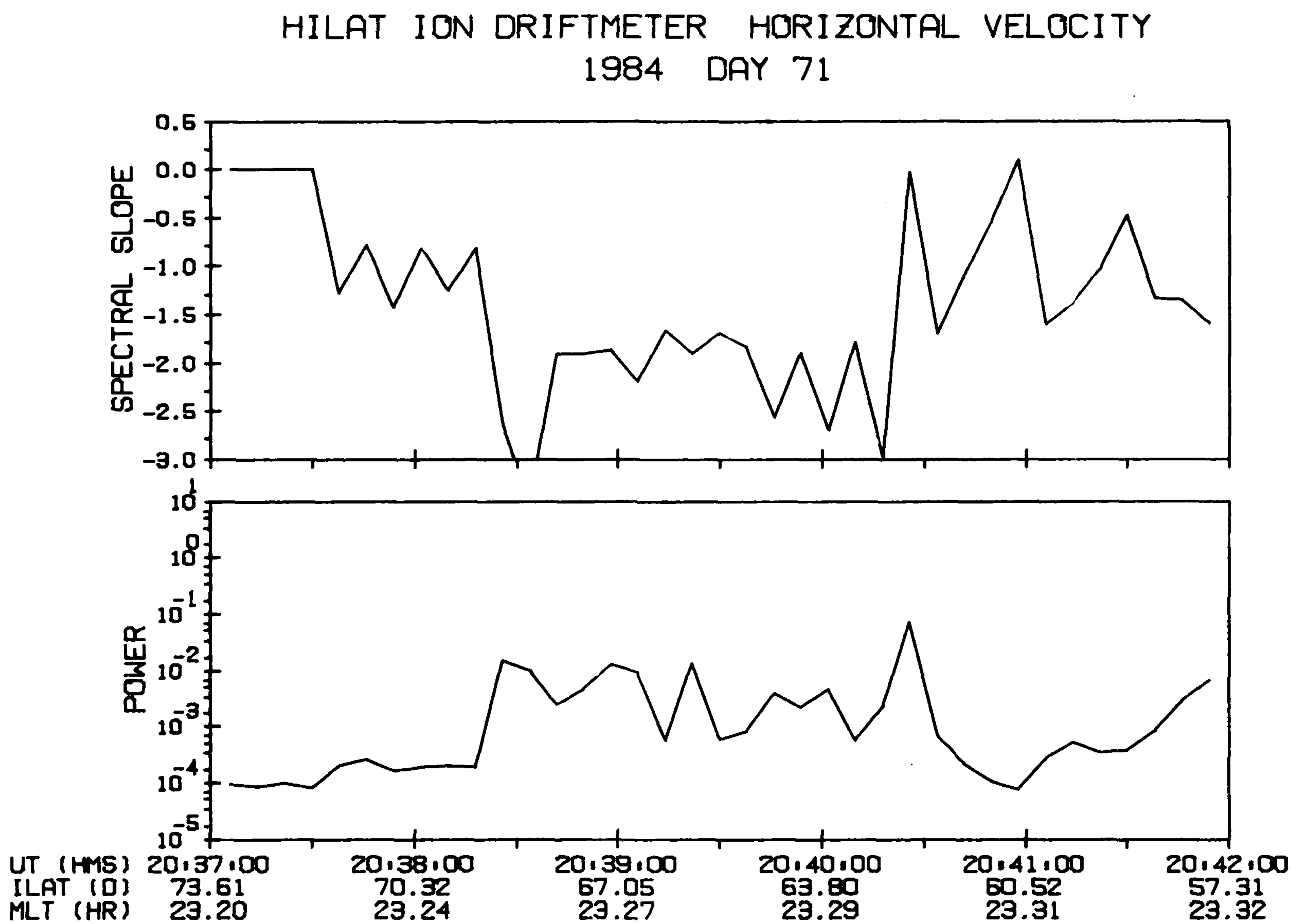
HILAT ION DRIFTMETER HORIZONTAL VELOCITY
1984 DAY 71
SPECTRAL SLOPE
0.5
0.0
-0.5
-1.0
-1.5
-2.0
-2.5
-3.0
POWER
UT (HMS) 20:37:00 20:38:00 20:39:00 20:40:00 20:41:00 20:42:00
ILAT (D) 73.61 70.32 67.05 63.80 60.52 57.31
MLT (HR) 23.20 23.24 23.27 23.29 23.31 23.32

Figure 6-11

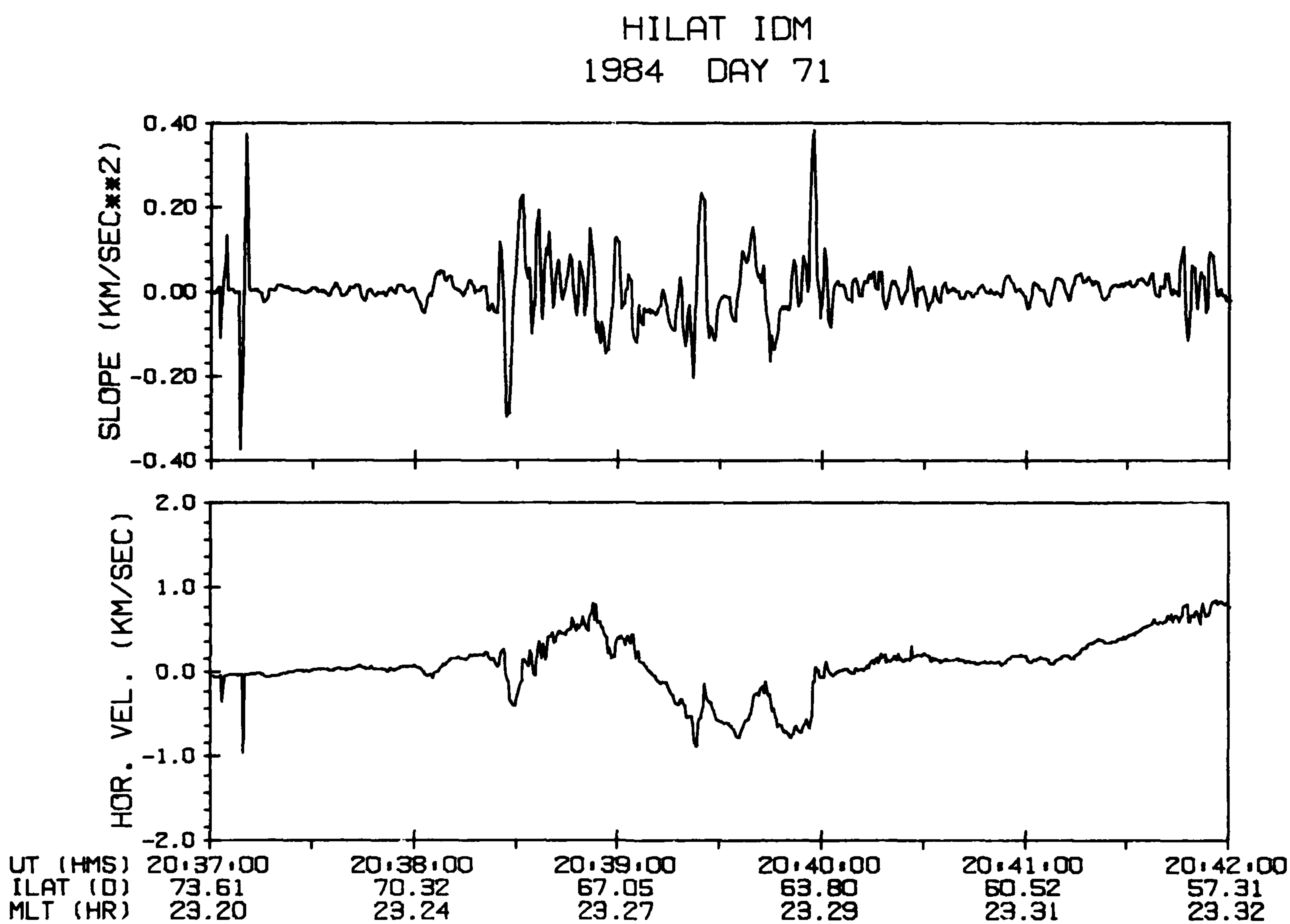
HILAT IDM
1984 DAY 71
SLOPE (KM/SEC**2)
0.40
0.20
0.00
-0.20
-0.40
HOR. VEL. (KM/SEC)
2.0
1.0
0.0
-1.0
-2.0
UT (HMS) 20:37:00 20:38:00 20:39:00 20:40:00 20:41:00 20:42:00
ILAT (D) 73.61 70.32 67.05 63.80 60.52 57.31
MLT (HR) 23.20 23.24 23.27 23.29 23.31 23.32

Figure 6-12

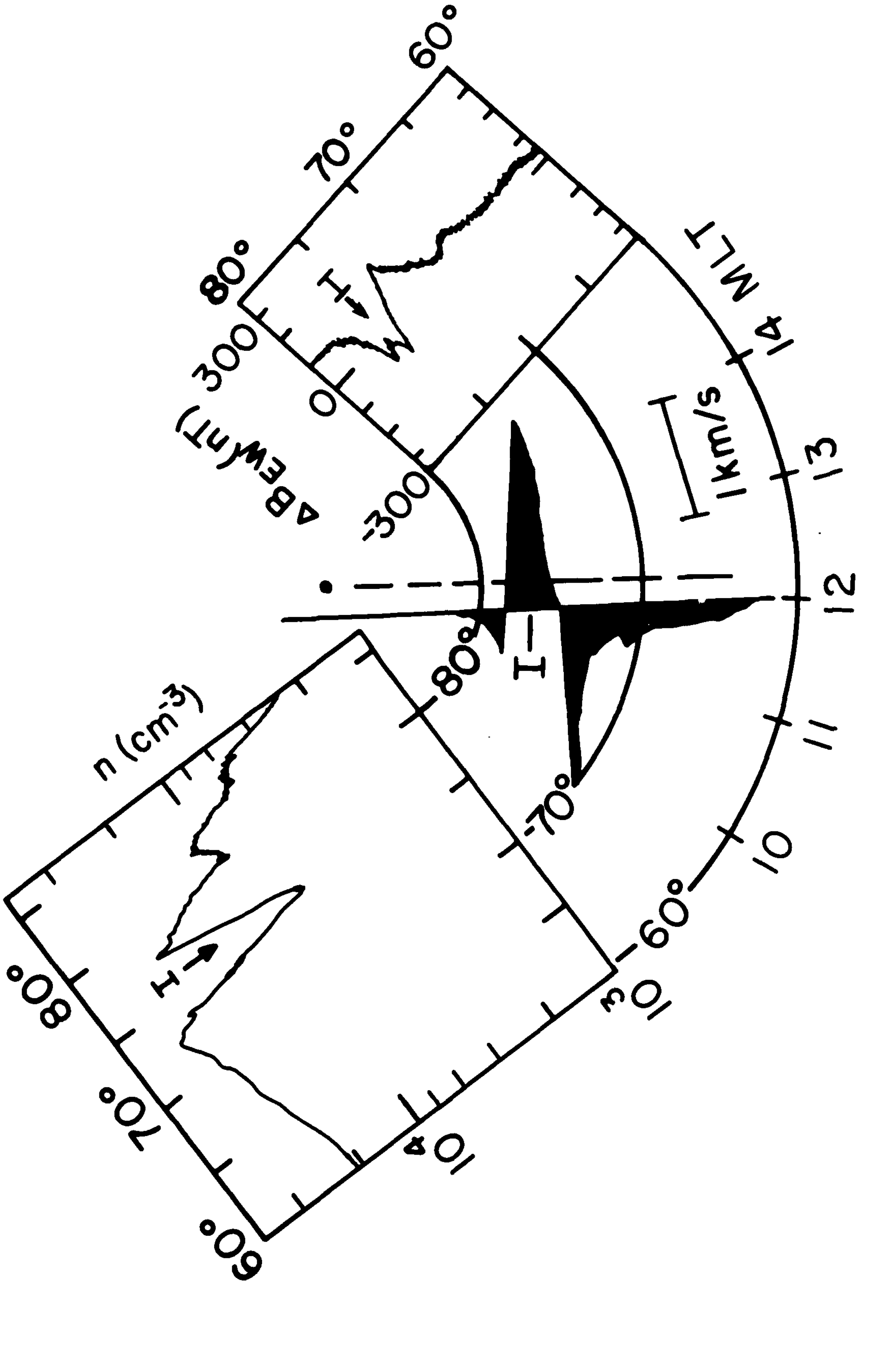
ΔBEW(nT)
300
0
-300
80°
70°
60°
MLT
14
13
12
11
10
1km/s
n (cm-3)
10⁴
10³
-80°
-70°
-60°

Figure 6-13

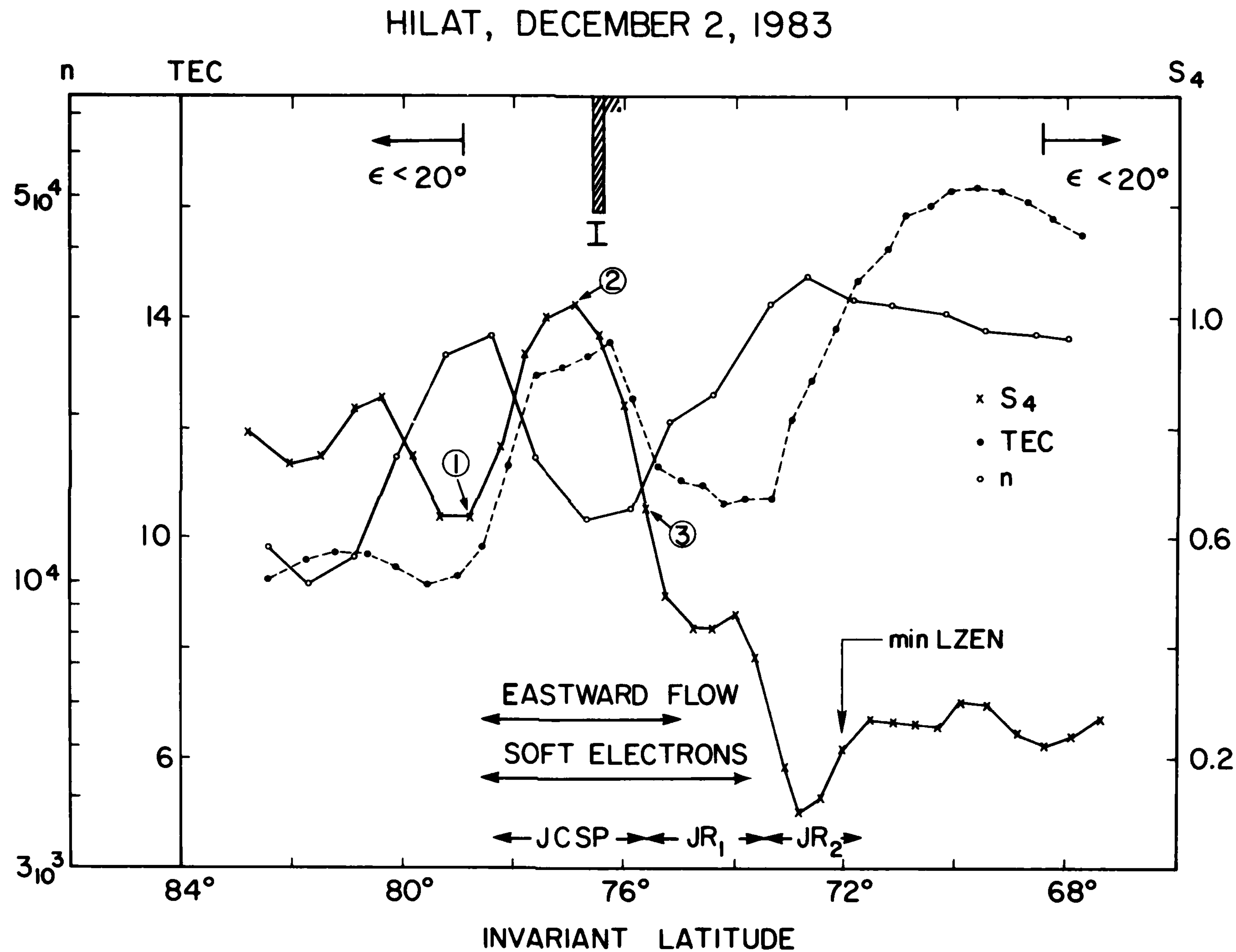

HILAT, DECEMBER 2, 1983
n
TEC
S4
ε < 20°
ε < 20°
5₁₀⁴
10⁴
3₁₀³
14
10
6
1.0
0.6
0.2
× S4
• TEC
∘ n
min LZEN
EASTWARD FLOW
SOFT ELECTRONS
JCSP
JR1
JR2
84°
80°
76°
72°
68°
INVARIANT LATITUDE

Figure 6-14

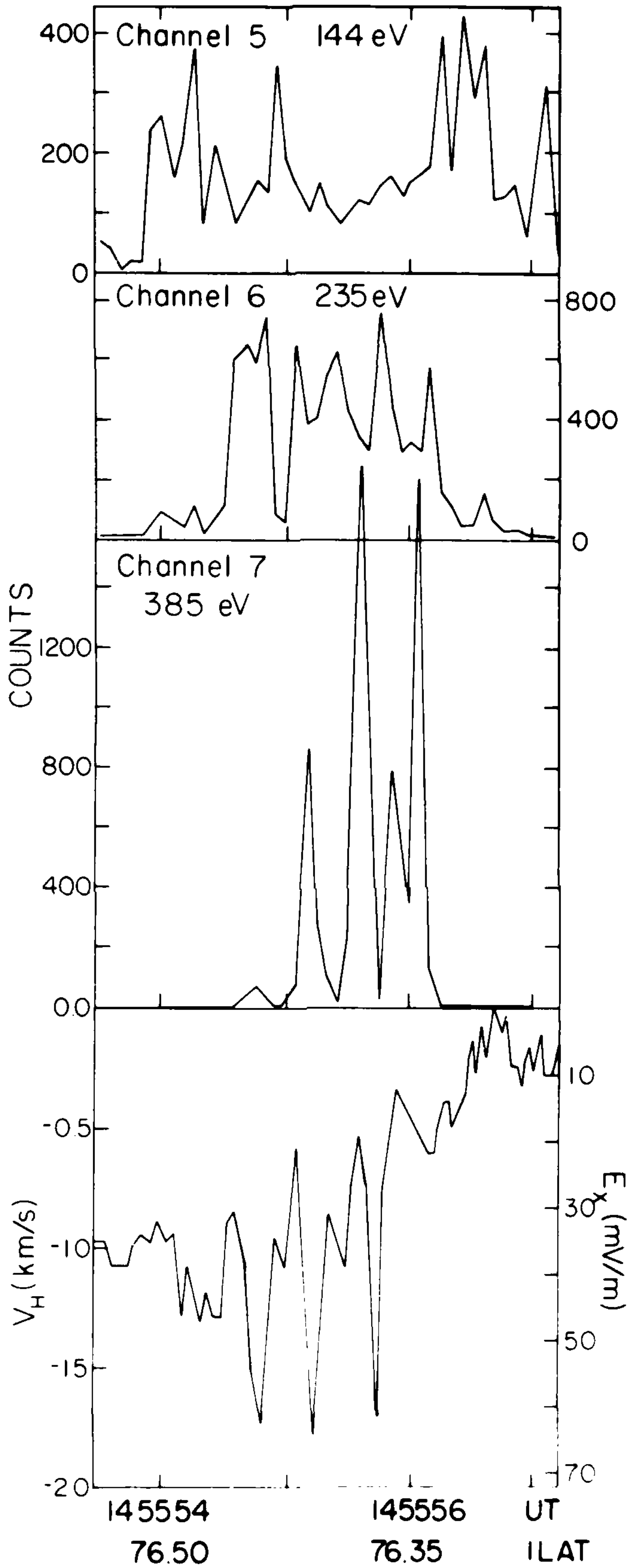
Channel 5 144 eV
400
200
0
Channel 6 235 eV
800
400
0
Channel 7
385 eV
COUNTS
1200
800
400
0.0
-0.5
-10
-15
-20
V_H (km/s)
10
30
50
70
E_x (mV/m)
145554
76.50
145556
76.35
UT
ILAT

Figure 6-15

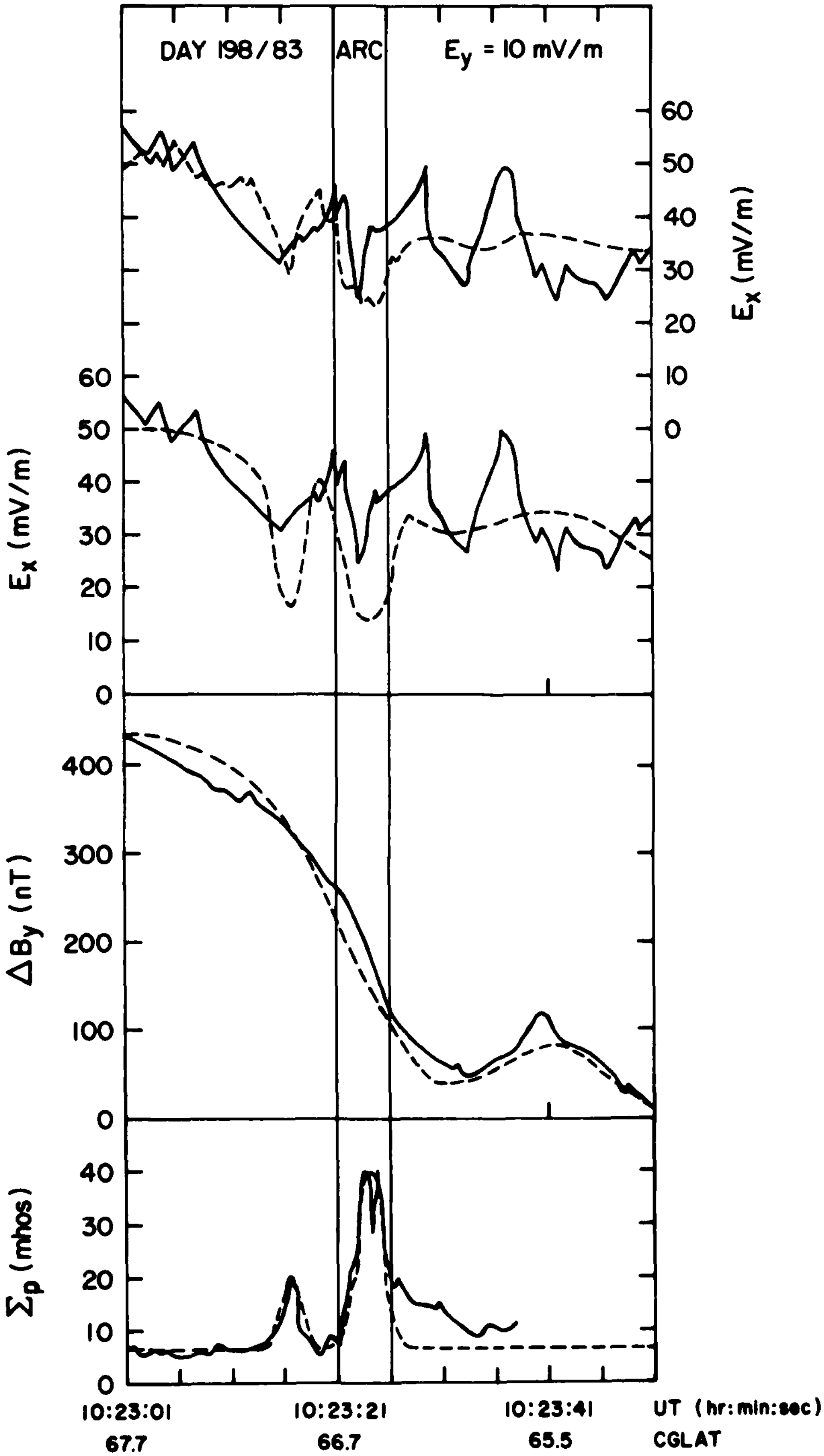

DAY 198/83
ARC
E_y = 10 mV/m
60
50
40
30
20
10
0
E_x (mV/m)
60
50
40
30
20
10
0
E_x (mV/m)
400
300
200
100
0
ΔB_y (nT)
40
30
20
10
0
Σ_p (mhos)
10:23:01
10:23:21
10:23:41
UT (hr:min:sec)
67.7
66.7
65.5
CGLAT

Figure 7-1

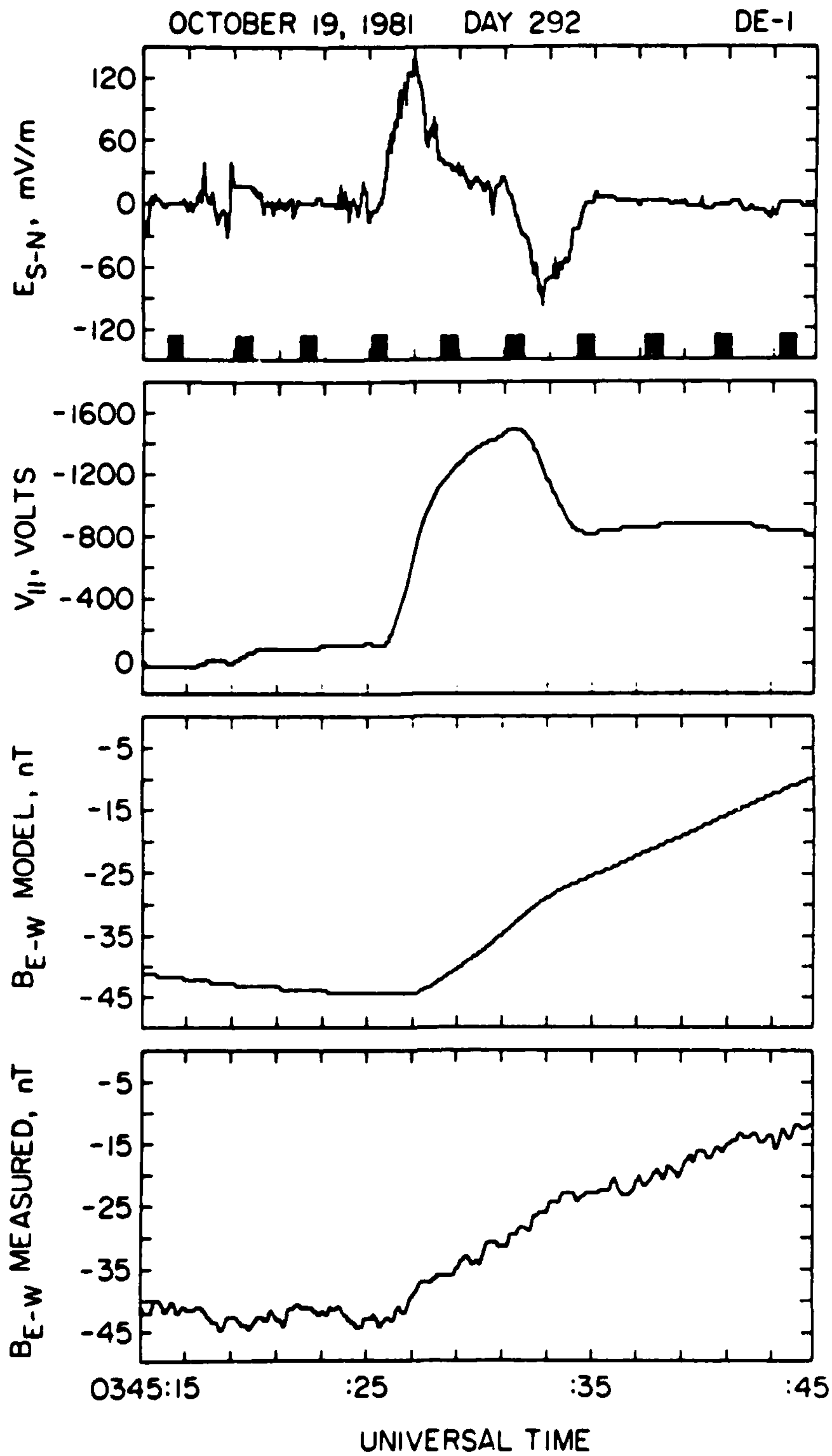

OCTOBER 19, 1981 DAY 292 DE-1
120
60
0
-60
-120
E_{S-N}, mV/m
-1600
-1200
-800
-400
0
$V_{\parallel}$, VOLTS
-5
-15
-25
-35
-45
B_{E-W} MODEL, nT
-5
-15
-25
-35
-45
B_{E-W} MEASURED, nT
0345:15
:25
:35
:45
UNIVERSAL TIME

Figure 7-2

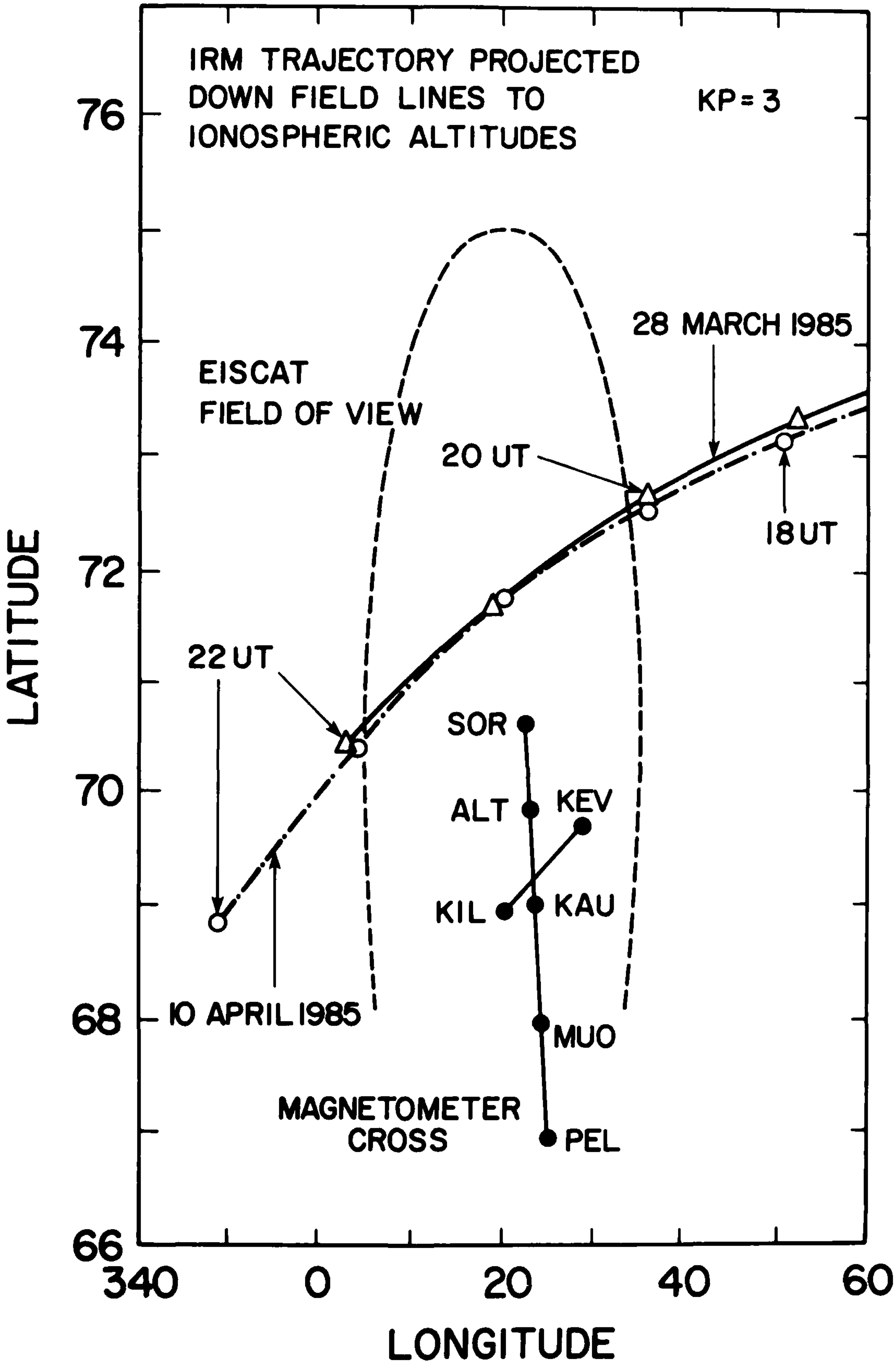

IRM TRAJECTORY PROJECTED
DOWN FIELD LINES TO
IONOSPHERIC ALTITUDES
KP=3
28 MARCH 1985
EISCAT
FIELD OF VIEW
20 UT
18 UT
22 UT
SOR
ALT
KEV
KIL
KAU
MUO
PEL
MAGNETOMETER
CROSS
10 APRIL 1985
LATITUDE
LONGITUDE
76
74
72
70
68
66
340
0
20
40
60

Figure 8-1

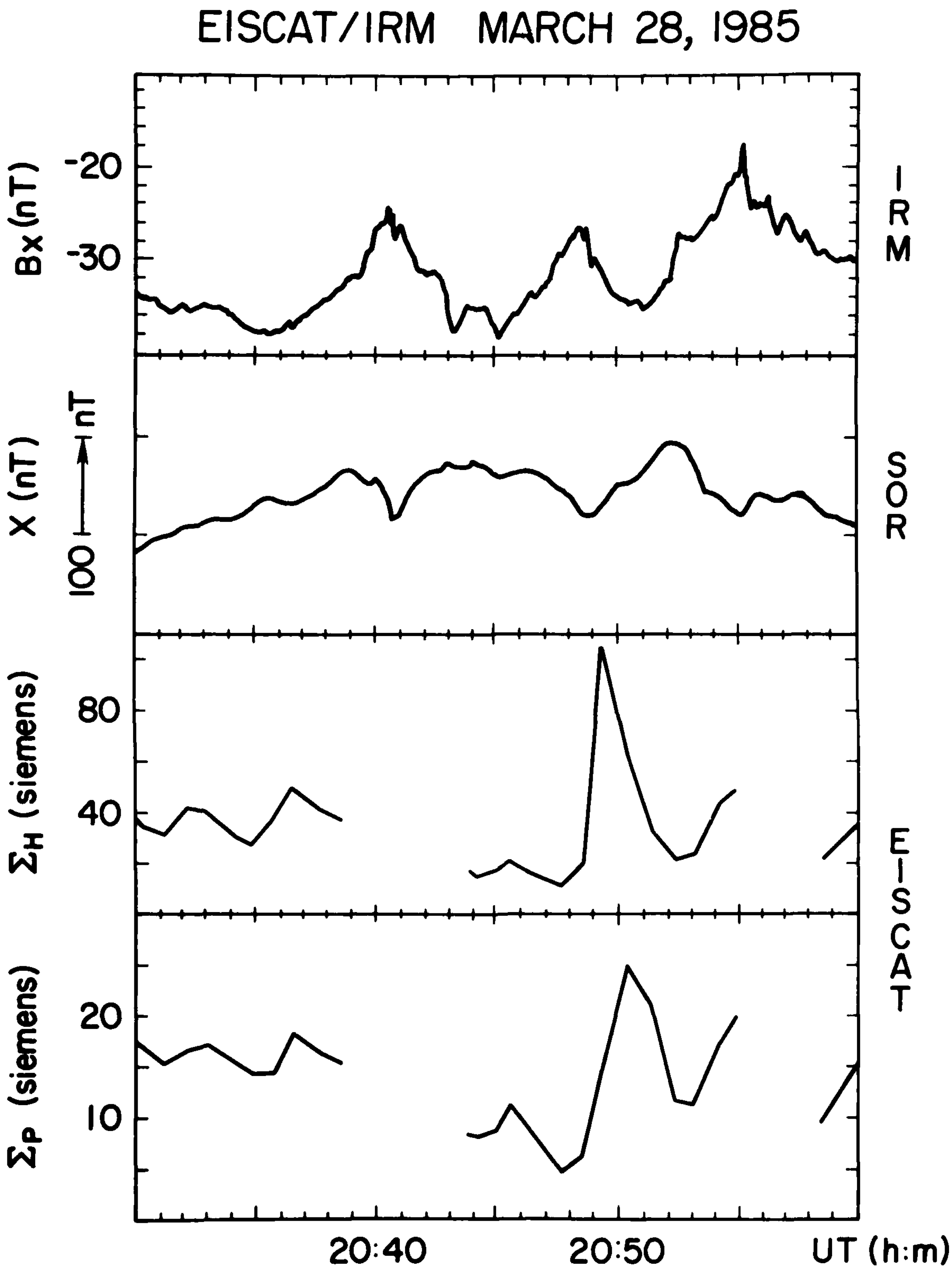

EISCAT/IRM MARCH 28, 1985
Bx (nT)
-20
-30
I R M
X (nT)
100 nT
S O R
Σ_H (siemens)
80
40
E I S C A T
Σ_P (siemens)
20
10
20:40
20:50
UT (h:m)

Figure 8-2

END

5-87

DTIC